

Copyright

by

Steven Wayne Rogers

2002

**Allowable Design Release Stresses for
Pretensioned Concrete Beams – Preliminary Results**

by

Steven W. Rogers, B.S.C.E.

Thesis

Presented to the Faculty of the Graduate School of

The University of Texas at Austin

in Partial Fulfillment

of the Requirements

for the Degree of

Master of Science in Engineering

The University of Texas at Austin

May 2002

**Allowable Design Release Stresses for
Pretensioned Concrete Beams – Preliminary Results**

**Approved by
Supervising Committee:**

Michael E. Kreger, Supervisor

Oguzhan Bayrak, Supervisor

Dedication

To my family and friends for their prayerful support.

Acknowledgements

This report was based on research performed at Ferguson Laboratory at Pickle Research Campus of the University of Texas at Austin. Research was funded through the generous support provided by the Texas Department of Transportation. My special thanks goes to Jeff Cotham, the project director.

Throughout my life, my parents have shown me unconditional love. They supported me throughout my college career with both prayers and finances, and never placed expectations on me, for which I am ever grateful. As the first in my family to attend graduate school, my parents encouraged me to walk my own path in life, trusting that I would make wise decisions and supporting me in those decisions. I thank God for my gracious parents, Laura and Ernest Davlin, and newly married sister, Kim Conlon.

I would like to thank Mike Kreger and Oguzhan Bayrak who served as supervisors on the project. Their intellectual expertise and guidance during the course of the project is much highly valued, along with their friendship.

I would also like to thank Alfredo Castro, who served alongside me during the last six months of the project. Without his tireless help during construction of the test setup, testing, and analyzing data, this thesis would have never come to fruition.

To the technicians at Ferguson Lab, Blake Stassney, Dennis Phillip, and Mike Bell, thank you for your competence and your professionalism. I appreciate

your patience in dealing with impatient students like us. Thanks for allowing me the opportunity to learn from you guys.

I would also like to thank many of my fellow graduate students who made the long, hot, exhausting days much more bearable, and many times, fun. I sincerely appreciate the sacrifice of their time on their own project to help with this one. I highly value the friendships of Alfredo Castro, Baris Binci, Jenny Tanner, Jorge Varela, Alexa von Mises, Gabriela Arce, Patrick Wagoner, Mike Hagenberger, Nat Attivitaves, and Joe Spadea.

Most importantly, I thank God my heavenly Father for the grace to see me through this project. His Word says, "I can do all things through Christ who strengthens me."

January 10, 2002

Table of Contents

TABLE OF CONTENTS	VI
LIST OF FIGURES.....	IX
CHAPTER 1 INTRODUCTION.....	1
CHAPTER 2 LITERATURE REVIEW	4
2.1 Introduction	4
2.2 History of Allowable Stresses	4
2.2.1 Allowable Stresses in Plain and Reinforced Concrete	5
2.2.2 Allowable Stresses in Prestressed Concrete (Hawkins, 1981).....	8
2.2.3 Research and the Development of Allowable Stresses in Prestressed Concrete	10
2.3 Recent Research Investigating Allowable Stresses.....	13
2.3.1 Allowable Compressive Stresses for Prestressed Concrete	14
2.3.2 Allowable Compressive Strength of Concrete at Prestress Release....	15
2.3.3 Strength Design of Pretensioned Flexural Concrete Members at Prestress Transfer	18
2.4 Summary.....	21
CHAPTER 3 OVERVIEW OF EXPERIMENTAL PROGRAM.....	23
3.1 Introduction	23
3.2 Background	23
3.2.1 Allowable Stress Design	23
3.2.2 Factors Affecting Prestressed Concrete Behavior.....	25
3.2.3 Summary	28
3.3 Scope of Research Program	28

3.4 Design of Beam Specimens.....	31
3.5 Prestressing Facility	33
3.5.1 General	33
3.5.2 Reaction Frame	35
3.5.2.1 Description of Elements	36
3.5.2.2 Redesign of Original Frame	41
3.5.2.3 Analysis of Modified Frame	45
3.5.3 Platform	48
3.6 Material Properties	50
3.6.1 Steel Strand Tension Tests	50
3.6.1.1 Strand Results Using V-Grips	51
3.6.1.2 Strand Test Using Chucks	54
3.6.1.3 Strand Results Using Upgraded Adhesive and Sealant for Strain Gauges	56
3.6.1.4 Summary of Strand Test Results	57
3.6.2 Concrete Compression Tests	59
3.7 Instrumentation.....	62
3.7.1 Strain Measurement.....	63
3.7.1.1 Electrical Strain gauges	63
3.7.1.2 DEMEC Gages	65
3.7.2 Camber Measurement	66
3.7.2.1 Linear Potentiometers	66
3.7.2.2 Dial Gauges	67
3.7.3 Temperature Measurement.....	67
3.8 Sure Cure.....	67
CHAPTER 4 FABRICATION OF TEST SPECIMENS.....	70
4.1 Introduction.....	70
4.2 Instrumentation of Prestressing Strand	70

4.3 Prestressing of Strands	71
4.4 Casting of concrete.....	71
4.5 Application of DEMEC Targets.....	72
4.6 Releasing of Prestressing Strands	72
CHAPTER 5 PRESENTATION OF PRELIMINARY RESULTS.....	74
5.1 Introduction	74
5.2 Strain Gauges	74
5.3 Concrete Fiber Stresses	75
5.3.1 Linear Analysis	76
5.3.2 Nonlinear Analysis.....	76
5.3.3 Discussion of Analysis	78
5.4 Specimen Behavior	79
5.4.1 Camber.....	79
5.4.2 Creep.....	81
5.4.3 Prestress Loss	81
CHAPTER 6 CONCLUSIONS AND RECOMMENDATIONS.....	84
APPENDIX A NOTATION.....	87
APPENDIX B CALCULATED CONCRETE STRESSES IN TEST SPECIMENS....	90
APPENDIX C PLOTS OF PRESTRESSING STRAND FORCE HISTORY.....	94
APPENDIX D MEASURED AND PREDICTED SPECIMEN CAMBER.....	97
APPENDIX E DEMEC STRAIN PROFILES.....	101
APPENDIX F PRESTRESSING STRAND TENSION TEST RESULTS.....	105
REFERENCES.....	110
VITA.....	113

List of Figures

Figure 2.1	Analysis Comparison for Prestressed Beam Section	17
Figure 3.1	Stress Gradients for Various force eccentricities	26
Figure 3.2	Typical AASHTO and Rectangular Cross-Section Comparison	31
Figure 3.3	Test Specimen Cross-Section and Length	32
Figure 3.4	Modified Reaction Frame	35
Figure 3.5	Modified Buttresses	36
Figure 3.6	Steel Bulkheads for Strand Anchors	37
Figure 3.7	Hole Spacing in Steel Bulkheads	38
Figure 3.8	12” Structural Steel Tube Compression Members	39
Figure 3.9	Buttress/Bulkhead Connections	40
Figure 3.10	Buttress/Bulkhead Connection Detail	40
Figure 3.11	Column/Buttress Connection	41
Figure 3.12	Post-Tensioning of Tie-Down Rods	42
Figure 3.13	Sketch of Buttresses Sliding Under Prestressing Loads	43
Figure 3.14	Sketch of Modifications Made to Original Buttresses	44
Figure 3.15	Free-Body-Diagram of Original Buttresses	46
Figure 3.15	Free-Body-Diagram of Modified Buttresses	47
Figure 3.16	Platform Framing	49
Figure 3.17	Lateral Bracing in N-S Direction; Plywood Decking	49
Figure 3.18	Ground Wire Instrumented with Strain Gauge; V-Grips	52

Figure 3.19	Photo of Failed Strand with Ground Wires.....	52
Figure 3.20	Stress-Strain Plot for Ground vs. Smooth Wires	53
Figure 3.21	Stress-Strain Plot for Strands Gripped with Chucks vs. V-Grips	54
Figure 3.22	Chucks Anchoring System; Failed Strand with Smooth Wires	55
Figure 3.23	Stress-Strain Plot for Strand Utilizing CN Adhesive.....	57
Figure 3.24	Calibration Curve for Stresses in Prestressing Strands.....	58
Figure 3.25	Cylinder Molds; Trial Specimen with Sure Cure Equipment	60
Figure 3.26	Strength and Temperature vs. Time Plot for Trial Specimen	61
Figure 3.27	Data Acquisition Computer and Scanner; Bridge Boxes.....	63
Figure 3.28	Photos of Strand Preparation Materials	64
Figure 3.29	DEMEC Targets and DEMEC Gage	65
Figure 3.30	Photo of Frame and Linear Potentiometers	66
Figure 3.31	Sure Cure System Computer and I/O Box; Sure Cure Cylinders	68
Figure 4.1	Instrumented Prestressing Strand for Test Specimen	70
Figure 4.2	Single-Strand Prestressing Ram; Hydraulic Pump	71
Figure 4.3	Casting of Test Specimens.....	72
Figure 4.4	Sketch of DEMEC Target Locations	73
Figure 5.1	Calculation of Concrete Fiber Stresses	77
Figure 5.2	Camber for South End Specimens	80
Figure 5.3	Camber for North End Specimens	80
Figure 5.4	Force vs. Time Plot for Specimens RS-75S and RS-75N.....	82
Figure 5.5	Force vs. Time Plot for Specimens RS-70S and RS-70N.....	82

Figure 5.6	Prestress Force vs. Time Plot for RS-60S and RS-60N.....	83
Figure B.1	Calculation of Concrete Stresses for RS-75S and RS-75N.....	91
Figure B.2	Calculation of Concrete Stresses for RS-70S and RS-70N.....	92
Figure B.3	Calculation of Concrete Stresses for RS-60S and RS-60N.....	93
Figure C.1	Prestress Force vs. Time Plot for RS-75S and RS-75N.....	95
Figure C.2	Prestress Force vs. Time Plot for RS-70S and RS-70N.....	95
Figure C.3	Prestress Force vs. Time Plot for RS-60S and RS-60N.....	96
Figure D.1	Camber of Specimen RS-75S	98
Figure D.2	Camber of Specimen RS-75N.....	98
Figure D.3	Camber of Specimen RS-70S	99
Figure D.4	Camber of Specimen RS-70N.....	99
Figure D.5	Camber of Specimen RS-60S	100
Figure D.6	Camber of Specimen RS-60N.....	100
Figure E.1	DEMEC Strain Profile for RS-75S	102
Figure E.2	DEMEC Strain Profile for RS-75N.....	102
Figure E.3	DEMEC Strain Profile for RS-75S	103
Figure E.4	DEMEC Strain Profile for RS-75S	103
Figure E.5	DEMEC Strain Profile for RS-75S	104
Figure E.6	DEMEC Strain Profile for RS-75S	104
Figure F.1	Stress vs. Strain plot for Strand with Ground Wires (V-Grips)	106
Figure F.2	Stress vs. Strain plot for Strand with Ground Wires (V-Grips)	106
Figure F.3	Stress vs. Strain plot for Strand with Ground and Smooth wires	107

Figure F.4 Stress vs. Strain plot for Strand with no Ground Wires	107
Figure F.5 Stress vs. Strain plot for Strand with no Ground Wires	108
Figure F.6 Calibration Curve for Prestressing Strands	108
Figure F.7 Stress-Strain Curve for Strand Utilizing CN Adhesive and Polyurethane Coating	109

CHAPTER 1

Introduction

Allowable stress limits for pretensioned members significantly impact the economy and productivity of precast plants. These limits dictate the required compressive strength of concrete prior to prestress transfer. Thus, the time that prestressed concrete members occupy prestressing beds while curing is likewise determined by the allowable release stress limits. By increasing these limits, precasters would be able to release prestressing strands earlier, and increase the turnover rate for their prestressing beds, favorably affecting the economy of pretensioned concrete members. Higher allowable release stresses would also permit precast concrete manufacturers to address current concerns about high early heat of hydration in the concrete, and potential premature deterioration of the concrete by delayed ettringite formation, by reducing cement content in concrete mixes.

The current allowable stress limits, set by American Concrete Institute (ACI) and American Association of State Highway and Transportation Officials (AASHTO) for pretensioned concrete members at transfer, are as follows:

ACI: (ACI 318-99)

Extreme fiber stress in compression	$0.60f'_{ci}$
* Extreme fiber stress in tension except as permitted below	$3\sqrt{f'_{ci}}$
* Extreme fiber stress in tension at ends of simply supported members	$6\sqrt{f'_{ci}}$

AASHTO: (AASHTO, 2000)

Compression	$0.60f'_{ci}$
-------------------	---------------

* Tension	200 psi or $3 \sqrt{f'_{ci}}$
Tension (with bonded reinf. to resist total tensile force)	$7.5 \sqrt{f'_{ci}}$

* Without bonded reinforcement to resist total tensile force in concrete

In order to satisfy the release strength requirements in current codes, multiple strands are often debonded near the ends of members, or harping of strands are introduced in some pretensioned members. The problems associated with debonding strands include: decreasing the shear strength of the member, possibly contributing to bond slip, and expediting corrosion by allowing water to flow along the sleeved ends of the strand (Tadros, 2001). Also, the process of harping strands, for instance in many tall slender members, can be quite dangerous. Often, the strands are depressed after stressing, rather than being held down during stressing. The device used to depress the strands is pulled out after prestress transfer, leaving a hole that is later filled with grout. This location can be susceptible to moisture penetration and premature corrosion of prestressing strands.

Primarily, stresses are limited to ensure that serviceability criteria are met, and also serve to prevent rapid creep resulting in concrete crushing at transfer. These serviceability criteria include deflection, camber control, crack control, and excessive creep of concrete. Even though increasing these allowable limits would favorably affect the production of pretensioned members, it may present serviceability problems.

If allowable stress limits can be safely increased without detrimental effects on the behavior of pretensioned members, there is no better time than the present to do so. The State of Texas is currently experiencing premature concrete deterioration of precast bridge girders, which has been linked to two chemical mechanisms within the concrete: alkali-silica reaction, and delayed ettringite

formation. To limit alkali-silica reaction, ACI now requires that producers meet one of several requirements listed in ACI Special Provisions 201. Many precast concrete producers have chosen to meet the requirement by using cement with lower alkali content. However, this cement type is more expensive and has been proven to gain strength considerably slower than the former type of cement. With low-alkali cement, pretensioned concrete beams must occupy prestressing beds longer, thus, disrupting the rate of production of the precast plant. To make this process more economical, less cement could be used in the mix, but would result in lower compressive strengths than required at the original scheduled time of release. An increase in the allowable stress limits would lower the required compressive strength at release and allow producers to release the strands earlier.

In an attempt to justify an increase in the allowable stress limits, an experimental program was proposed. Researchers plan to cast, instrument, and monitor small-scale beams subjected to stresses higher than the current limit. The current phase of the experimental program involved a preliminary series of rectangular cross-section test specimens. The specimens were stressed at the bottom fiber to a level as high as $0.71f'_{ci}$. Specimen behavior will be monitored for approximately six months. However, due to time limitations, the specimen behavior for approximately three weeks after transfer is presented in this thesis. Background information documenting the history of the development of allowable concrete stresses is also presented.

CHAPTER 2

Literature Review

2.1 INTRODUCTION

The author conducted a thorough review of available documents on the subject of allowable concrete stresses in prestressed concrete members. The literature review included researching technical papers, journal entries, building codes, theses and dissertations, as well as other technical documents on the subject, dating from the early 1900's to the late 1990's. The objectives of this literature review were to discover the rationale behind the values for compressive and tensile stress limits in prestressed members at release, and to gain insight from past researchers' experience that investigated allowable concrete stresses. However, in order to understand the reasoning behind the specified stresses allowed in prestressed members, one must first understand the origin of allowable stresses in plain and reinforced concrete.

2.2 HISTORY OF ALLOWABLE STRESSES

Allowable stresses for concrete were set at prescribed values in the early years of the ACI Code. Concrete at this time was very low strength (approximately 2000 psi). Later, accumulated design experience, coupled with substantial laboratory tests and the development of reliable methods for guaranteeing concrete strengths (w/c ratio, etc...), resulted in less restrictive allowable stresses specified as percentages of the ultimate concrete strength at 28 days (Kerekes, 1954). This development in the early years of the building code will be examined further in this chapter. The use of linear prestressing in concrete effectively dates from 1949 with the successful completion of the Walnut Lane

Bridge in Philadelphia (Hawkins, 1981). However, the use of allowable concrete stresses in design originated much earlier in the design of plain and reinforced concrete.

2.2.1 Allowable Stresses in Plain and Reinforced Concrete (Kerekes, 1954)

In 1904, the First Joint Committee on Reinforced concrete was established. This committee was made up of representatives from four major societies interested in the uniform control of reinforced concrete. Shortly after its formation, the United States government granted aid to a number of universities to maintain a program of research in this area. Following the establishment of the First Joint Committee, the National Association of Cement Users (later to become the American Concrete Institute) was founded.

The first attempt of the National Association of Cement Users (NACU) at writing a reinforced concrete code appeared in 1907 in a report by the committee on Laws and Ordinances (Henley, 1907). Little that is definite was said about design procedure for reinforced concrete. Unit stresses of 500 psi in direct compression, 800 psi for “cross bending,” 300 psi for direct shear, and 30 psi for “secondary tension” were permitted. The limits were introduced for concrete with a compressive strength of 2000 psi.

In 1908, a second report of the NACU recommended an ordinance for reinforced concrete construction submitted by the National Board of Fire Underwriters. It proposed a slight increase from 300 psi to 350 psi in the allowable concrete stress in direct compression (Henley, 1908). Also proposed in the report was an interesting approach to the design of members. The board suggested using a factor of safety of four for the working loads and an extreme compressive fiber stress in the concrete of 2000 psi, producing a stress in the steel equal to the elastic limit. The NACU did not adopt these recommendations, but it

is important to note that the approach is similar to the current strength design method.

During the following year, there was a flurry of proposed building regulations, including a report submitted by the Joint Committee, and a report submitted by the Committee on Reinforced Concrete, newly formed by the NACU (Henley, 1909). In comparison with 15 municipal codes in 1909, with the exception of two, the NACU's proposed value for the allowable fiber stress was easily the most liberal. The NACU proposed an allowable compression fiber stress of 650 psi versus 500 psi stated in the New York City code. The Association also added that the 650 psi limit could be increased 15 percent near the supports in continuous beams.

In 1910, following a few revisions, NACU adopted the first Standard Building Regulations, which were based on another report of the Joint Committee completed that year. The Regulations stated that the allowable compressive stress at the extreme fiber be 650 psi with an increase of 15 percent near the ends of continuous members (same as in 1909). These values were based on 2000 psi concrete and could be increased up to 25 percent if using higher strength concrete (Committee on Building Laws, 1910).

Experimental work between 1903 and 1910 was chiefly laboratory work, but over the next five years, results from tests made on actual buildings were considered and correlated with many design methods of the day. By 1916, members of the building industry determined the need for revisions. Therefore, in 1916, proposed revisions to the regulations of the American Concrete Institute (ACI) appeared that incorporated findings from the many tests conducted in the previous years (Moore, 1916). This year also marked the transition from prescribed allowable stresses (i.e. 650 psi), to allowable stresses expressed as a percentage of the 28-day concrete compressive strength (i.e. $0.325f'_c$). In 1909, a

similar procedure was employed in the Joint Committee's Report by allowing a 25 percent increase in allowable stresses for concrete strengths higher than 2000 psi. Because the 1916 revisions incorporated stress limits that were a function of the concrete compressive strength, and compressive strengths up to 3300 psi were recognized, the allowable stresses could easily exceed the 25 percent increase in the 1909 Joint Committee Report allowed for concrete strengths exceeding 2000 psi. The allowable stresses for concrete stated in the 1916 Revised Regulations were as follows: $0.25f'_c$ for direct compression; $0.375f'_c$ for extreme fiber stress ($0.475f'_c$ adjacent to the support of continuous members); $0.50f'_c$ for bearing; and $0.075f'_c$ for shear (reinforced concrete).

By 1917, the ACI Code and that of the Joint Committee were considerably different. Members of the ACI and the Joint Committee had differing opinions in several areas, including the increase of allowable fiber stress at the ends of continuous members. The increase in allowable stress at the ends of continuous members was limited to $0.410f'_c$ in the 1917 ACI Code rather than $0.475f'_c$ proposed by the Joint Committee.

In 1925, ACI once again adopted allowable stress limits that were lower than those proposed by the Joint Committee. ACI limited the allowable extreme fiber stress to $0.375f'_c$ ($0.41f'_c$ at ends of continuous members) in compression versus $0.40f'_c$ ($0.45f'_c$ at ends of continuous members) recommended by the Joint Committee. No further changes were made in the ACI Code until the 1936 edition. The new code followed the form of its predecessor with a few important changes, but none regarding allowable concrete stresses.

ACI presented its new Building Code Requirements for Reinforced Concrete in 1941, ACI 318-41 (Committee 501, 1940). Generally speaking, the code was very similar to the final report of the Third Joint Committee submitted in 1940. The ACI code adopted a single value of $0.45f'_c$ for the allowable fiber

stress in compression. According to ACI 318-99, this is also the current allowable fiber stress for prestressed concrete members subjected to sustained loads.

2.2.2 Allowable Stresses in Prestressed Concrete (Hawkins, 1981)

A committee on prestressed concrete was first organized by ACI in 1942. Its mission was to review present knowledge of prestressed concrete, to develop design procedures, and to recommend needed research. The impetus provided by the Walnut Lane Bridge led to a reorganization and expansion of that committee in 1949 and subsequently to further expansion in 1952 as the joint ACI-ASCE Committee 323 on Prestressed Concrete. Despite the lack of specifications, the prestressed concrete industry began to flourish and by 1952, contracts had been let for over 100 bridges and buildings. Interestingly, prestressed concrete is the only major construction medium that postdates the introduction of building codes.

In 1952, development of tentative recommendations for prestressed concrete bridges became the main task of Joint Committee 323. Along the way, the committee had a major influence on the Design Criteria for Prestressed Concrete published by the Federal Bureau of Public Roads in 1952 and 1954.

The first attempt at writing a set of recommendations for prestressed concrete was endeavored by the Federal Bureau of Public Roads (now the Federal Highway Administration) and was titled, "Criteria for Prestressed Concrete Bridges" (Bureau of Public Roads, 1954). Although there were considerable differences in opinion, the Bureau decided to allow a temporary fiber stress (stress at transfer, before losses due to creep and shrinkage) of $0.60f'_c$ in compression for pretensioned members but only $0.55f'_c$ for post-tensioned members. The allowable compressive stress due to dead, live, or impact loads (after prestress losses) was limited to $0.40f'_c$. The allowable fiber stress for concrete in tension

was limited to $0.05f'_{ci}$ at transfer, and 0 after prestress losses had taken place. It is important to note that this document was not regarded as a code, but it did serve as guidelines much needed for the prestressed concrete industry at that time.

Following the Bureau's publication, the ACI-ASCE Joint Committee submitted its *Tentative Recommendations for Prestressed Concrete* in 1958 (Joint Committee 323, 1958). Allowable extreme fiber stress limits were recommended both at release and after all prestress losses had taken place. Concrete compressive stresses at release were limited to $0.60f'_{ci}$ for pretensioned members and $0.55f'_{ci}$ for post-tensioned members. At the service load stage (accounting for all prestress losses), the allowable compressive fiber stress was limited to $0.45f'_c$ for building members and $0.40f'_c$ for bridge members. It is important to note that many interpreted these recommendations as code, but the fact that the Joint Committee 323 report was a recommended practice and not a code was very significant for the subsequent development of prestressed concrete.

The first officially recognized code provisions for prestressed concrete were incorporated in the 1961 AASHTO bridge specifications (Siess, 1960; AASHTO, 1961). First developed by a subcommittee of the Structural Engineers Association of Northern California, the first building code provisions for prestressed concrete were included in the 1963 ACI Building Code (ACI Committee 318, 1963). In ACI 318-63, allowable fiber stresses for concrete in compression were limited to $0.60f'_{ci}$ for pretensioned members at release and $0.45f'_c$ for pretensioned members at design loads (after prestress losses). Since these provisions were adopted by ACI in 1963, the allowable compressive stress limit for the extreme fiber in prestressed concrete members for sustained loads has not changed. However, in part, due to research conducted by Huo and Tadros (Huo, 1995), the allowable compressive stress limit was revised in ACI 318-95 and the AASHTO Specifications (1996) to allow $0.60f'_c$, due to the prestress force

and total loads, at the extreme fiber for pretensioned members. The tensile stress limits of $3\sqrt{f'_{ci}}$ and $6\sqrt{f'_{ci}}$, have remained unchanged, with the exception of a few minor additions dealing with serviceability issues.

In comparison, the allowable limit for compressive concrete stress for building members is somewhat higher than for bridge members. Today, the AASHTO code (primarily for bridge members) limits the allowable compressive stress in concrete to $0.40f'_c$ for sustained loads (AASHTO, 2000), due to the likely adverse service conditions such as corrosive environments, weather, and fatigue that may degrade the concrete.

2.2.3 Research and the Development of Allowable Stresses in Prestressed Concrete

At the time of the release of the Joint Committee's Tentative Recommendations for Prestressed Concrete in 1958, there was still no significant research that targeted allowable stresses. Therefore, it was no surprise that the limits set by the Bureau of Public Roads and Joint Committee came under constant scrutiny. Following are opinions and comments made by two key researchers of prestressed concrete from that era.

Undoubtedly, the allowable stress values selected for the Joint Committee's recommendations in 1958 had very little research support. These values were, for the most part, based exclusively on experience and very limited data. It is evident, by the vast number of differing opinions within the Joint Committee, that the values agreed upon were unsubstantiated. Also, when discussing the limits to recommend for the Bureau of Public Roads, suggested limits from authorities within the committee varied as much as $0.15f'_{ci}$ (Bureau of Public Roads, 1954). Apparently, some attempted to rationalize the selected

limits by relating to experience with allowable stresses in reinforced concrete, about which, Professor Chester Seiss made important comments.

During the years 1950 to 1952, C. P. Seiss, a leading authority on the subject of prestressed concrete provisions, headed the sub-committee of ACI-ASCE Committee 323 that developed definitions and notation for prestressed concrete. His views on the function of codes and the correlation between the behavior of reinforced and prestressed concrete left a lasting impact on prestressed concrete concepts (Hawkins, 1981). Prof. Seiss presented a paper in 1960 describing his views, which were later endorsed by ACI Committee 318 in their commentary for the 1963 ACI Code (Seiss, 1960). He emphasized that codes are almost entirely empirical, based primarily on research and experience. He posed the question: “We have design specifications for ordinary reinforced concrete, a specification essentially empirical in nature and based on years of experience with reinforced concrete. Can we extend such a specification to cover the design of prestressed concrete?” His answer was, “No.” He added, however, that reinforced concrete provisions could serve as a guide for prestressed concrete provisions, but reinforced concrete provisions could not be carried over directly to prestressed concrete.

In a private conversation with Prof. Seiss regarding the origin of the allowable compressive release stress for prestressed concrete, he recalled that the value arose from a meeting (Siess, 2000). He could recall no rationalization or supporting research for the chosen value of $0.60f_{ci}$. In fact, at that time, he disapproved of permitting a compressive stress of $0.60f_{ci}$ even as a temporary stress. He gave three reasons: First, concrete strengths vary as much as 15 percent; second, the ultimate strength of concrete for sustained loads is perhaps only 90 percent of that for instantaneous loads; and third, some allowance should

be made for the eccentricity of the prestress force. He was only one of many with differing opinions on the subject.

T.Y. Lin, a distinguished emeritus professor at the University of California at Berkeley and expert in the field of prestressed concrete stated his dissention about the allowable stress limits in the discussion of the Tentative Recommendations for Prestressed Concrete (Lin, 1958). Lin wrote, “While it is true that such simple sets of allowable stresses have been used for some time and have apparently yielded safe results, it must be realized that this was more a matter of coincidence than of rational justification. Most of the values were empirically employed by pioneers of prestressed concrete...We as engineers who endeavor to seek the truth and to apply the laws of nature should not blindly follow these empirical values.” Lin went on to state that, based on an investigation at the University of California, the behavior of beams at transfer cannot be simply described by stresses, but are dependent on a number of factors, such as the shape of the section, the amount and location of prestress, etc. “At this stage in our knowledge regarding prestressed concrete,” Lin continued, “we are not in a position to fix definite allowable values for all the stresses under all conditions. Arbitrary values as now recommended ... could be misleading, and therefore dangerous.” Lin felt strongly that the recommendations should guide engineers in their thinking rather than force them to blindly follow arbitrary rules of thumb.

Despite the dissenting opinions, allowable stress limits were adopted in many building codes and still exist today. However, there has been an overall shift in the design process since the early 1900’s, most recently for prestressed concrete design, to a strength design approach. This design approach is based on assigning load factors for possible overloads, and strength reduction factors to account for material variations, failure modes, etc. Currently, ACI and AASHTO

require that a prestressed flexural member be designed to satisfy allowable stresses as well as strength requirements.

2.3 RECENT RESEARCH INVESTIGATING ALLOWABLE STRESSES

It was clear that the building codes of the mid 1900's were in need of research to justify the allowable stresses prescribed for prestressed concrete design. However, significant research was not conducted on the topic until the 1900's. With years of acceptable performance of prestressed beams designed using the allowable stress limits specified in ACI 318-63, it is assumed that researchers saw no reason for change.

In recent years, precast, prestressed concrete manufacturers have indicated a desire to increase allowable concrete stresses at release in order to improve the efficiency and/or economy of their production process. Higher allowable concrete release stresses would not only permit earlier release of prestress forces on elements, but alternatively, would also permit less expensive concrete with reduced cement content to be used without affecting current production rates. Use of concrete with reduced cement content has the added benefit of avoiding undesirable material damage mechanisms triggered by high early heat of hydration, such as delayed ettringite formation (DEF). With these objectives in mind, there have been a number of research projects conducted in recent years to investigate the effects of increased allowable concrete stresses at prestress transfer. In the following sections, results from a few of these research studies are presented.

2.3.1 Allowable Compressive Stresses for Prestressed Concrete: Pang and Russell

In 1995, the Precast/Prestressed Concrete Institute funded a research project conducted by Pang and Russell (Pang, 1996) to investigate the strength

reduction experienced by concrete cylinders when subjected to large sustained compression loads. Concrete cylinders with two different design mixes, a 7-sack mix and an 8 ½-sack mix, were tested. Both mixes with their high early strengths are common to the prestressing industry. The 7-sack mix had an average 1-day compressive strength of 5800 psi and an average 28-day strength of 7420 psi. The 8.5-sack mix had an average strength of 7010 psi in one day and 8710 psi in 28 days.

After 22 hours of steam curing at 100° F, the concrete cylinders were subjected to compressive stresses equal to or higher than the allowable stress specified by ACI and AASHTO ($f_c = 0.60f'_{ci}$). Compressive stresses of $0.60f'_{ci}$, $0.70f'_{ci}$, and $0.80f'_{ci}$ were sustained 7 days, 28 days, 63 days, 90 days, or 180 days. Control cylinders, used to determine the 1-day breaking strength, were made from the same concrete batches as the “test” cylinders, and were placed alongside the loaded cylinders to assure identical curing conditions. After the prescribed load duration, the cylinders were tested to determine the compressive strength and modulus of elasticity.

Strength testing revealed that the specimens loaded to $0.70f'_{ci}$ suffered no reduction in compressive strength. Two of the specimens that were loaded to $0.80f'_{ci}$ failed under the sustained load, but the cylinders that survived the sustained load exhibited no reduction in strength. Creep of the specimens loaded to $0.70f'_{ci}$ and $0.80f'_{ci}$ was also monitored, and the behavior was found to be similar to that for specimens loaded with a lower sustained stress.

Researchers concluded that there were no detrimental effects to the strength of concrete by applying sustained stresses higher than allowed by current codes. The acceptable observed creep behavior also supports a higher limit for allowable concrete stresses at prestress transfer. However, because this research project only dealt with the behavior of concrete cylinders nominally in pure

compression, further research should be conducted to examine flexural behavior (ie. camber, prestress loss, creep, etc...) in order to fully support increasing allowable stress limits.

2.3.2 Allowable Compressive Strength of Concrete at Prestress Release: Huo and Tadros

In their paper published in the Precast/Prestressed Concrete Institute (PCI) Journal in 1997, Huo and Tadros (Huo, 1997) proposed the implementation of higher allowable release stresses based on the nonlinear behavior of concrete. The authors stated that the allowable stress limits exist to guard against concrete crushing at the time of prestress release. They indicated that because the concrete fails at a critical strain and not a critical stress, nonlinear behavior should be considered when limiting the allowable concrete compressive stress. It is demonstrated in many stress-strain curves from concrete compression tests that this approach is undoubtedly the most accurate. Also, because of the self-relieving nature of prestressed members due to elastic shortening, relaxation, creep, and shrinkage, the authors suggest that nonlinear section analysis is the only realistic method for determining the prestress force in a member. Although accurate and realistic, this procedure may be undesirable for use by designers because of the complexity involved.

In this paper an 18"x18" cross-section was analyzed with varying amounts of prestressing steel stressed at 189 ksi and with no eccentricity. The initial strength of the concrete (f'_{ci}) assumed for the analysis was 3500 psi. With the steel stress and concrete strength known, the number of strands in the cross-section was varied in the analysis. As more prestressing strand was added to the cross-section, the corresponding ratio of concrete stress (f_c) to concrete strength

(f'_{ci}) was increased to a limiting value. Also, the ratio of concrete strain (ϵ_c) to ultimate strain ($\epsilon_{cu} = .003$) was analyzed.

A linear approach was presented first. Utilizing common design techniques, an estimate of the concrete stress due to prestressing was calculated using the transformed section. This is equivalent to the iterative approach and is slightly more accurate for calculating prestress loss than the standard assumption of 10 percent elastic prestress loss stated in the PCI Design Handbook (PCI, 1995). For 45 prestressing strands, f_c was computed to be f'_{ci} , which would theoretically crush the concrete. The number of strands required to stress the concrete to the current allowable limit ($0.60f'_{ci}$) was 25 strands.

The following method used by the author was based on the Hognestad nonlinear stress-strain model for concrete. Using the model, the authors calculated the number of strands required to reach the crushing strain of the concrete, based on an ultimate strain ϵ_{cu} of 0.003, rather than the ultimate stress ($f'_c = f'_{ci}$). Using a spreadsheet program the authors iterated to solve the concrete stress-strain relationship (Equation 1), the steel stress-strain relationship (Equation 2), and the equilibrium condition (Equation 3), then generated the relationship shown in Fig. 2.1.

$$f_c = f'_{ci} \left[2\epsilon_c/\epsilon_o - (\epsilon_c/\epsilon_o)^2 \right] \text{ where } \epsilon_c < 0.003 \quad (2.1)$$

$$f_{po} = f_{pi} - \epsilon_c E_{ps} \quad (2.2)$$

$$f_{po} A_{ps} = f_c A_c \quad (2.3)$$

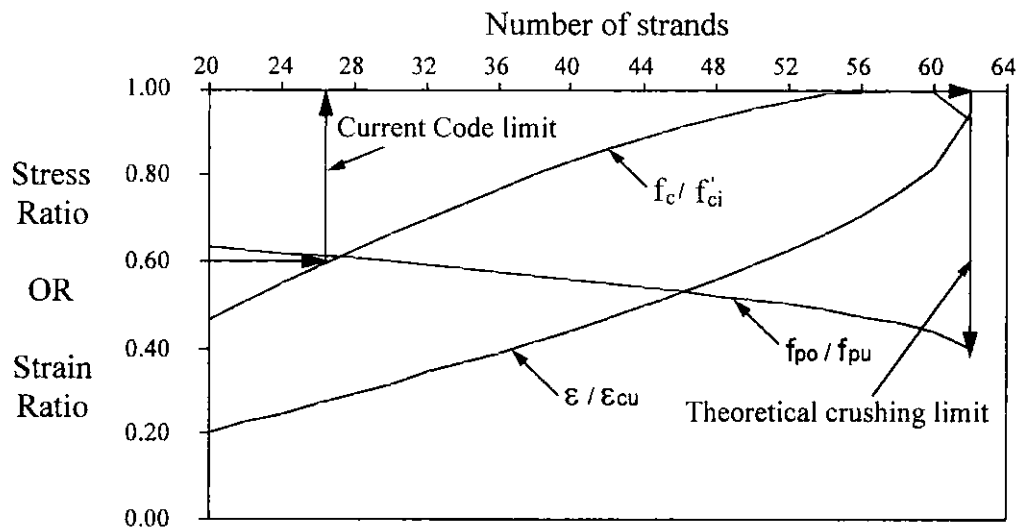


Figure 2.1 Linear and Nonlinear Analysis Comparison for Concentrically Prestressed Beam Section (Huo, 1997)

Using linear analysis, 25 strands were required to stress the section to the current allowable limit, $0.60f'_{ci}$. The nonlinear analysis predicted that 26 strands would be needed. This indicates that the linear approach is reasonably accurate up to the current allowable limit of $0.60f'_{ci}$. As the stress and strain ratio increase, it is shown in Fig. 2.1 that the difference in number of strands required to reach these ratios increases.

By using nonlinear analysis, the number of strands can be increased up to 58 to reach the peak stress, f'_{ci} , and 62 to reach the ultimate strain, versus 45 strands calculated based on linear-elastic analysis. This suggests that the section has approximately a 50 percent reserve capacity when the member is stressed to the current allowable limit of $0.60f'_{ci}$.

Although designers do not want to approach a concrete crushing failure at release, nonlinear analysis illustrates the inherent safety in current linear design

practice. When one designs a prestressed beam assuming linear behavior, the maximum compressive stress the concrete actually experiences could be significantly less than calculated. Although the authors made no definitive recommendations, their research does lend support to arguments for increased allowable concrete stresses at release.

A major limitation of this research is the lack of consideration of steel relaxation, creep, and shrinkage effects on prestress loss and camber. These effects, along with accidental eccentricity in the prestress force, need to be considered for a thorough analysis. There were also no tests carried out to support the findings of this study. However, the study does present a rational approach for calculating concrete stresses and, perhaps for revising allowable stress limits.

2.3.3 Strength Design of Pretensioned Flexural Concrete Members at Prestress Transfer: Noppakunwijai and Tadros

In another research project funded by PCI, Noppakunwijai and Tadros (Noppakunwijai, 2001) investigated the effectiveness of a strength design approach for the design of prestressed members. They state that, in practice, the proposed method will generally lead to higher allowable prestress levels than permitted by the $0.60f'_{ci}$ empirical limit. Also included in the report is a simple equation for calculating a more realistic limit for allowable stresses in members having various cross-sectional properties.

Load factors and strength reduction factors were introduced as part of the proposed strength design method. A load factor of 1.2 was applied to the prestress force in prestressing steel just before transfer, P_t . A load factor of 0.8 or 1.2 was applied to the self-weight moment, M_g , due to the uncertainty of lifting locations. The load factor of 1.2 would be used when the member self weight acts

in the opposite direction of the prestress moment, and the load factor of 0.8 would be used when the member self-weight acts in the same direction as the prestress moment. A conservative strength reduction factor, ϕ , of 0.7, was applied to the nominal axial capacity, P_n , and bending moment capacity, M_n .

These load factors and strength reduction factors were used in calculating the required strength of the cross-section by satisfying equilibrium and strain compatibility conditions. Assumptions common to the strength design method for reinforced concrete were made. The equations are listed below.

$$\text{Strain Compatibility Equations:} \quad \varepsilon'_s = [(c - d')/c] \cdot 0.003 \quad (4)$$

$$\varepsilon_s = [(d - c)/c] \cdot 0.003 \quad (5)$$

$$\text{Assume:} \quad f'_s = \varepsilon'_s E_{ps}; f_s = \varepsilon_s E_{ps}$$

$$\text{Equilibrium Equations:} \quad 0.85f'_{ci} b a + A'_s f'_s - A_s f_s = \frac{1.2 Pi}{\phi} \quad (6)$$

$$0.85f'_{ci} b a [a/2 - d'] - A_s f_s [d - d'] = \frac{0.8 Mg}{\phi} \quad (7)$$

In solving the equations of equilibrium and strain compatibility, one could specify the known properties of the cross-section (prestressing force, amount of top reinforcement, etc...) and calculate the desired unknown (required release strength, required top reinforcement, etc...).

In order to provide design engineers with an alternative to the $0.60f'_{ci}$ limit currently used, while still permitting the use of familiar allowable stress design procedures, the researchers attempted to derive a simple empirical formula for calculating the allowable stress at release (Equation 8).

$$(0.6 + y_b/5h) f'_{ci} \leq 0.75f'_{ci} \quad (8)$$

where:

y_b = distance from section centroid to extreme compressive fiber

h = overall depth of member

The authors developed this relationship analyzing various cross-sections included in the 1995 edition of PCI Design Handbook using the strength design method. It was found that the geometry of the cross-section was one of the most important parameters. Stress limits for the NU inverted tee section varied from $0.66f'_{ci}$ to $0.67f'_{ci}$, while values for the PCI double tee sections were the highest, ranging from $0.73f'_{ci}$ to $0.76f'_{ci}$. The proposed formula, which limits concrete compressive stresses at release to a maximum of $0.75f'_{ci}$, gives more conservative results, but is much less rigorous than the strength design method.

To support their analytical study, the authors prepared two test specimens. Both specimens were inverted tee beams with a span length of 32 feet. Note that this section shape allows only a slight increase in the allowable concrete release stress based on the formula presented earlier. Following release, one test specimen experienced a maximum concrete stress level at its ends of $0.84f'_{ci}$, and the other experienced a stress level of $0.79f'_{ci}$. Both of these values are significantly higher than that currently allowed or that calculated by the strength design method. However, no adverse behavior was observed for the prestress levels reported for each test. The camber and creep behavior of the specimens also followed closely the predicted behavior.

The conclusions and recommendations in the paper included:

- 1.) Eliminating the allowable compressive stress limit at transfer
- 2.) Using the alternative strength design approach to replace the allowable stress design.

- 3.) Using the empirical formula (equation 4) to replace the $0.60f'_{ci}$ value as a transitional measure.

The authors presented much theoretical data supporting the relationship between the strength design method and transitional empirical formula for determining allowable compressive stresses at release. However, the experimental data was limited to only two specimens. Although the specimens behaved well when subjected to the prestress forces, the method employed for determining the stresses at the ends of the members ($0.79f'_{ci}$ and $0.84f'_{ci}$) is unclear. Because prestress losses can vary substantially from those based on nominal calculations, it is difficult to accurately report prestress forces applied to the beams at transfer without some type of instrumentation on the prestressing strand.

2.4 SUMMARY

Since the introduction to allowable stress design in the early 20th century, allowable stresses have become a thing of the past for plain and reinforced concrete design. Prestressed concrete design, however, is still governed by allowable stresses established in the mid 1900's. For some time, these limits have worked well, but recently, researchers and professional societies have become interested in reevaluating the limits for prestressed members at transfer.

During the early years of prestressed concrete use, concrete properties were much less reliable and there was little prior experience with prestressed concrete behavior. Therefore, it is reasonable that the limits for allowable stresses were conservative. However, because concrete properties are now more reliable and because years of experience with prestressed members have yielded safe results, a reevaluation of the allowable limits needs to be conducted.

Most of the recent research reports included in this literature review include a recommendation for increasing the allowable compressive stress limit for concrete at the extreme compressive fiber. In a proposed PCI Committee Report in 1996, the PCI Technical Activities Council and the PCI Committee on Building Code indicates that no problems have been reported by allowing compression stresses at release to go as high as $0.75f'_{ci}$ in order to avoid debonding or harping of strands. It was brought to the author's attention that in some prestressing plants it is common to allow compressive stresses in double-tee sections to go as high as $0.70f'_{ci}$ to $0.75f'_{ci}$.

According to contemporary research, allowable compressive stress limits for prestressed concrete members at transfer should be increased. However, there has not been significant experimental research to support the theories presented in this chapter by a number of researchers. This thesis will present the initial stages of an experimental investigation to study the effects of subjecting prestressed members at transfer to stresses higher than that allowed in current codes.

CHAPTER 3

Overview of Experimental Program

3.1 INTRODUCTION

This chapter discusses preliminary design of test specimens, design and construction of the prestressing facility, material testing, and instrumentation used to monitor specimens. The experimental program planned to date involves a series of scaled pretensioned girders fabricated and tested at Ferguson Structural Engineering Laboratory at The University of Texas at Austin. This thesis reports only preliminary results from the first series of beams fabricated at Ferguson Laboratory.

3.2 BACKGROUND

This section discusses basic principles used in the design of test specimens. Included is the current design method for pretensioned members and a discussion of factors that potentially affect the time-dependent properties of concrete, such as creep and camber.

3.2.1 Allowable Stress Design

The allowable stress design method, currently used by designers of pretensioned flexural members, utilizes linear analysis of concrete cross-sections (ACI 318-99). Stresses calculated at the extreme fibers are based on the assumptions that plane sections remain plane, and the stress-strain relationship for concrete is linear. Given the prestress force, eccentricity of the prestress force, and cross-sectional properties, one can easily calculate the extreme fiber stresses for a prestressed member. In comparison with a common nonlinear stress-strain

relationship, such as the Hognestad model, this method is fairly accurate for calculating compressive fiber stresses up to the current allowable limit of $0.60f'_{ci}$ (Tadros, 1997). It is important to note that this may not be an accurate method for calculating extreme concrete fiber stresses when stresses computed using these assumptions exceed $0.60f'_{ci}$, but it may be conservative and is the method implemented in the design of specimens discussed in this thesis.

The allowable stress design equations (Equations 3.1 and 3.2) below illustrate the relationship between concrete strength at release and the prestressed force at transfer for cross-sections near the ends of simply supported members.

$$\frac{F_o}{A_g} + \frac{F_o \cdot e \cdot y_b}{I_g} \leq 0.60f'_{ci} \text{ (at bottom extreme fiber)} \quad (3.1)$$

$$-\frac{F_o}{A_g} + \frac{F_o \cdot e \cdot y_t}{I_g} \leq 6 \sqrt{f'_{ci}} \text{ (at top extreme fiber w/ no top reinf.)} \quad (3.2)$$

To facilitate the discussion that follows, the ratio of the extreme compressive fiber stress due to the applied prestress to concrete compressive strength at release will be referred to as the Applied Stress Ratio (ASR).

In some cases, design of pretensioned beams is governed by the allowable compressive stress equation. The required concrete compressive strength at release (f'_{ci}) is calculated based on the maximum allowable applied stress ratio (ASR) which is currently 0.60. Using the calculated value for f'_{ci} , the top fiber stress is then checked to be sure it is less than allowable tensile stress limit which is currently $6 \sqrt{f'_{ci}}$. Prestressed members must also meet strength requirements as well, but these do not commonly control the design.

A better representation of how the minimum concrete compressive strength at release is calculated based on an allowable compressive stress is illustrated by Equation 3.3.

$$f'_{ci(min)} = \frac{\frac{F_o}{A_g} + \frac{F_o \cdot e \cdot y_b}{I_g}}{\text{ASR}} \quad (3.3)$$

Note that the release strength is inversely proportional to the ASR. Thus, by increasing the allowable ASR, the concrete strength requirement at release can be reduced and release can occur earlier.

Because the allowable stress in compression commonly governs the design of pretensioned members, and the limit is strictly empirical, the experimental program will focus primarily on designing members with a maximum compressive fiber stress equal to or exceeding the allowable limit. Tensile stresses will be targeted above the allowable limit as well, but will not govern the designs. As a result, the tensile stress in some specimens may not exceed the allowable limit.

3.2.2 Factors Affecting Prestressed Concrete Behavior

Although increases in allowable stresses at release would be favorable for precasters, subjecting members to stresses higher than the current limits may have adverse effects on the behavior of pretensioned girders at transfer or while in service. Anticipated signs of distress in the beams may include microcracking in the concrete, increased creep deformations, and related increases in camber. In an extreme case, a prestressed girder may experience excessive creep, resulting in a catastrophic failure.

Creep and camber behavior of concrete beams is primarily governed by the modulus of elasticity of the concrete, which depends greatly on the concrete mix made with local materials (Tadros, 1997). A change in the type of aggregate (hard rock vs. soft rock) will likely change the properties of the hardened concrete. A soft-rock aggregate may decrease the modulus of elasticity of concrete while a hard-rock aggregate may increase the modulus of elasticity.

Another factor affecting the behavior of pretensioned concrete beams is the location of the prestress force in relation to the centroid of the section, and the resulting stress gradient on the cross-section. If the stress gradient is relatively high (Fig. 3.1 (a)), and the stresses at the bottom and top exceed the current allowable limits, the creep and camber behavior may be much different than a case in which the stress gradient is relatively low (Fig. 3.1 (b)).

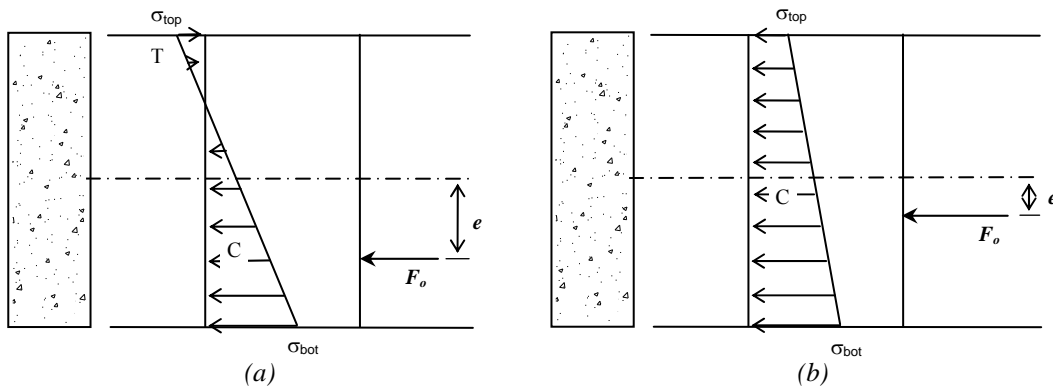


Figure 3.1 (a) and (b) Stress Gradients for Various force eccentricities

One could argue that the former case would be more critical because the section may experience cracking at the top fiber, resulting in excessive camber. However, the compressive stress at the bottom fiber decreases quickly over a small distance and may be within the allowable limit a short distance from the

extreme fiber. It is the author's understanding that typical double-tee sections, which tend to be designed with a stress gradient similar to Figure 3.1 (a), are commonly allowed to experience stresses as high as $0.75f'_{ci}$ at transfer. In the latter case, one could argue that the camber behavior would not be excessive, but due to the high, sustained compressive stresses, the member may experience a crushing failure. Both of these cases are critical and represent typical design scenarios for pretensioned members.

The rate of strength gain at the time of release may also significantly affect the time-dependent behavior of prestressed members. Precasters commonly desire to release the strands well within 24 hours of casting, when the concrete strength could be as low as 60 percent of its 28-day compressive strength. Because the modulus of elasticity of concrete is a function of compressive strength, the effective modulus of elasticity some time after prestress release will be higher than that estimated at transfer. If the ratio of f'_{ci} to f'_c at release is relatively low (i.e. 60 percent) and the rate of strength gain is high, the modulus of elasticity of the concrete will increase substantially after release in a short period of time. Thus, time-dependent camber estimations based on the modulus of elasticity of the concrete at prestress release should be slightly higher (conservative) than that observed in real precast elements. If the ratio of f'_{ci} to f'_c is relatively high and the rate of strength gain is low, the modulus of elasticity of the concrete will not change significantly, and camber can be estimated more accurately using the concrete compressive strength at prestress release. Therefore, a precast element subjected to a prestress force producing an extreme fiber stress of $0.70f'_{ci}$ when the concrete is experiencing a high rate of strength gain should behave more favorably than an element subjected to the same stresses when experiencing a lower rate of strength gain.

In an attempt to justify increasing the allowable compressive stress limit of $0.60f'_{ci}$, Tadros argued that the fiber stress allowed on a cross section is mostly affected by its size and shape (Tadros, 2001). Tadros conducted a parametric study of his proposed design technique, and determined that for standard inverted tee sections, rectangular, and double tee sections, the allowable limits should be $0.66f'_{ci}$ to $0.67f'_{ci}$, $0.69f'_{ci}$ to $0.70f'_{ci}$, and $0.73f'_{ci}$ to $0.76f'_{ci}$, respectively. This indicates that as the geometric property for a flexural member, y_b (distance to extreme compressive fiber), increases, the allowable stress should increase, respectively.

3.2.3 Summary

All factors discussed in this section that might affect the behavior of pretensioned beams after release were considered for this research project. The variables planned to be examined during the course of this research project include:

- 1.) Concrete compressive strength at release,
- 2.) Stress gradient on the cross-section,
- 3.) Cross-sectional shape, and
- 4.) Type of coarse aggregate (hard or soft) in the concrete mix.

The only variable considered in the preliminary results presented in this thesis is the concrete compressive strength at release.

3.3 SCOPE OF RESEARCH PROGRAM

The experimental program is intended to investigate the effects of applying flexural stresses at release that are higher than the allowable limits. A series of reduced-scale test specimens will be fabricated at Ferguson Structural Engineering Laboratory to investigate the behavior of beams subjected to various

release stresses and stress gradients. The series of beams is intended to include cross-sections fairly representative of standard cross-sections used by industry, the use of high early-strength cement (commonly Type III cement), and the use of concrete mixes that are similar to standard mixes used at prestressing plants. The research program will investigate the effects of subjecting pretensioned beams to extreme fiber stresses higher than currently allowed for both tension and compression at prestress transfer. The design of some test specimens will target a condition that exceeds both allowable limits within the same beam. This will represent beams with high prestress force eccentricity, and a high strain gradient. Other specimens will be designed for different target stresses at the top and bottom extreme fibers, thus producing a lower stress gradient.

Prior to casting test specimens, researchers constructed a prestressing facility to accommodate the proposed series of beams. The facility was designed to safely pretension the desired number of strands without exceeding the capacity of the restraining elements (i.e. the structural floor, buttresses, bulkhead, compression members, etc...). Details of the design and installation of this facility are included in Section 3.4.

Once constructed, The prestressing facility should accommodate three lines of specimens. For every concrete casting operation, each line of specimens will be fabricated with the same batch of concrete and will be identical in cross-section, prestress force, and eccentricity of the prestress force. Release strength for each line of specimens will be controlled. This will effectively subject each beam to a maximum applied stress equal to a desired percentage of the compressive strength at release. For the preliminary series of specimens described here, the nominal maximum compressive stresses at release were targeted to be $0.60f'_{ci}$, $0.65f'_{ci}$, and $0.75f'_{ci}$ for the three lines of specimens, respectively. The required concrete compressive strength at release can be easily calculated using Equation 3.3.

Target extreme fiber stresses for each line of beams for future concrete castings will be reevaluated based on results from the preliminary specimens.

It is intended that researchers may fabricate beams with different cross-sections including rectangular, tee, and inverted tee shapes when the experimental program is complete. These shapes were chosen to represent the geometry of cross-sections commonly used in industry, such as I-beams, double tees, and U-beams.

In later series, researchers will investigate the effects of using soft rock versus hard rock aggregates. It is likely that the hardness of the aggregate will affect the modulus of elasticity of the concrete.

This thesis reports the results from the first six specimens cast in Ferguson Laboratory. All six beams were rectangular in cross-section, and spanned 15 feet. Two beam specimens occupied each bay of the prestressing facility. At release of each line of specimens, both beam specimens were nominally subjected to an identical prestress force and eccentricity. Each line of specimens was prestressed with six straight tendons, each stressed to approximately $0.75f_{pu}$ before release. Details of these specimens will be presented in Section 3.4.

The overall behavior of the specimens was monitored by strain gauges attached to the prestressing strand, DEMEC points installed on the sides of the beam, and linear potentiometers located at midspan. Details about the instrumentation will be presented in Section 3.7. Strength data from 6 x 12-inch concrete cylinders was obtained periodically to estimate the strength of the concrete beams for timing the release of the strands. *Sure Cure* cylinders were also tested to more accurately estimate the concrete compressive strength in the beams by accounting for the elevated curing temperature of the beams. An explanation of the *Sure Cure* equipment and its function are included in Section 3.8.

3.4 DESIGN OF BEAM SPECIMENS

As discussed in Section 3.3, the small-scale beams designed for fabrication in Ferguson Laboratory were intended to represent standard cross-sectional shapes used in industry. With this in mind, researchers decided to begin the experimental program with a series of rectangular beams. Because the web of flexural members contributes little to its flexural capacity, a rectangular cross-section behaves similarly to an I-beam with a flange thickness equal to the width of the rectangular section (Fig. 3.2).

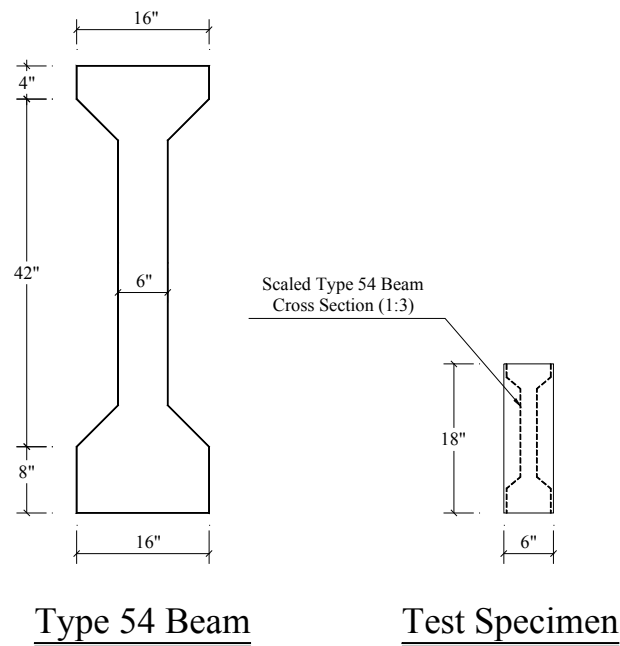


Figure 3.2 Typical AASHTO Type-54 Cross-Section (left); Scaled (1:3) Type-54 Section and Representative Rectangular Section (right)

Dimensions for the first series of beams are shown in Figure 3.3. The cross-section dimensions are fairly representative of a scaled AAHSTO Type-54 girder (Fig. 3.2), but the size was primarily chosen based on the prestress force and eccentricity that could be supplied with the prestressing facility. A deep and narrow section allows for higher stresses to develop at the extreme fibers with a limited amount of prestressing. For the first series of test specimens, it will serve as the shape used to examine higher allowable fiber stresses at release as well as the effect of a high stress gradient versus a relatively low stress gradient on the behavior of prestressed concrete beams. The length chosen allowed for two specimens to be cast within the same bay of the prestressing facility, thus, producing two specimens with identical prestress force and eccentricity.

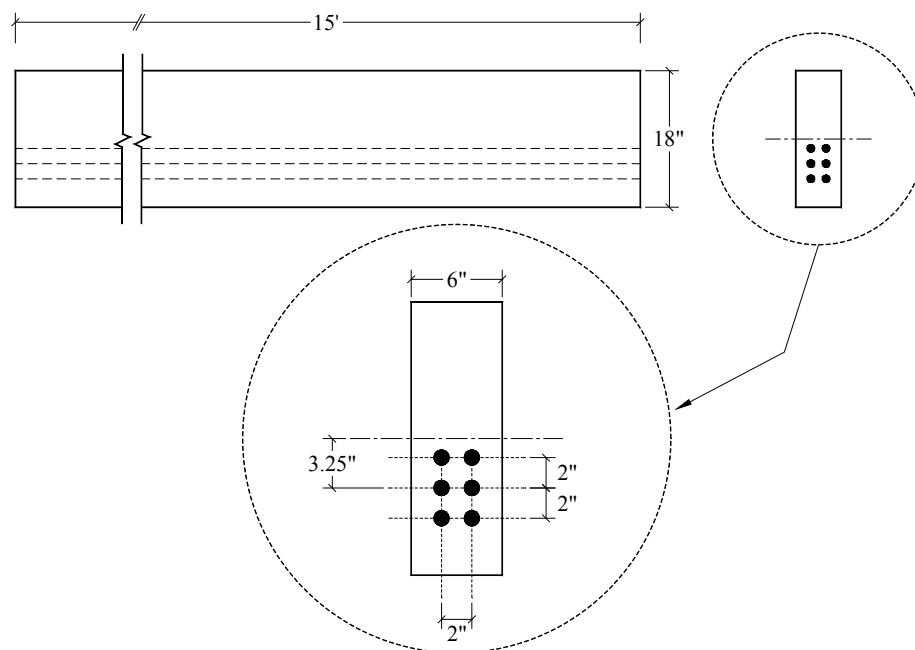


Figure 3.3 Test Specimen Cross-Section and Length for First Cast

The first cast of beams was designed for a prestress force of 171 kips with an eccentricity of 3.25 inches. Depending on the release strength, this produced a bottom extreme fiber stress, σ_{bot} , between $0.60f'_{ci}$ and $0.75f'_{ci}$ (Table 3.1). The resulting top fiber stress, σ_{top} , was calculated to be 132 psi in tension. Note that this does not exceed the allowable limit of $6\sqrt{f'_{ci}}$ (390 psi for the lowest release strength). It was impossible to exceed the allowable stress in tension for these specimens due to the position of the strands, while targeting the extreme compression fiber stress. The release strengths calculated in Tables 3.1 and 3.2 are based on gross section properties (I_g , and A_g). This is an approximate method of calculating stresses, but it is the most common method used by designers. A more rigorous approach using the transformed section properties and a comparison with the approximate method is included in Section 5.3. The release strengths calculated with gross section properties in Table 3.1 were targeted with the test specimens fabricated in Ferguson Laboratory.

For the next beam cast, the specimens will be subjected to a prestress force of 285 kips with an eccentricity of 1.1 inches. This orientation of the prestressing strands will produce a relatively low stress gradient in the cross-section with the bottom fiber stress varying from $0.60f'_{ci}$ to $0.75f'_{ci}$ and the respective top fiber stress varying from $0.28f'_{ci}$ to $0.35f'_{ci}$ in compression.

3.5 PRESTRESSING FACILITY

3.5.1 General

The prestressing facility used for this research project was constructed from many of the same elements used in Bruce Russell's research at the University of Texas at Austin in 1992 (Russell, 1992). The facility accommodates up to three bays of specimens, separated by four buttresses on each end. For Russell's research, it was never required to tension more than a

Table 3.1 Details for Preliminary Series of Beams

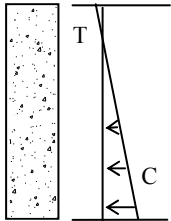
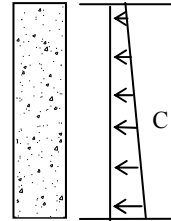
Stress Gradient	Specimen Designation	Target σ_{bot}	F_o (kips)	e (in)	σ_{bot} (psi)	σ_{top} (psi)	Required Release strength, f'_{ci} (psi)
	RS-75N	$0.75f'_{ci}$	171	3.25	-3300	132	4400
	RS-75S	$0.75f'_{ci}$	171	3.25	-3300	132	4400
	RS-70N	$0.70f'_{ci}$	171	3.25	-3300	132	4710
	RS-70S	$0.70f'_{ci}$	171	3.25	-3300	132	4710
	RS-60N	$0.60f'_{ci}$	171	3.25	-3300	132	5500
	RS-60S	$0.60f'_{ci}$	171	3.25	-3300	132	5500

Table 3.2 Details for Following Series of Beams

Stress Gradient	Specimen Designation	Target σ_{bot}	F_o (kips)	e (in)	σ_{bot} (psi)	σ_{top} (psi)	Required Release strength, f'_{ci} (psi)
	RF-75N	$0.75f'_{ci}$	285	1.1	-3606	1670	4810
	RF-75S	$0.75f'_{ci}$	285	1.1	-3606	1670	4810
	RF-70N	$0.70f'_{ci}$	285	1.1	-3606	1670	5150
	RF-70S	$0.70f'_{ci}$	285	1.1	-3606	1670	5150
	RF-60N	$0.60f'_{ci}$	285	1.1	-3606	1670	6010
	RF-60S	$0.60f'_{ci}$	285	1.1	-3606	1670	6010

total of 16 strands (8 strands in opposite bays), which is a demand far less than that estimated for the current research program. Therefore, the prestressing facility was redesigned for the anticipated loads required for the current test specimens. This section discusses the process of re-design and construction of the prestressing facility.

3.5.2 Reaction Frame

The steel members of the prestressing facility create a structure similar to a reaction frame. The original frame used by Russell consisted of steel bulkheads and buttresses, which were tied down to the floor with threaded rods. The modified frame used for the current research consists of the same elements, along with additional stiffeners welded on the buttresses, and compression members added between the buttresses (see Fig 3.4). A description of these elements and the analysis of the reaction frame are included in the following sections.



Figure 3.4 Photo of Modified Reaction Frame

3.5.2.1 Description of Elements

3.5.2.1.1 Buttresses

The buttresses consist of standard steel wide flange shapes welded together to form a structure similar to half of an A-Frame. Attached to the bottom are 1-inch base plates used to bolt the buttresses to the structural floor. After careful redesign and analysis, additional stiffeners were welded near the point of concentrated load from the added compression columns (horizontal elements in Fig. 3.4).



Figure 3.5 Photo of Modified Buttresses

3.5.2.1.2 Bulkheads

Connected outside of the buttresses on each end of the facility were steel bulkheads (Fig. 3.6) that distributed the force from the prestressing strands to the buttresses. The bulkheads were made up of an overly stiffened steel plate girder, 35.5-inch deep, modified with 0.75-inch plate backing for bearing against the buttresses, and 0.75-inch and 1-inch thick layered bearing plates at mid-depth on the opposite side for anchoring tendons. As shown in Figure 3.7, these elements have holes drilled at a 2-inch spacing for 0.5-inch strand, and are designed for prestressing a maximum of three bays. Holes were also drilled for 0.6-inch strands with slightly larger spacing during Russell's research, explaining the additional holes in the bearing plate.



Figure 3.6 Steel Bulkheads for Strand Anchors

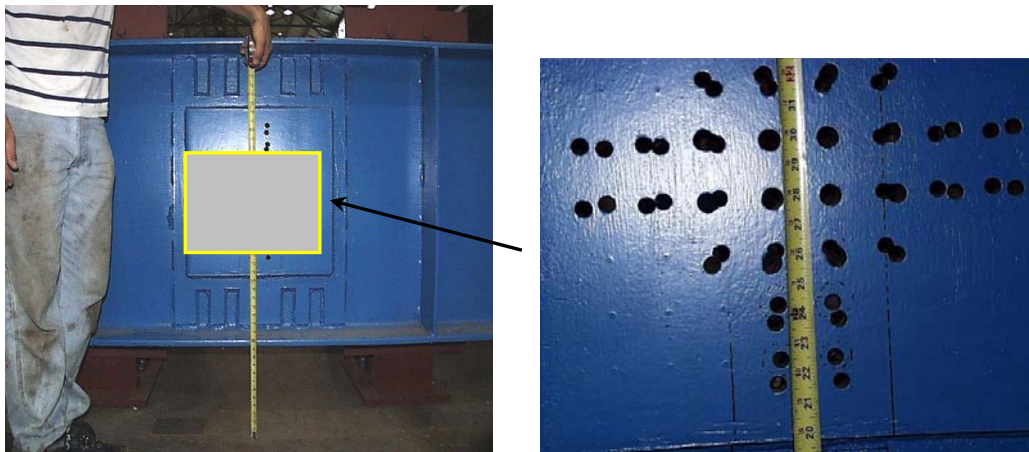


Figure 3.7 Hole Spacing in Steel Bulkheads

3.5.2.1.3 Columns

The columns chosen in the re-design of the prestressing facility are shown in Figure 3.8. The cross-section was specified as a 12-inch steel structural tube with a wall thickness of 0.5-inch. The span length for the members was 35 feet. Once received, the columns were painted, then hoisted into place using the crane in Ferguson Laboratory, and set on blocks. 1.5-inch thick end plates were then welded into place.

3.5.2.1.4 Connections

Most connections involved in this reaction frame were highly over-designed, and the shapes and sizes chosen for connection elements were most commonly due to clearance limitations and available steel in Ferguson Laboratory. The only load carried any connection, excluding the floor tie-down connection, was the dead weight of the connected members.

In connecting the bulkheads to the buttresses, steel angles were bolted to a 0.75-inch plate extending outside the width of the buttresses to align the angles with the pre-drilled holes in the bulkheads (Fig. 3.9). It was important that the

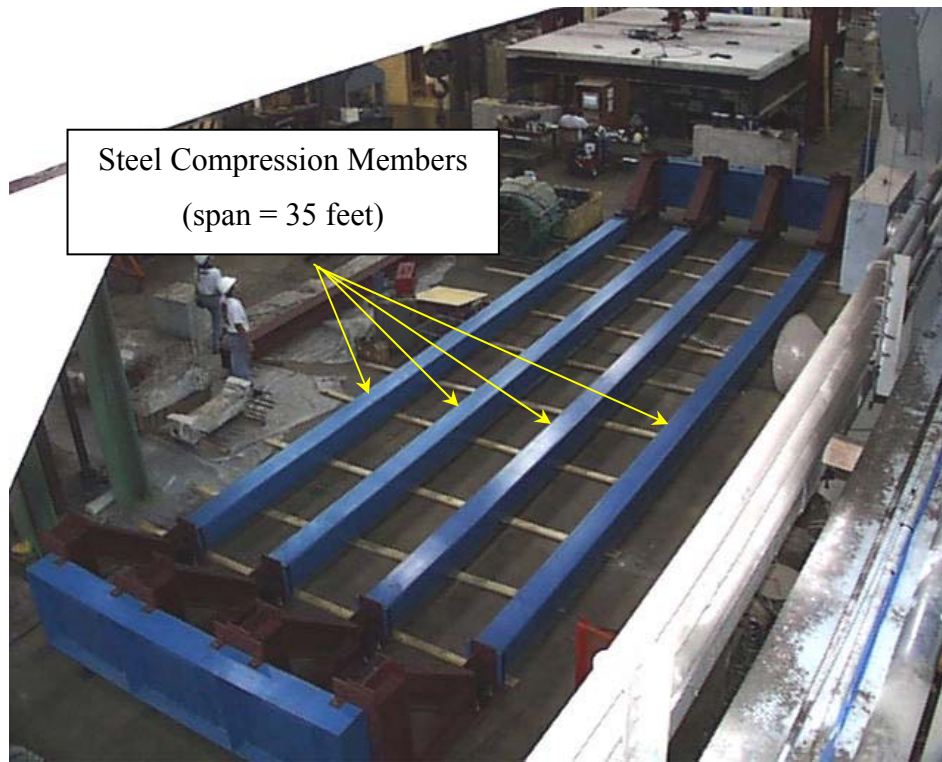


Figure 3.8 12” Structural Steel Tube Compression Members

plates be installed on the buttresses above the top and below the bottom of the bulkheads to create the maximum amount of bearing area on the buttresses. The 0.75-inch plate was connected to the buttresses with 0.75-inch diameter bolts, and the angles were connected to the 0.75-inch plate and bulkheads by 0.375-inch diameter bolts. A sketch of this connection detail is shown in Figure 3.10.

Note, as shown in the detail in Figure 3.10, the bulkhead weight is transferred directly to the angle in the bottom connection, but is carried by the bolt and then transferred to the angle in the top connection. In either case, the connection was not in danger of experiencing overloads due to the dead weight of the bulkhead.



Figure 3.9 Buttress/Bulkhead Connections

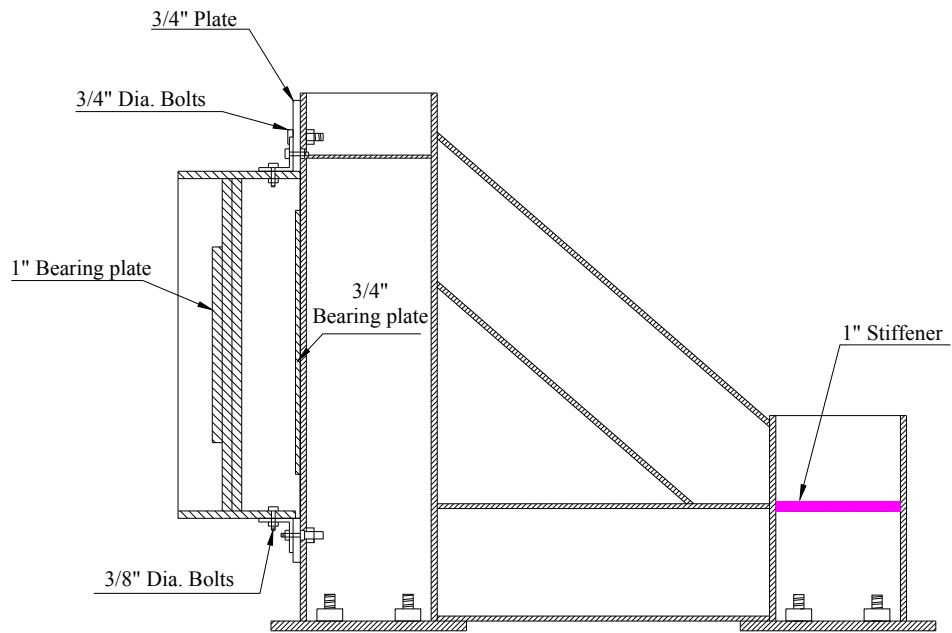


Figure 3.10 Buttress/Bulkhead Connection Detail

In the column/buttress connection, the end plates of the column rest on a steel angle that is bolted to the buttress with 0.375-inch bolts (Fig 3.11). There was no bolted connection between the end plates and the steel angle. Thus, the columns are essentially simply supported by the steel angles before prestressing occurs.



Figure 3.11 Column/Buttress Connection

The tie-down connection to the floor was the only significant load-bearing connection. The buttresses were attached to the structural floor by fully threaded, 1-inch diameter high-strength steel rods. Fortunately, the buttresses had been previously tied down to the structural floor, and the anchors in the floor aligned perfectly with the drilled holes in the base plates of the buttresses. Once the buttresses, bulkheads, and columns were all in place, the buttresses were tied down to the floor by post-tensioning the steel rods to the specified capacity of the floor (120 kips), and tightening the nuts to lock in the tension (Fig 3.12). This tie-down procedure was followed to minimize uplift of the buttresses once loads from the prestress force were applied.

3.5.2.2 Redesign of Original Frame

3.5.2.2.1 Addition of compression columns

The limitation found in the original test setup used by Russell was the inability of the buttresses to resist the anticipated prestressing loads by friction alone. As illustrated in Figure 3.13, the steel threaded rods used to tie down the



Figure 3.12 Post-Tensioning of Tie-Down Rods

buttresses would bear against the edge of the holes in the floor once friction was overcome and the buttresses slid inward. This would likely result in local crushing of concrete in the structural floor. Multiple ideas were entertained in an attempt to alleviate potential sliding of the buttresses including:

- 1.) Grouting buttresses to the floor in addition to post-tensioning steel tie-down rods, and
- 2.) Adding spacers between buttresses to resist the compressive loads due to prestressing.

The researchers decided to add the compression columns on the basis that it would produce a safe environment and the most predictable behavior of the reaction frame. It would also allow more varied use of the facility in the future, when higher prestress forces may be desired.

The compression member design was governed by the most critical demand (30 fully-tensioned 0.5-inch diameter strands) predicted for the facility. This demand was multiplied by a factor of 1.5 to account for possible future use with higher prestressing forces. Once the loads were calculated, researchers proceeded to follow LRFD guidelines for the design of compression members, considering the boundary conditions and member orientation (AISC, 1998). The compression member chosen was a 12-inch steel structural tube with a wall thickness of 0.5-inch.

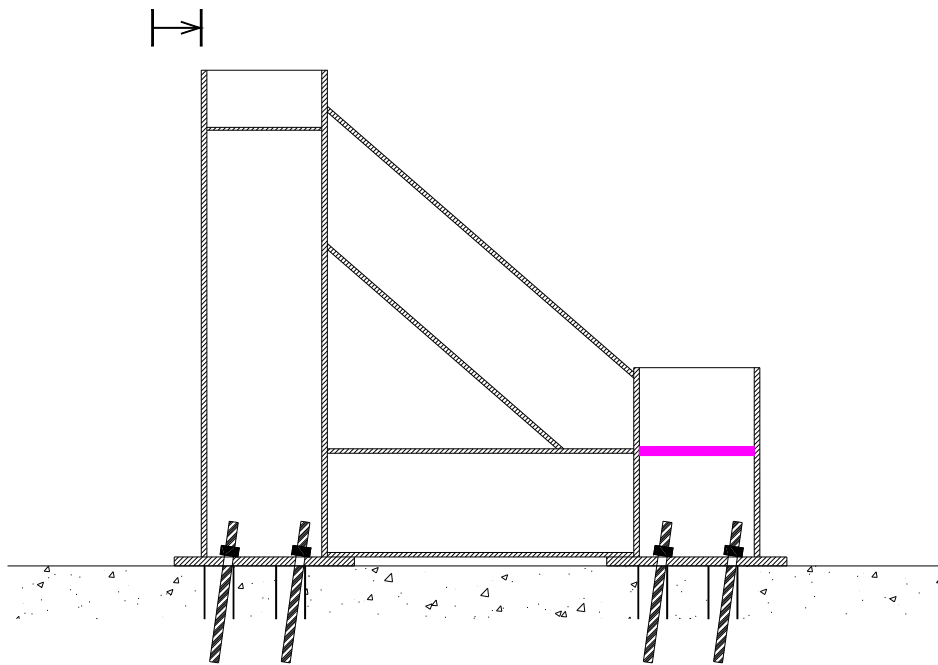


Figure 3.13 Sketch of Buttresses Sliding Under Prestressing Loads

3.5.2.2.2 Modification of Buttresses

By adding the compression members to the test setup, a concentrated load was created at the points of contact between the columns and the vertical W14x61 section of the buttresses. A section analysis proved the web of the W14x61 inadequate, and researchers proceeded to design stiffeners for the buttresses at the location of the concentrated load. One-inch thick stiffeners were found to be adequate for the anticipated loads and higher loads for possible future use.

Another limitation found in the original setup dealt with the location of the bulkhead when attached to the buttresses. Theoretically, when prestressing forces were applied to the buttresses at the original height of the bulkhead, the uplift forces exceeded the capacity of the structural floor. To lessen the uplift forces, additional holes were punched in the buttresses, and the bulkheads were lowered. This modification is shown in Figure 3.14.

Note, with this modification alone, the uplift forces still exceeded the capacity of the floor. The compression members were critical in decreasing the uplift forces applied to the buttresses.

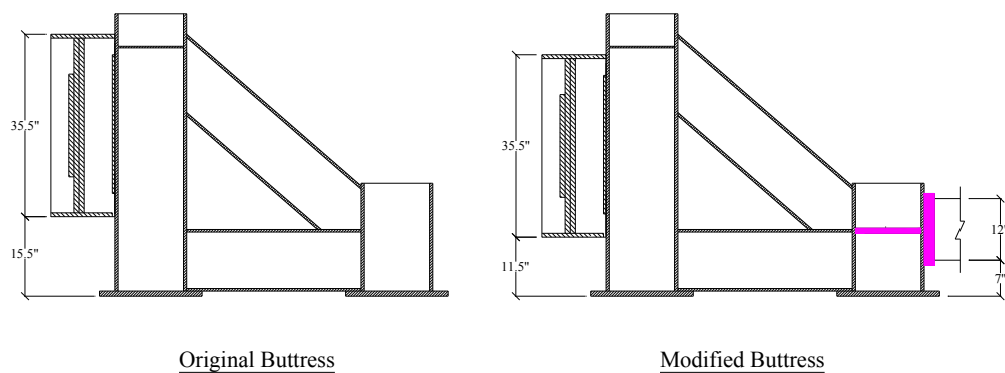


Figure 3.14 Sketch of Modifications Made to Original Buttresses

3.5.2.3 Analysis of Modified Frame

Most of the analysis of the modified reaction frame was performed locally for the design of stiffeners and compression members, and when making other modifications to the setup. However, a 2-D analysis was also conducted for the completed reaction frame subjected to the maximum loads anticipated during the experimental program.

At each tie-down location for the buttresses, the floor capacity was 120 kips for uplift forces. As shown in the free-body diagram for the original test setup (Figure 3.15) and Table 3.3, the uplift force resulting from the prestressing force of 240 kips, exceeds the floor capacity. In order to reduce the overturning moment and uplift forces, the bulkhead was lowered. The added compression members also significantly reduced the overturning moment by providing an additional reaction force just 13 inches below the prestress force. Reaction forces for the modified test setup are shown in Figure 3.16 and Table 3.4. Once the compression members were added, no friction force was required to resist the applied prestress force.

The analysis demonstrated that when a greater portion of the reaction force is carried by the compression members, the uplift forces are reduced. In addition, as more reaction force is carried by friction between the buttresses and the floor, the compression members carry less force, causing higher uplift forces. So, to reduce the frictional force, the tie-down rods on the inside of the buttresses were not post-tensioned. The frictional force would be reduced more if the outside tie-down rods were not post-tensioned, but the uplift of the buttresses was more of a concern than the small amount of additional friction force contributed by the post-tensioning.

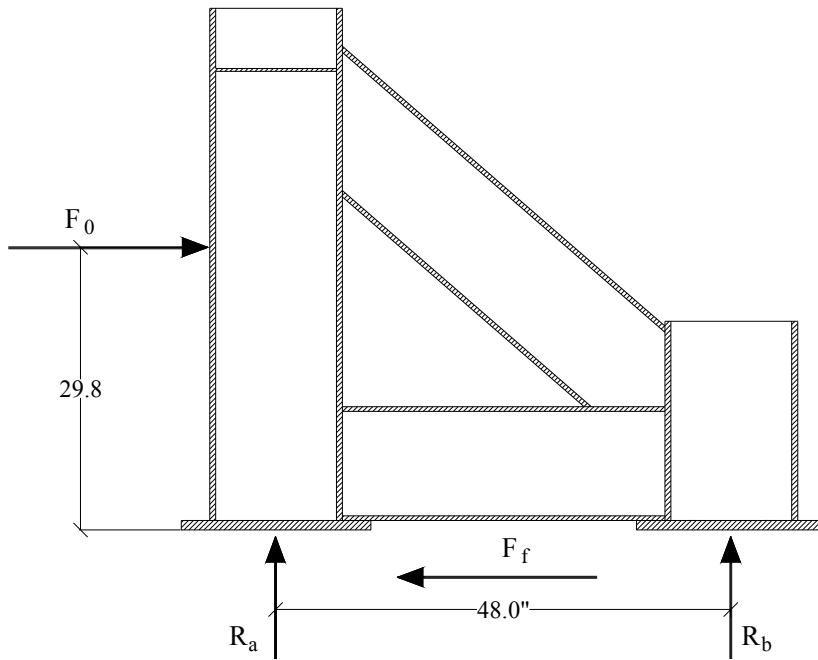


Figure 3.15 Free-Body-Diagram of Original Buttresses Subjected to Prestressing Forces

Table 3.3

	F_o	Height	R_a	R_b	F_f
Required Forces	240 kip	29.8 in.	-150 kip	150 kip	240 kip
Capacity	-	-	120 kip (T)	-	60 kip
Comment			Capacity Exceeded		Capacity Exceeded

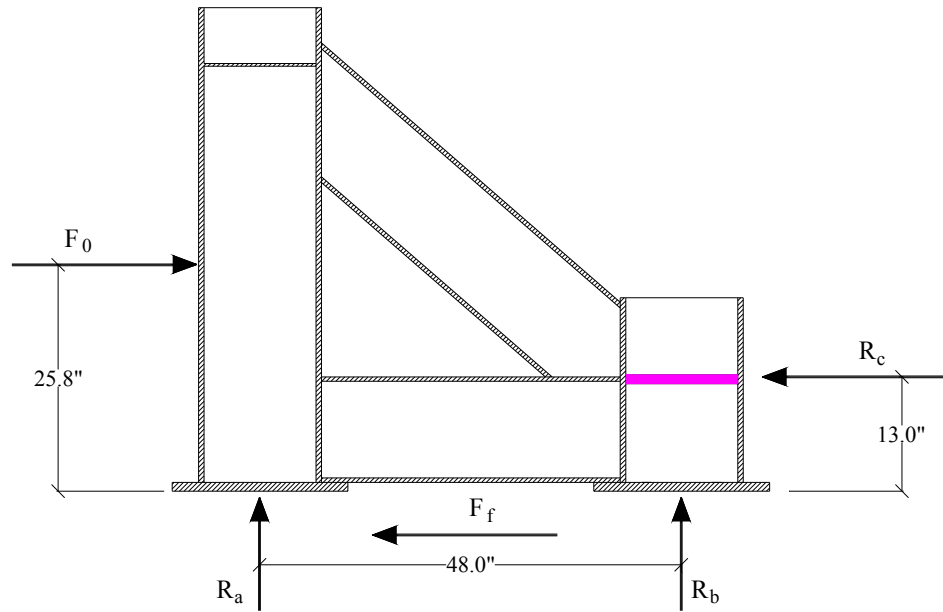


Figure 3.15 Free-Body-Diagram of Modified Buttrresses Subjected to Prestressing Forces

Table 3.4

	F_o	Height	R_a	R_b	F_f	R_c
Required Forces	240 kip	25.8 in.	-72 kip	72 kip	29 kip	211 kip
Capacity	-	-	120 kip (T)	-	-	> 450 kip
Comment			Capacity Adequate			Capacity Adequate

The possibility of local yielding or failures was theoretically alleviated with the added modifications to the structure. Considering these modifications, a linear analysis was conducted for the complete structure using a program package called Visual Analysis (IES, 1998). The results showed that no members were overstressed, and member deformations and deflections were well within acceptable levels.

3.5.3 Platform

After the reaction frame was completed, construction of a wooden platform to support test specimens began. The platform consisted of a timber frame, made of 2 x 4-inch flexural members and 4 x 4-inch columns, and topped with a 0.75-inch plywood deck. The frame was braced laterally in the N-S direction with 2 x 4-inch members, and braced in the E-W direction by the plywood deck's snug fit between the steel compression members. This platform was largely overdesigned to permit very small deflections under dead load of the test specimens. The frame before and after applying the decking is shown in Figures 3.16 and 3.17.

With the bulkheads bolted to the buttresses, the elevation of the prestressing strands was fixed. The platform height, therefore, must be varied to achieve the desired eccentricity of the prestressing strand for test specimens. The platform was originally built at the height required to achieve an eccentricity of 3.25 inches for the first set of specimens. For future casts, the platform height will need to be adjusted according to the desired prestress eccentricity for the specimens.



Figure 3.16 Platform Framing



Figure 3.17 Lateral Bracing in N-S Direction (left); Plywood Decking (right)

3.6 MATERIAL PROPERTIES

3.6.1 Steel Strand Tension Tests

The tension tests conducted on Grade 270 0.5-inch diameter prestressing strands were pertinent for this research project. Despite conflicting reviews on the durability and accuracy of strain gauges installed on prestressing strand (Russell, 1992), researchers desired to accurately estimate the prestress force applied to each test specimen, both at transfer and after release, through the utilization of strain gauges. Accurate estimates of prestress force are crucial for determining the extreme fiber stresses applied to each beam. Current methods of estimating prestress losses due to steel relaxation, wedge seating, and elastic shortening may be acceptable for design, but are unacceptable for a laboratory investigation.

Six tests were conducted on strands instrumented with strain gauges. ASTM procedure A370 was followed in four of the tension tests. Two tests were conducted using the same anchoring system used during the prestressing process prior to casting. Results from strand tension tests for strands having different surface conditions and end-gripping conditions are discussed in the following sections.

It is important to note the results presented in this section are strains measured on individual wires that are oriented at a small angle relative to the axis of the strand. The plots should be considered as calibration curves rather than accurate stress-strain behavior for the prestressing strands. The stress in the strand was calculated based on the measured force from a load cell in the testing machine divided by the nominal cross-sectional area of 0.153 in². To calculate the axial strains in a strand, a correction factor should be applied to measured strains to account for the approximate 9° pitch of the prestressing wire. For the

purposes of this research, only a calibration curve was needed to relate strand force to measured strains up to approximately $0.80f_{pu}$. This calibration curve is shown in Section 3.6.1.4. The full stress-strain behavior of the prestressing strand was not needed for the scope of this research project.

3.6.1.1 Strand Results Using V-Grips (ASTM A370, A7.3.2)

3.6.1.1.1 Ground surface (See Figures F1 and F2)

In the first two tension tests conducted, all six exposed wires were instrumented, and the strand surface was ground slightly to secure the strain gauges to a flat surface (Fig. 3.18). Gluing the strain gauge to a flat surface was first thought to be the most effective way to assure its durability and increase the life of the gauge.

The strain readings from each of the gauges on separate wires gave fairly consistent results (Appendix F). The stress in the strand could be computed based on the strain readings with an accuracy of $\pm 2.25\%$. However, the process of grinding the wire surface resulted in reduced strand area and failure at the ground strand locations. The variance in the readings was most likely due to inconsistent grinding techniques from wire to wire. The ground surface on one wire could be deeper or wider than others, thus, creating higher reduction in strand area. It is important to note that most strain gauges failed prior to strand failure and prior to reaching the nominal capacity during these tests.

3.6.1.1.2 Smooth vs. Ground surface (See Figures 3.29 and F3)

One tension test was conducted with strain gauges attached to both grinded and smooth surfaces on the same wire to investigate the effect that grinding has on the strain readings and the durability of the gauge. Results from this test are shown in Figure 3.20.



(a)



(b)

Figure 3.18 Ground Wire Instrumented with Strain Gauge (a); V-Grips Used to Grip Strands (b)

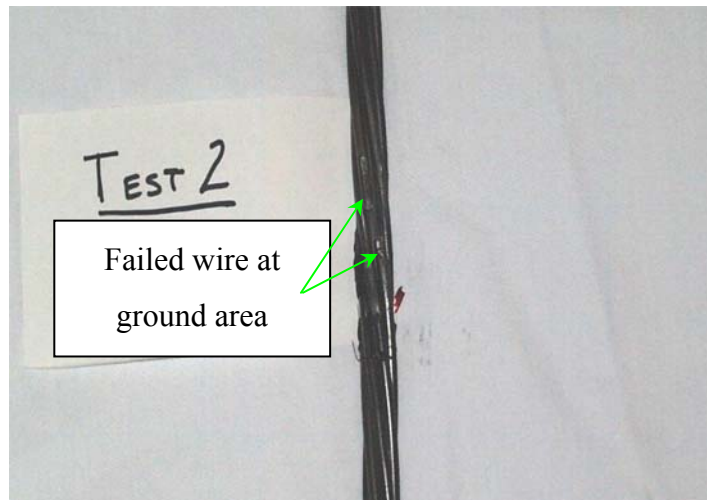


Figure 3.19 Photo of Failed Strand with Ground Wires

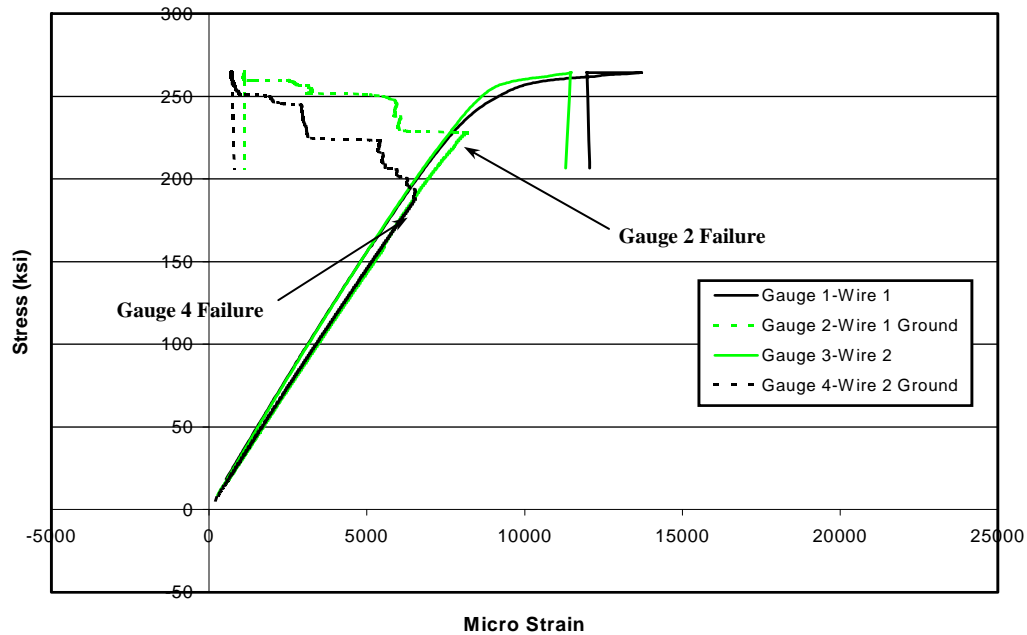


Figure 3.20 Stress-Strain Plot for Ground vs. Smooth Wires

Note the higher strain readings on the ground surfaces versus the smooth surfaces of the wire for the same load level. The readings from the ground wire averaged 7.5% higher for stress levels above 150 ksi. The gauges installed on smooth wires also survived until failure of the strand, while both gauges on the ground wires failed before reaching a stress of 240 ksi in the strand.

From this test, it is observed that when gauges are installed on smooth wires, they provide more accurate results, and are much more durable than when installed on ground wires. Also, by grinding, the cross-sectional area and capacity of the strand is reduced which causes premature failure at the grinding location. In light of these findings, researchers decided against grinding wires to install strain gauges on prestressing strand, and proceeded to test the effects of more realistic gripping conditions at the ends of the strands.

3.6.1.2 Strand Test Using Chucks

Two tests were conducted to investigate the effects that realistic gripping conditions using anchoring chucks have on the behavior of prestressing strand in tension. The anchoring chucks used for the test (Fig. 3.22) were also utilized for prestressing the strands in the test specimens. All six wires were instrumented with strain gauges on both strands. No wire surfaces were ground; they were prepared as discussed in Section 3.7.1.1. To assure the safety of the test administrators, the strand ends were capped with a protective unit to catch the anchoring chucks in case of complete strand failure, or wedge slipping.

A comparison of the results from this test and the results from the previous test with v-grips is illustrated in Figure 3.21. Note that the stress-strain curves are virtually indistinguishable up to more than 200 ksi.

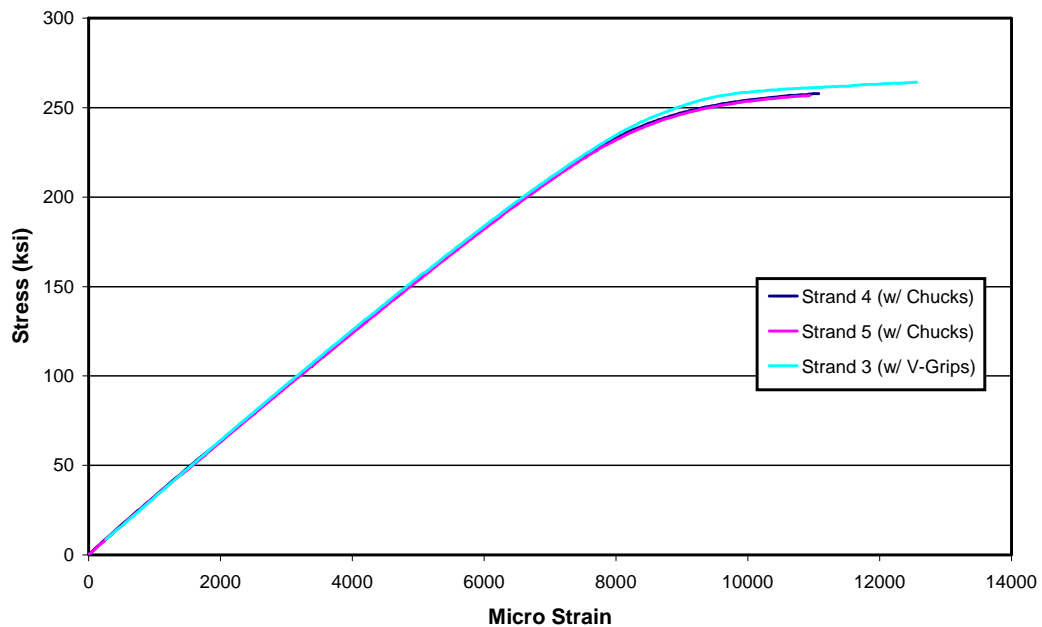


Figure 3.21 Stress-Strain Plot for Strands Gripped with Chucks vs. V-Grips

Out of twelve strain gauges installed for both tests with chucks, only one failed prior to strand failure. This confirmed the increased durability of the strain gauges when applied to a smooth wire rather than a ground wire. This test also demonstrated that tests conducted with v-grips provide reasonable results up to stresses exceeding 200 ksi. Both strands tested with the anchoring chucks failed at the gripping location (Fig. 3.22).



**Figure 3.22 Photo of Barrel and Wedge Anchoring System (Chucks) (left);
Photo of Failed Strand with Smooth Wires (right)**

3.6.1.3 Strand Results Using Upgraded Adhesive and Sealant for Strain Gauges

One tension test was conducted on a strand that had been submerged in water for 48 hours. The purpose of the test was to subject the strain gauge to conditions similar to, or more extreme than when cast in concrete, and afterwards, test its ability to function properly.

The preparation of the strand for this test was identical to the previous tests. However, a different adhesive, called CN and manufactured by Tokyo Sokki Kenkyujo Co. of Japan, was used to apply the strain gauges to the strand. Afterwards, two coats of a polyurethane material were spread over the gauge for waterproofing.

After the prescribed amount of time submerged in water, the strand showed no signs of corrosion around the gauge, indicating that the waterproofing material performed well. Researchers proceeded to test the strand to failure and found that the CN adhesive was much durable and reliable than the adhesive used in prior tests. As shown in Figure 3.23, the strain gauges consistently measured strains up to 40,000 microstrain, which is much higher than the average maximum strain reading from the previous tests. Both gauges in this test exceeded their specified capacity of 30,000 microstrain. In light of these results, researchers decided to use this adhesive and waterproofing material when installing strain gauges on the strands for test specimens.

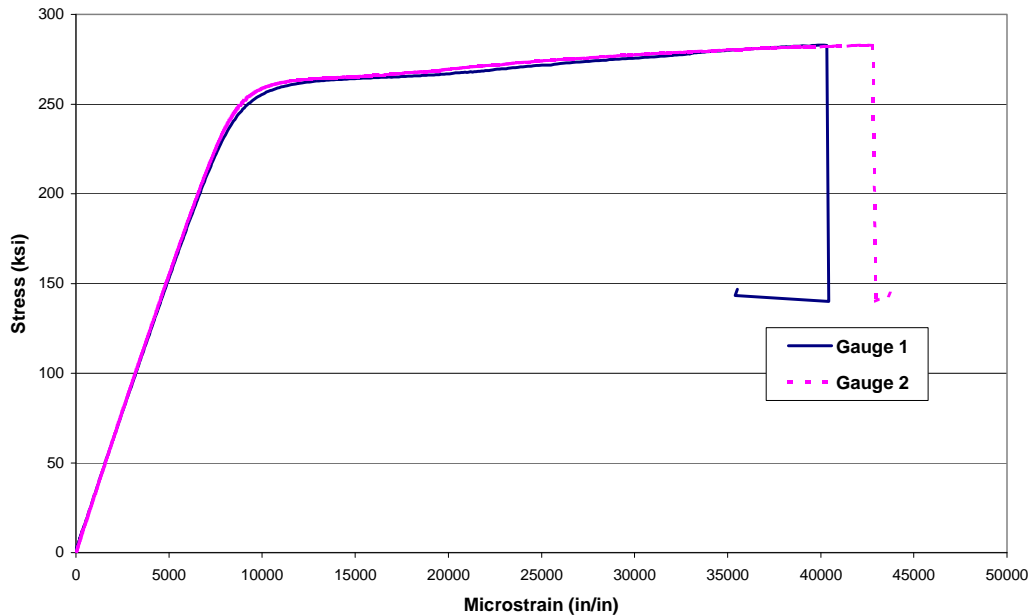


Figure 3.23 Stress-Strain Plot for Strand Utilizing CN Adhesive and Polyurethane Coating

3.6.1.4 Summary of Strand Test Results

The results from the ground wires showed poor gauge durability and elevated local strains in the strand due to the decreased cross-sectional area. However, results from prestressing strands with smooth (unground) wires indicated that with CN adhesive, the life and durability of the strain gauge could be increased substantially. Based on data from the three tension tests conducted on the strands with smooth wires, researchers generated a calibration curve and equation for estimating the stress in the prestressing strands used in the concrete test specimens. This calibration curve is shown in Figure 3.24.

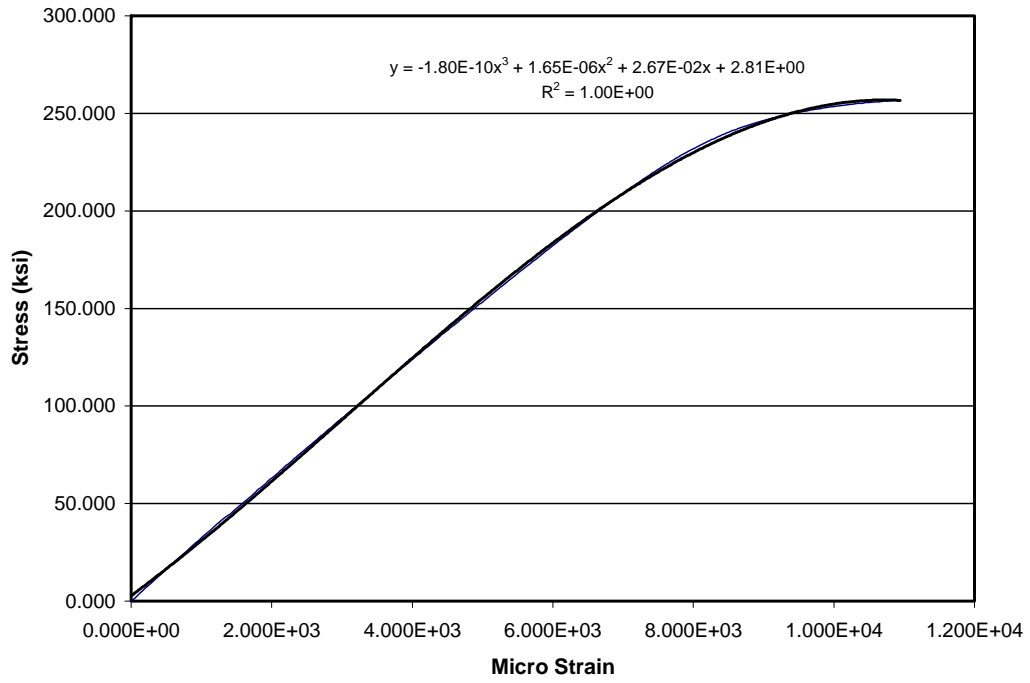


Figure 3.24 Calibration Curve for Estimating Stresses in Prestressing Strands Compared with Measured Stress-Strain Response

3.6.2 Concrete Compression Tests

Concrete compression tests were conducted on cylinders from a trial batch of concrete prior to casting the first series of test specimens. Six x 12-inch cylinders were cured in plastic molds (Fig 3.25) and tested according to ASTM C 39 for the purpose of developing a strength vs. time curve. Researchers planned to use this data to estimate the time of prestress release for the test specimens. The concrete mix was similar to a standard mix used in a prestressing plant in Victoria, Texas. It was a 6-sack Type III cement mix, with river gravel coarse aggregate and a w/c ratio of 0.34. This was a concrete trial batch that was no longer unavailable at the time the first series of test specimens was cast.

In addition to the cylinders, a non-prestressed beam with the same dimensions as the test specimens (6 x 18 inches x 15 feet) was cast to experiment with the *Sure Cure* equipment. This equipment is designed to cure 4 x 8-inch cylinders at the same temperature as the core of the beam. Because the beam contains a larger mass of concrete, it generates more heat during the hydration process than a 6 x 12-inch cylinder, and as a result, cures at a higher temperature. Therefore, the cylinders cured in the *Sure Cure* cylinder molds tend to provide a better representation of the concrete strength in the beam. Twelve *Sure Cure* cylinders were cast in addition to standard 6 x 12-inch cylinders. A thorough explanation of the *Sure Cure* equipment is included in Section 3.8.



Figure 3.25 Compression Test Cylinder Molds (a); Trial Test specimen with Sure Cure Equipment (b)

Due to a considerable amount of retarder added to the mix, the concrete remained retarded for approximately seven hours before the hydration process began. Once the chemical reaction started, the temperature and strength of the concrete increased rapidly. These properties are shown in Figure 3.26. The temperature of the test specimens was measured using thermocouples filtered through the *Sure Cure* equipment. Thermocouples were embedded at the bottom and mid-height at midspan and at one end of the specimen to monitor the difference in temperature between the two locations. Cylinders were cured at the lowest temperature measured in the beam. This location was at the bottom of the beam near the end.

The *Sure Cure* cylinders consistently displayed higher strength than the 6 x 12-inch cylinders. The behavior was expected, due to the elevated curing temperature of the cylinders.

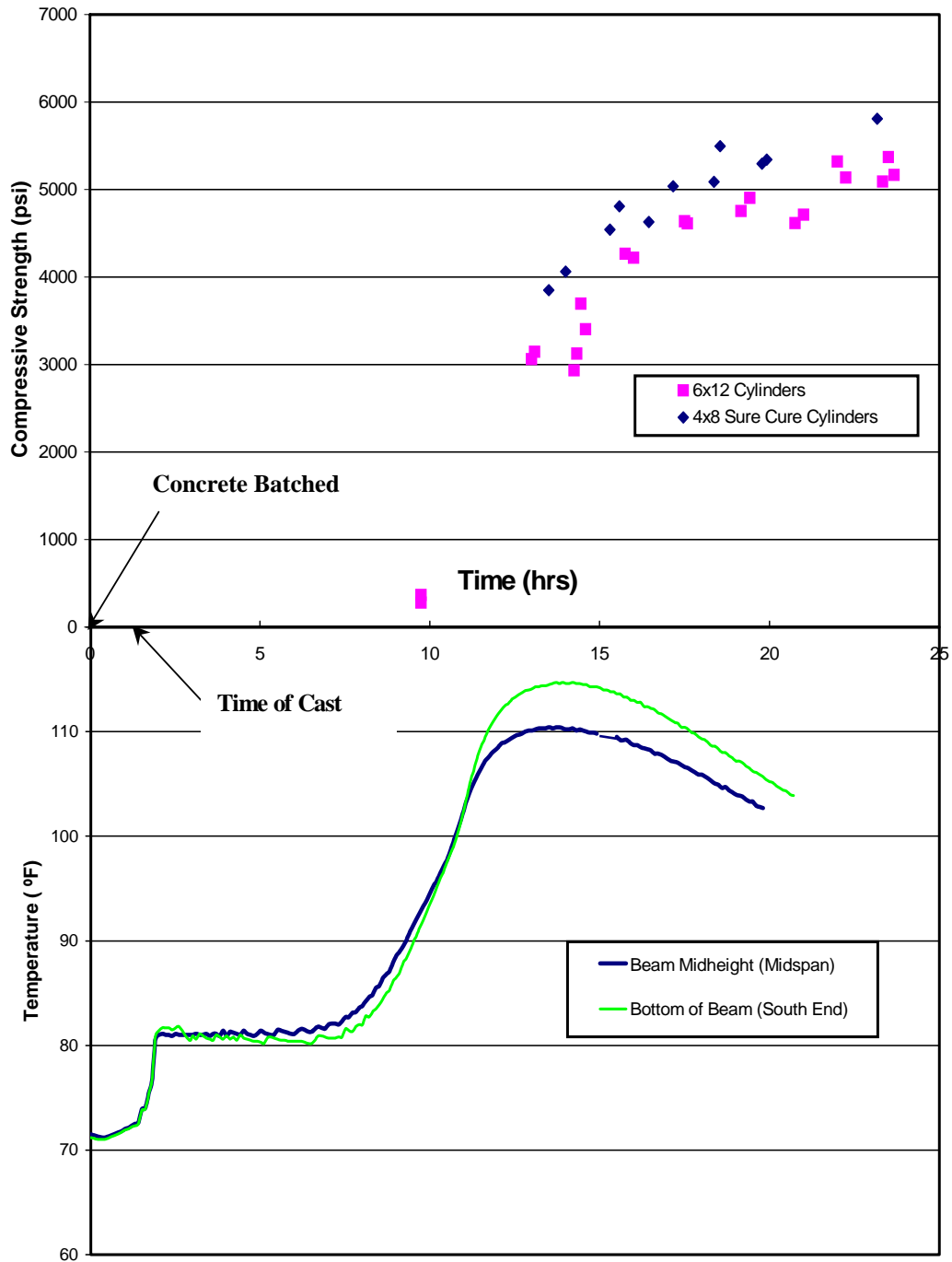


Figure 3.26 Strength and Temperature vs. Time Plot for Trial Specimen

3.7 INSTRUMENTATION

The instrumentation utilized for the first series of test specimens included:

1. Strain gauges attached to prestressing strands
2. DEMEC points installed on the sides of test specimens
3. Linear potentiometers located at midspan
4. Thermocouples located at one end of each test specimen

All instrumentation, with the exception of thermocouples, was connected to a data acquisition system. The data acquisition system consisted of bridge boxes, wires, cables, and a computer system to manage the data. This system is shown in Figure 3.27. The computer ran an Excel program called Measure that controlled the data acquisition process. The software converted the measured changes in voltage to engineering units of microstrain from the strain gauges and inches from the linear potentiometers. This system took readings every 30 seconds during the tensioning of the strands prior to casting, and during the release of prestressing strands. Readings were generally taken every 30 minutes for three weeks following release of the strands. A 2-volt excitation was supplied for all strain gauges, and a 10-volt excitation was supplied for all linear potentiometers.

A separate system was used for running the *Sure Cure* software and hardware. This system was used to set the temperature of the *Sure Cure* cylinders to the curing temperature of each of the test specimens.



(a)



(b)

Figure 3.27 Data Acquisition Computer and Scanner (a); Bridge Boxes and Connectors (b)

3.7.1 Strain Measurement

3.7.1.1 *Electrical Strain gauges*

The strain gauges used in the prestressing steel tension tests were also used to instrument the prestressing strand for the test specimens. These strain gauges were required to be small enough to fit on a single wire of a 0.5-inch diameter prestressing strand. FLA-5-3LT strain gauges by Tokyo Sokki were found to be reliable gauges that met that requirement. The gauges have a resistance of $119.5\Omega (\pm 0.5)$, and have 1.5 x 5-mm dimensions.

To install the gauges, the surface of the strand was prepared with sterile swabs and acetone, neutralizer, and conditioner. The gauges were then attached

to the prestressing wires using CN adhesive. This proved to be the most effective adhesive during the trial tension tests. Once the adhesive dried, the exposed gauge wires were embedded in black mastic to alleviate the chance of a short circuit. The wires and gauges were then covered with two coats of a polyurethane substance and wrapped in aluminum tape. This waterproofed the gauges and provided protection when the strands were cast in the concrete.

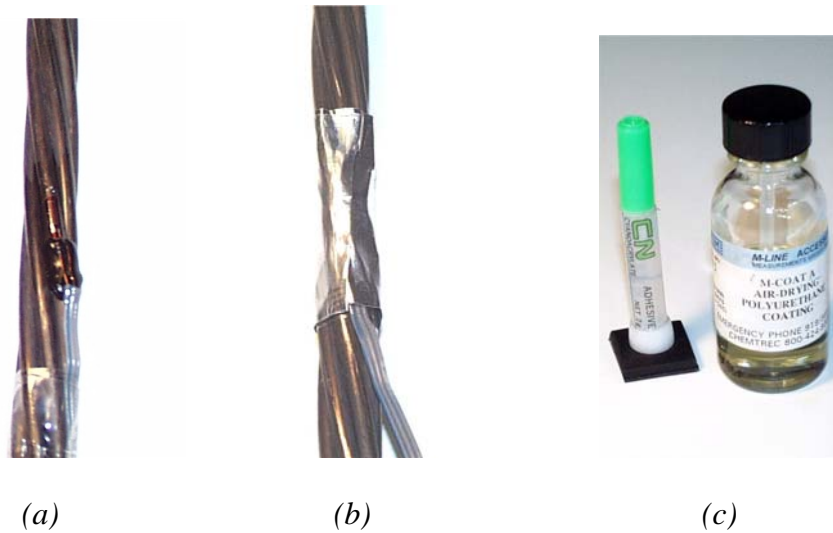
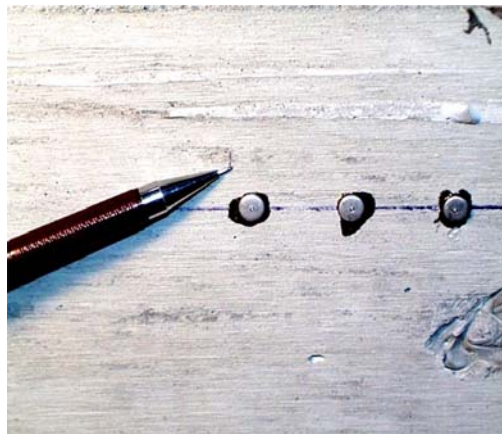


Figure 3.28 Instrumented Strand with Electrical Strain Gauge (a); Photo of Protected Strain Gauge (b); CN Adhesive and Polyurethane Coating (c)

3.7.1.2 DEMEC Gages

Strains on the outside surface of the concrete were measured with detachable mechanical strain gages (DEMEC gages). The DEMEC gages are used in conjunction with DEMEC targets, small stainless steel discs with a machined hole in the center. The DEMEC gage is received by the holes in the center of the DEMEC targets, and a change in length is measured between points. The DEMEC gage and DEMEC targets are shown in Figure 3.29. The DEMEC gage used on the specimens described in this thesis had a 50 mm gage length and was made by Hayes Manufacturing Company in England.



(a)



(b)

Figure 3.29 Photo of DEMEC Targets (a) and DEMEC Gage (b)

3.7.2 Camber Measurement

3.7.2.1 Linear Potentiometers

Camber measurement was used to monitor rate of creep in the specimens. In order to recommend higher allowable stresses at transfer, the growth of camber in test specimens must be monitored carefully. Two stiff timber frames were constructed over the beams to support 2-inch linear potentiometers (Fig. 3.30 (b)) that could accurately measure the deflection of the test specimens with time. The timber frames were positioned over the test specimens to allow measurements to be taken at midspan of the beams (Fig. 3.30 (a)).

Because the beams were expected to displace 1 inch or more horizontally at release, short pieces of smooth aluminum plate were glued to beam at the point of contact between the linear potentiometer and the top of the test specimen to accommodate movement at release. This minimized erroneous data due to imperfections on the concrete surface. The linear potentiometers were used to take camber measurements for three weeks after release of the strands.



(a)



(b)

Figure 3.30 Photo of Frame (a) and Linear Potentiometers (b) Used in Monitoring Midspan Camber of Specimens

3.7.2.2 Dial Gauges

Upon removal of the linear potentiometers and test specimens from the prestressing facility, the camber measurements will be taken manually using dial gauges. Once a location is secured for future storage of the test specimens, a frame similar to the timber frame used to support the linear potentiometers will be constructed and dial gauges will be installed to monitor long-term camber.

3.7.3 Temperature Measurement

Curing temperature of the beams was monitored using thermocouples wrapped in shrink tubing and embedded in the concrete. The thermocouples were located at the bottom of the beam near one end of each test specimen. The thermocouples were used in conjunction with the *Sure Cure* equipment discussed in the following section. In addition to monitoring the temperature of the beams, a thermocouple was also embedded in one 6 x 12-inch cylinder to measure the difference in curing temperature from the *Sure Cure* cylinders.

3.8 SURE CURE

Sure Cure is a concrete curing system implemented in several prestressed concrete plants (Fig. 3.31). It is used to control the curing temperature of 4 x 8-inch cylinders. It is a very conservative practice for precasters to rely on the breaking strength of common cylinders to determine when they release the strands in their prestressing beds. In large precast elements, such as those cast at a plant, the rate of strength gain can be much different than for a typical 6 x 12-inch cylinder, because the large elements cure at a much higher temperature. *Sure Cure* allows precasters to cure small 4 x 8-inch cylinders at the same temperature as a selected location within a precast element, thus providing a better representation of the strength of the concrete in the precast element.



(a)

(b)

Figure 3.31 Sure Cure System Computer and I/O Box (a); Sure Cure Cylinders (b)

The *Sure Cure* system can be used to set a curing cycle to follow any number of temperature paths, or more commonly, to mimic the temperature of a location within a precast concrete beam. To set the cure cycle to a temperature equal to the temperature of the interior of a precast beam, the thermocouple end must be imbedded in the precast element and the lead end connected to the *Sure Cure* input/output box. Another thermocouple that is connected to the *Sure Cure* cylinder must also be connected to the *Sure Cure* input/output box. Following the guidelines set forth in the *Sure Cure* user's manual, the cylinder channel is designated as a slave to the channel containing the thermocouple imbedded in the precast element. Once the curing cycle length is set, the *Sure Cure* system heats the cylinder to the temperature of the channel to which it is a slave, commonly the channel corresponding to the thermocouple imbedded in the test specimen.

For this research project, two *Sure Cure* cylinders were set to cure at the temperature measured in one assigned test specimen. Thus, twelve *Sure Cure* cylinders were cast, and four could be tested to determine the average

compressive strength of the concrete beams when prestress for each line of specimens was released.

The *Sure Cure* software was also used to produce time vs. temperature curves for all desired channels. These plots are shown in Section 3.6. There are many other features the Sure Cure system offers, but they were not of interest for this study.

CHAPTER 4

Fabrication of Test Specimens

4.1 INTRODUCTION

This chapter discusses the tasks completed during the fabrication of the first six test specimens in Ferguson Laboratory. In subsequent beam casts, some of these tasks may be modified or omitted. However, this procedure was followed for the series of specimens included in this thesis.

4.2 INSTRUMENTATION OF PRESTRESSING STRAND

All strands used to prestress the test specimens were instrumented with strain gauges as stated in Chapter 3. Two strain gauges were installed on each strand near midspan of every test specimen, for a total of 72 strain gauges on 18 strands. The strain gauges proved to be fairly durable with minimal failures. Every strand had at least one working strain gauge prior to release. Most gauge failures occurred during curing and stripping of formwork, with no failures at release.



Figure 4.1 Instrumented Prestressing Strand for Test Specimen

4.3 PRESTRESSING OF STRANDS

The strands were stressed with a single-strand ram and hydraulic pump as shown in Figure 4.2. Each strand was initially stressed to 50 ksi, and respective strain gauges were zeroed at this time. This process alleviated much of the erroneous data readings observed during the initial stages of stressing in prior tension tests. After each gauge was initialized at 50 ksi, the strands were fully stressed to $0.80f_{pu}$, or 216 ksi, to target a stress in the strands of $0.75f_{pu}$ after seating losses. Researchers tensioned each strand multiple times in order to reach the desired strand stress. Due to small deformations in the prestressing bed during prestressing, it was difficult to stress each strand to precisely $0.75f_{pu}$, so there were slight variances in prestress from strand to strand.



Figure 4.2 Single-Strand Prestressing Ram (left); Hydraulic Pump (right)

4.4 CASTING OF CONCRETE

The test specimens cast using with a 7-sack Type III cement mix, with river rock coarse aggregate, and a 0.4 w/c ratio. Due to the unavailability of ready-mix concrete, an on-site concrete mixing company supplied the concrete. Concrete was placed in the forms using a hopper transported by the overhead crane, then the concrete was consolidated using mechanical vibrators. Each

concrete-filled hopper would cast approximately 1½-test specimens. Much care was taken to keep the vibrators a clear distance from the strain gauges to avoid damaging them. The specimens were cured for nine hours under plastic sheeting before stripping the form sides.



Figure 4.3 Casting of Test Specimens

4.5 APPLICATION OF DEMEC TARGETS

Immediately after stripping the forms, DEMEC targets were applied to the concrete surface on each side of the beams. They were applied using a 5-minute epoxy and the 50 mm standard length bar included with the DEMEC gage. A sketch showing the locations of DEMEC targets is shown in Figure 4.4.

4.6 RELEASING OF PRESTRESSING STRANDS

At the prescribed compressive strength for each of the beams, the prestressed strands were cut in the space between the beams using an acetylene torch: They were cut in this location to minimize movement of the beam specimens at release. Individual strands were heated gradually until failure of each wire occurred. This process was followed to avoid loading the beams suddenly and possibly causing excessive transfer lengths.

7

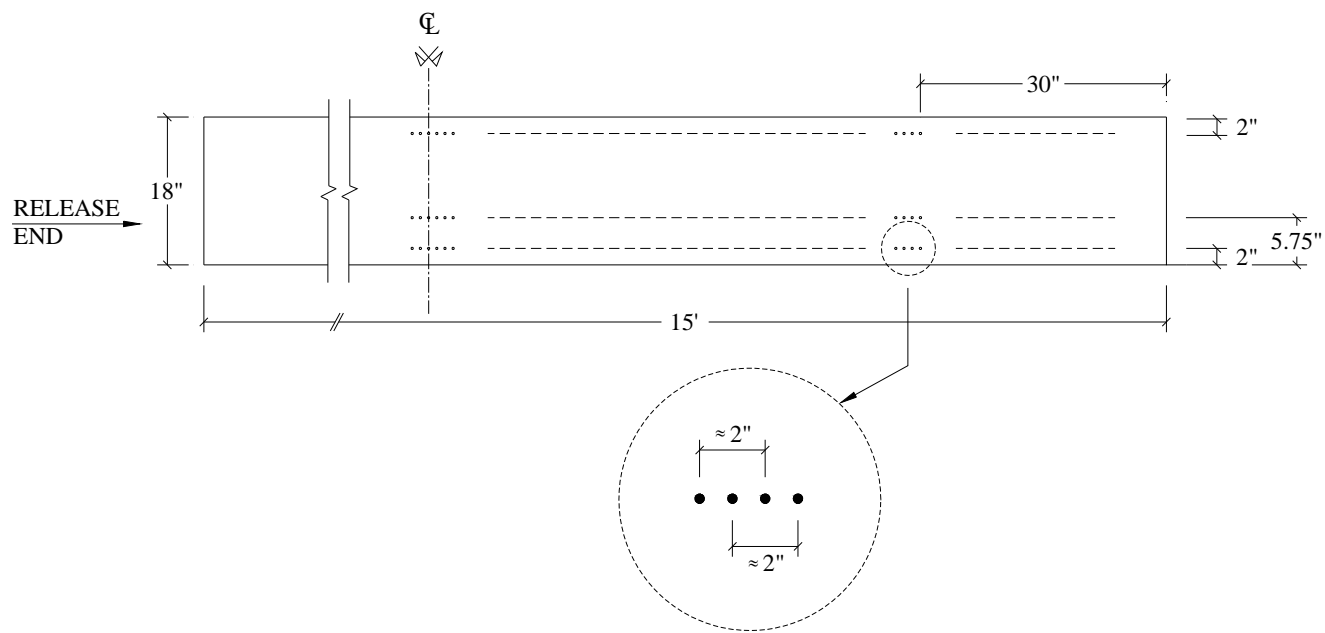


Figure 4.4 Sketch of DEMEC Target Locations

CHAPTER 5

Presentation of Preliminary Results

5.1 INTRODUCTION

This chapter discusses preliminary results from the first six test specimens cast in Ferguson Laboratory to investigate allowable release stresses. Included is a presentation of multiple methods for calculating extreme fiber stresses, and measured short-term prestress losses and camber. The data presented here were collected by monitoring the specimens for approximately three weeks after releasing the strands.

Generally, data obtained prior to release were reliable. However, following release, anomalies in strain readings made with surface-mounted DEMEC points and strain gauges mounted on prestressing strands were observed. Some readings suggested that the concrete was expanding. This unconfirmed expansion, along with possible electrical interferences, adversely affected much of the strain data obtained, so an identical cast of test specimens using a different concrete supplier and revised instrumentation is currently being planned.

5.2 STRAIN GAUGES

The most reliable data from this first series of beams were collected at release using the electrical strain gauges installed on the prestressing strand. The gauges permitted an extremely accurate estimate of the prestress force, F_i , prior to release, rather than using a force based on calculated prestress losses due to relaxation and wedge seating. This was quite important because the

effective prestress is crucial for accurately determining maximum compression and tensile stresses in specimens at release.

Data obtained from the DEMEC gages were deemed to be unreliable. Large variations were experienced from reading to reading, likely due to I proper attachment of DEMEC points to the side faces of the concrete beam specimens, and perhaps, inconsistent time-dependent behavior of the concrete mix. For this reason, the data obtained from the DEMEC gages are not included in this chapter. Strain profiles plotted from measured DEMEC readings are included in Appendix E.

5.3 CONCRETE FIBER STRESSES

Extreme fiber stresses were calculated for all test specimens considering both linear and nonlinear material behavior. Example calculations for specimens RS-75S and RS-75N are shown in Figure 5.1, and results for all specimens are summarized in Table 5.1. Calculations for other test specimens are shown in Appendix B. For the calculations shown, the following assumptions were made:

1. Strains vary linearly over the section depth
2. $E_{ci} = 57000 \sqrt{f'_{ci}}$ (Linear Analysis)
3. $E_{ci} = 2f'_{ci} / \epsilon'_c$ (Nonlinear Analysis)
4. Prestress Force = F_o (after elastic shortening)

The initial prestress force prior to transfer, F_i , for each beam was calculated from strain measurements, based on the calibration equation included in Chapter 3, and the average strain readings from all working gauges on the strands in each beam. This value was used to determine an effective prestress force, F_o , using two different methods, to calculate concrete flexural stresses.

5.3.1 Linear Analysis

For the linear analysis, two methods were used to calculate the fiber stresses. Both methods first calculated an effective prestress force, F_o . One method used transformed-section properties, while the other used gross-section properties. Extreme fiber stresses were then calculated using the two different section properties and the respective F_o value.

The transformed section-section approach will likely yield more accurate estimates of concrete stresses, but is a more rigorous approach and is seldom used by designers. Most commonly, gross-section properties are used by designers for analysis. Both methods yield similar results, but the method using gross-section properties provides slightly higher estimates of maximum compressive fiber stresses.

5.3.2 Nonlinear Analysis

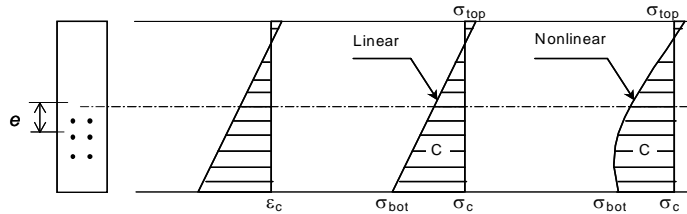
A software program written at the University of Toronto, called *Response* (Collins, 1990), was used to consider the nonlinear behavior of concrete in compression (i.e. not assume linear behavior). This program also accounted for the nonlinear behavior of the prestressing strand. Hognestad's parabolic model described the concrete behavior in compression, and a Ramberg-Osgood function was used to model the prestressing strand response. Using the F_o computed for a transformed section, *Response* calculated the concrete strain at the top and bottom fibers. Concrete stresses were calculated assuming a linear stress-strain relationship for concrete in tension, and Hognestad's model for concrete in compression.

Concrete Stresses

Specimens: RS-75S, RS-75N

Material Properties				Cross-sectional Properties				Prestress Force Calculation							
Nonlinear		Linear		Gross		Transformed		Strand No.	Microstrain (in/in)				Avg.	f_{ps} (ksi)	F_i (kip)
f'_{ci} (psi)	4225	f'_{ci} (psi)	4225	A_G (in ²)	108	A_T (in ²)	114		Gauge 1	Gauge 2	Gauge 3	Gauge 4			
E_{ci} (ksi)	4225	E_{ci} (ksi)	3705	I_G (in ⁴)	2916	I_T (in ⁴)	2981	1	6292.54	6205.5	6333.16	6309.7	6285	191	173.1
ϵ'_{ci} (in/in x 10 ³)	2.00			y_{bG} (in)	9	y_{bT} (in)	8.83	2	6235.3	6138.38	6191.24	-	6188	189	
σ_c (psi) = $f'_{ci} [2(\epsilon_c/\epsilon'_c) - (\epsilon_c/\epsilon'_c)^2]$				y_{iG} (in)	9	y_{iT} (in)	9.17	3	-	6231.7	6202.25	-	6217	189	
f_{ps} (ksi) = (see Calibration curve)				S_{bG} (in ³)	324	S_{bT} (in ³)	338	4	6054.31	6064.16	-	6040.1	6053	185	
				S_{iG} (in ³)	324	S_{iT} (in ³)	325	5	-	-	6113.18	5955.4	6034	185	
								6	6334.2	-	-	6332.3	6333	192	

M_D (kip-in) = 37.969
 F_i (kips) = 173
 e (in) = 3.25
 A_{ps} (in²) = 0.918
 E_{ps} (ksi) = 28500
 n_L = 7.7
 n_{NL} = 6.7



Linear Analysis

Transformed Section Method:

Effective Prestress Force (Elastic Shortening):

$$F_o = [F_i/A_{ps} - (n_L * F_i)/(A_G + (n_L - 1) * A_{ps})] * A_{ps}$$

$$F_o = \mathbf{162.4 \text{ kips}}$$

$$\sigma_{top} = -F_o/A_T + (F_o * e)/S_{iT} - (M_D * y_{iT})/I_T$$

$$\sigma_{top} = \mathbf{23 \text{ psi}}$$

$$\sigma_{bot} = -F_o/A_T - (F_o * e)/S_{bT} - (M_D * y_{bT})/I_T$$

$$\sigma_{bot} = \mathbf{-2872 \text{ psi}}$$

Gross Section Approximate Method:

Effective Prestress Force (Elastic Shortening):

$$F_o = [F_i/A_{ps} - (n_L * F_i)/A_G] * A_{ps}$$

$$F_o = \mathbf{161.8 \text{ kips}}$$

$$\sigma_{top} = -F_o/A_G + (F_o * e)/S_{iG} - (M_D * y_{iG})/I_G$$

$$\sigma_{top} = \mathbf{8 \text{ psi}}$$

$$\sigma_{bot} = -F_o/A_G - (F_o * e)/S_{bG} - (M_D * y_{bG})/I_G$$

$$\sigma_{bot} = \mathbf{-3003 \text{ psi}}$$

Nonlinear Analysis

Nonlinear Analysis Program: Response

(see Appendix)

$$F_o: \text{Sub. } n_{NL} \text{ for } n_L \text{ in trans. section eqn. } \epsilon_{top} (x10^{-3}) = \mathbf{0.053}$$

$$F_o = \mathbf{163.6 \text{ kips}} \quad \epsilon_{bot} (x10^{-3}) = \mathbf{-0.789}$$

$$\sigma_{top} = \epsilon_{top} * E_{ci}$$

$$\sigma_{top} = \mathbf{224 \text{ psi}}$$

$$\sigma_{bot} = f'_{ci} [2 (\epsilon_{bot} / \epsilon'_{ci}) - (\epsilon_{bot} / \epsilon'_{ci})^2]$$

$$\sigma_{bot} = \mathbf{-2676 \text{ psi}}$$

Figure 5.1 Calculation of Concrete Fiber Stresses

Table 5.2 Extreme Fiber Stresses* for Test Specimens

	RS-75S, RS-75N			RS-70S, RS-70N			RS-60S, RS-60N		
	Linear (Gross)	Linear (Trans.)	Nonlinear	Linear (Gross)	Linear (Trans.)	Nonlinear	Linear (Gross)	Linear (Trans.)	Nonlinear
f'_{ci} (psi)	4225	4225	4225	4550	4550	4550	5225	5225	5225
E_{ci} (ksi)	3705	3705	4225	3845	3845	4550	4120	4120	5225
F_i (kip)	173.1	173.1	173.1	171.5	171.5	171.5	173.8	173.8	173.8
F_o (kip)	161.8	162.4	163.6	160.7	161.2	162.8	163.6	164.1	166.1
σ_{top} (psi)	-8	-23	-224	-7	-22	-214	-9	-24	-225
σ_{bot} (psi)	3003	2872	2676	2982	2852	2707	3039	2904	2841
$\frac{\sigma_{bot}}{f'_{ci}}$	71.0%	68.0%	63.3%	65.5%	62.7%	59.5%	58.1%	55.6%	54.4%

* (-) Signifies tensile stress

5.3.3 Discussion of Analysis

As shown in Table 5.2, the bottom (compressive) fiber stresses calculated using gross-section properties were considerably higher than when computed using a transformed-section linear analysis or nonlinear approach. Most designers, therefore, are acting conservatively when estimating the required release strength based on gross-section properties. A bottom fiber stress computed with gross-section properties to be $0.71f'_{ci}$ may only be $0.63f'_{ci}$ when accounting for the nonlinear behavior of the concrete.

Also, note that as f'_{ci} increases, the percentage difference in maximum compressive stresses based on linear (gross section) versus nonlinear analysis reduces (i.e. % difference in linear (gross section) versus nonlinear results for

Specimen RS-75S was 7.7%, compared to 3.7% for Specimen RS-60S). This trend was expected because lower stresses relative to f'_{ci} correspond with the “more linear” portion of the nonlinear stress-strain model. This observation also agrees with Tadros’ observation that a linear analysis is fairly accurate up to the current compressive stress limit of $0.60f'_{ci}$ (Tadros, 1997).

It is important to note that the maximum tensile stress computed from the nonlinear analysis was significantly higher than that computed from both linear methods. Since most designs of pretensioned concrete beams are governed by the maximum compressive fiber stress, this is not too alarming. However, if a beam were designed to crack at transfer, the amount of steel required to resist the total tensile force would be unconservative and could result in excessive camber or crack widths.

5.4 SPECIMEN BEHAVIOR

5.4.1 Camber

The midspan camber is plotted for all test specimens in Figures 5.2 and 5.3. A best-fit curve was used to help illustrate the behavior of each specimen. In comparison with the two specimens that met code requirements (RS-60N and RS060S), the four test specimens that did not meet code allowable stress requirements behaved somewhat similarly. Initial camber measurements were higher due to the lower E_{ci} , but long-term camber seemed to be relatively stable.

All camber measurements were well below predicted values. The measured camber for specimens RS-75S and RS-75N at transfer was 0.092 in. and 0.088 in., respectively. The estimated camber for these specimens at release was 0.22 in. This estimate was based on an approximation listed in the PCI Design Handbook, Fifth Edition (PCI, 1992). A plot of all measured test specimen cambers with their respective predicted values is found in Appendix D.

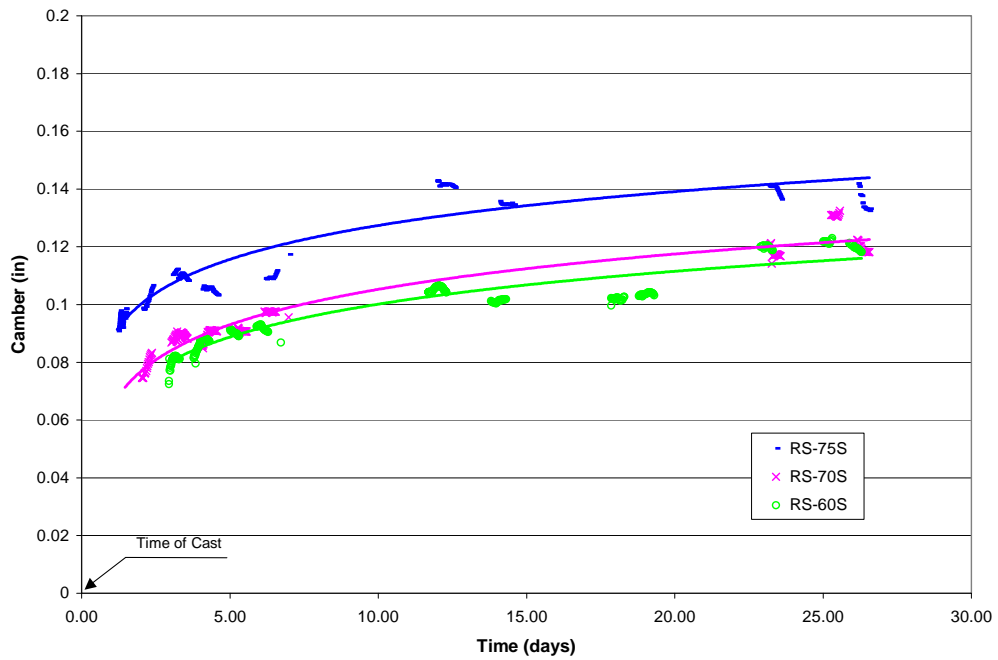


Figure 5.2 Camber for South End Specimens

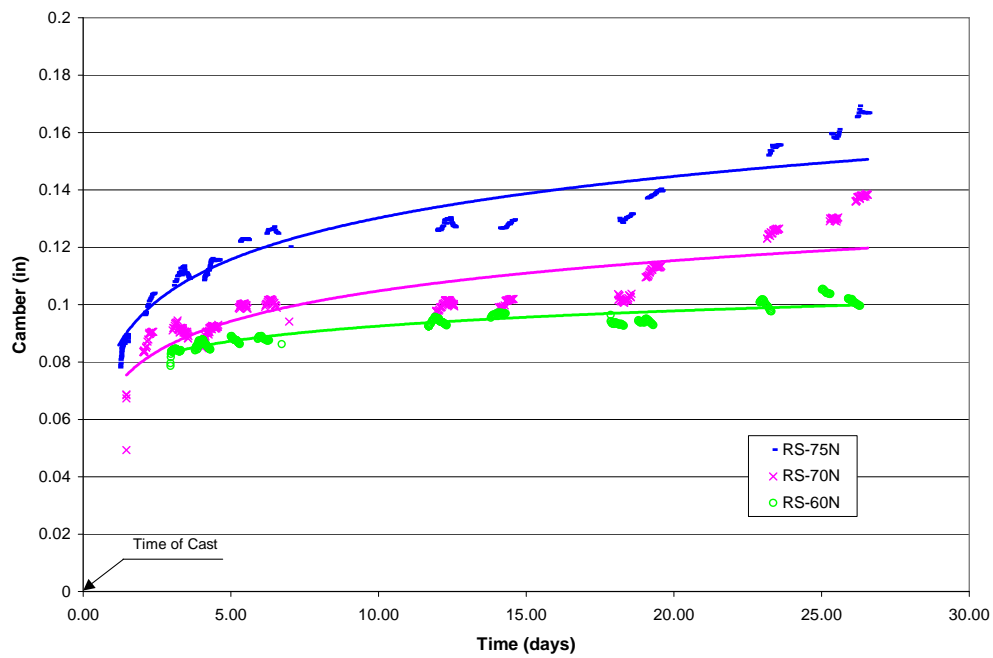


Figure 5.3 Camber for North End Specimens

It is important to note that the measured readings may be subject to significant error. Large variations between readings taken over a limited number of days leads the author to believe that external factors played a significant role in the measurements obtained from the linear potentiometers. The frames used to support the linear potentiometers may have been jarred, or even undergone time-dependent deflection, as well. Researchers are currently considering a more stable and reliable frame for future specimens. Due to the small amount of camber, factors such as temperature, relative humidity, shrinkage, and excitation voltage variations likely had a significant affect on measurements.

5.4.2 Creep

Concrete strains were intended to be measured using a DEMEC gage and target points mounted on the sides of beams. However, this data proved to be unreliable for most specimens and is included in Appendix E. Researchers are currently investigating ways to obtain more reliable surface strain readings for future beam casts.

5.4.3 Prestress Loss

The time allowed for monitoring the test specimens was not sufficient to record much time-dependent change in prestress force. Prestress force versus time plots for the test specimens are shown in Figures 5.4 through 5.6. Following release (15 to 50 hours later), prestress forces increased for some time in five of the six specimens. It was not clear whether these increases were related to electrical drift in the strand strain gauges or due to a suspected expansion mechanism in the concrete. Currently, researchers are seeing a significant decrease in the stress in the steel due to creep and shrinkage. Prestress force data over a longer time period are presented in Appendix C.

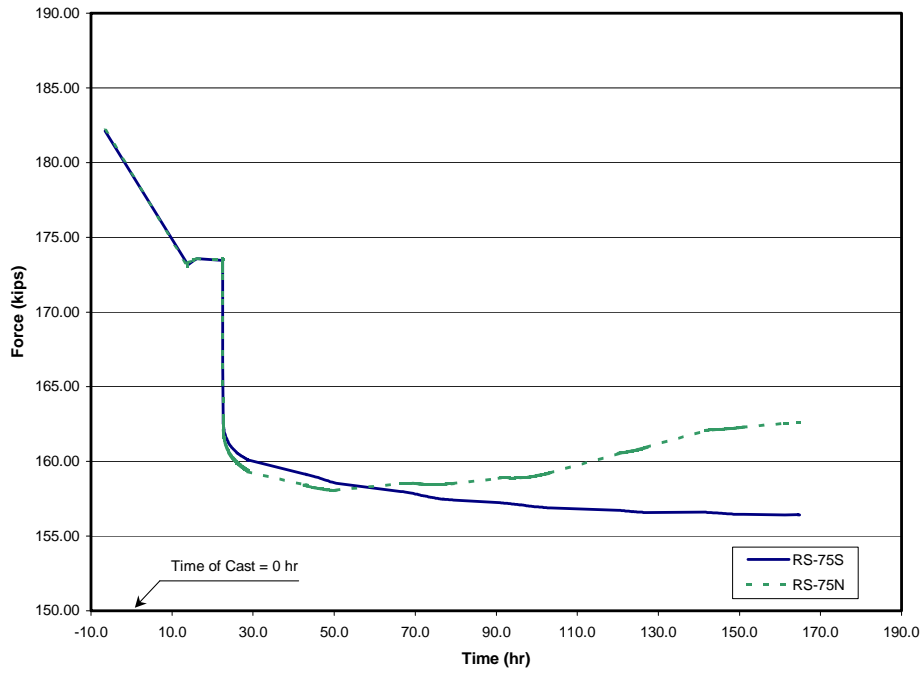


Figure 5.4 Prestress Force vs. Time Plot for Specimens RS-75S and RS-75N

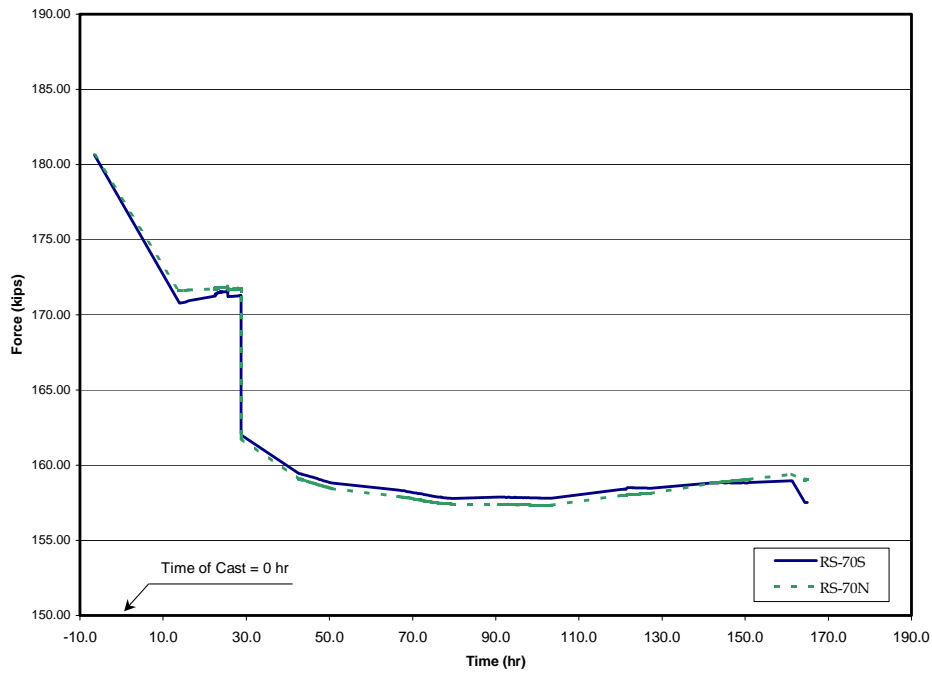


Figure 5.5 Prestress Force vs. Time Plot for Specimens RS-70S and RS-70N

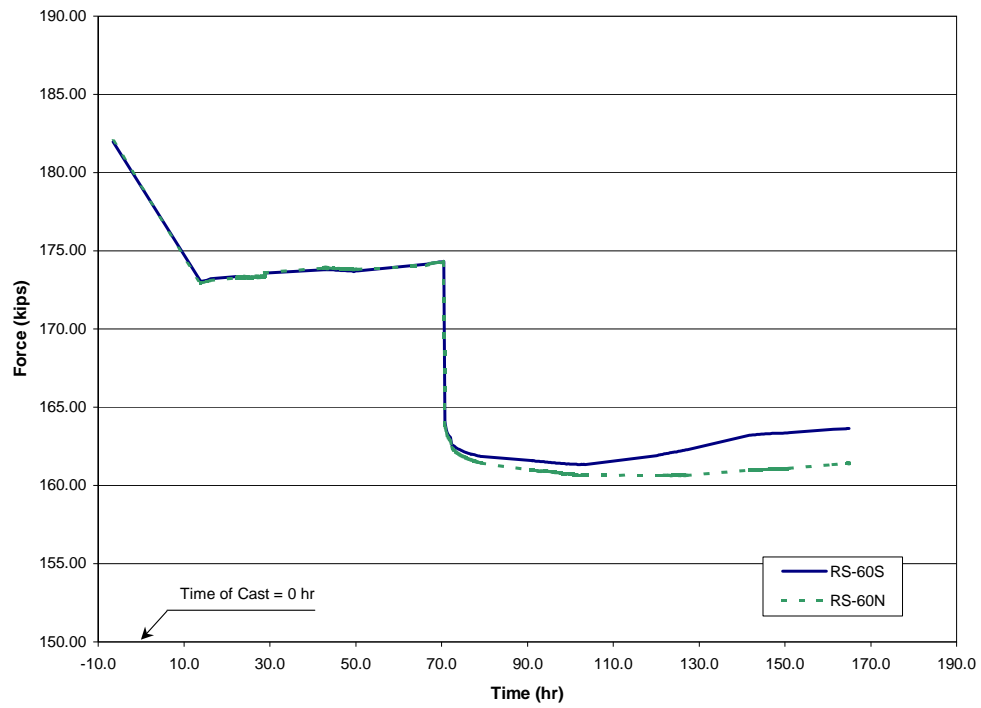


Figure 5.6 Prestress Force vs. Time Plot for Specimens RS-60S and RS-60N

CHAPTER 6

Conclusions and Recommendations

Based on the results from this experimental study, the following conclusions can be drawn:

- 1.) Results from this preliminary series of test specimens are not sufficient to warrant an increase in the allowable concrete fiber stresses at transfer. More specimens should be fabricated and tested before safely recommending a higher allowable compressive stress limit. However, other recent research supports raising the current limit of $0.60f'_{ci}$ to $0.70f'_{ci}$. The Precast/Prestressed Concrete Institute also currently suggests a compressive stress limit at transfer of $0.70f'_{ci}$.
- 2.) When subjecting these test specimens to higher compressive stresses at release than allowed by current codes, they did not fail. Researchers designed the test specimens to target compressive stresses at the bottom fiber of $0.60f'_{ci}$, $0.70f'_{ci}$, and $0.75f'_{ci}$. The actual stresses applied to each line of specimens were $0.58f'_{ci}$, $0.66f'_{ci}$, and $0.71f'_{ci}$, based on linear elastic, gross-section analysis used by designers for estimating concrete stresses. All test specimen behavior was relatively consistent, with no adverse affects recorded due to higher release stresses. The measured camber of all specimens was consistent, and well below the predicted values.
- 3.) The current linear elastic, gross-section method employed by most designers significantly overestimates the extreme fiber stresses for concrete flexural members. As higher stresses, relative to the compressive strength, are applied to a concrete member, the estimated

fiber stresses from linear versus nonlinear analysis become increasingly different. In this experimental study, the extreme fiber stress calculated from linear analysis for two specimens was $0.71f'_{ci}$, while the fiber stress calculated from nonlinear analysis was only $0.63f'_{ci}$. By accounting for the nonlinear behavior of concrete, researchers can calculate a much more realistic estimate of concrete fiber stresses. This would be especially significant for nominal stresses as high as $0.80f'_{ci}$, which will be investigated further in this experimental program.

As with many preliminary tests, changes in the data acquisition process are recommended to obtain more reliable results. Several unforeseen problems in these preliminary specimens were encountered during the data acquisition process, which raised important issues to be addressed before casting another series of test specimens. Following are recommendations for researchers to consider for future casts of test specimens.

- 1.) Researchers should further investigate the effects of voltage excitation drift on the measured strain and displacement readings or find ways to alleviate these fluctuations. During monitoring of the current series of specimens, a significant amount of excitation difference and drift from channel to channel was experienced making it necessary to adjust the readings from the instrumentation. This issue must be resolved for researchers to have considerable confidence in the data obtained.
- 2.) Researchers should consider building a more stable and protected frame for supporting the linear potentiometers. Due to the long period required for monitoring the test specimens, a lightweight steel frame is

suggested. Because the properties of wood are highly sensitive to moisture and temperature, its use for this purpose is discouraged. These frames should also be protected as much as possible from external interference such as people and mechanical equipment.

- 3.) Researchers should investigate a way to take automated readings continuously with the data acquisition system at a prescribed level, rather than relying on periodic readings initiated by the researchers. This will help researchers clearly distinguish between actual changes in specimen camber, and outside interference. It may also help to answer questions raised about the drift in voltage excitation for the instrumentation.

In summary, the results from this preliminary phase of the research program indicate that it is safe to proceed with the fabrication of more test specimens with applied stresses higher than that allowed by current codes. Further research should experiment with various shapes and sizes of cross-sections, with various types of concrete mixes.

APPENDIX A

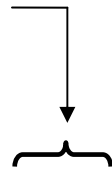
Notation

a	depth of equivalent rectangular stress block
A_c	cross-sectional area of concrete
A_{ps}	total cross-sectional area of prestressing strand
A_s	area of tension reinforcement
A'_s	area of compression reinforcement
A_G	gross cross-sectional area of concrete
A_T	transformed cross-sectional area of concrete
b	width of compression face of member
c	neutral axis depth
d	effective depth of section
d'	distance from extreme compression fiber to centroid of compression reinforcement
e	distance from section centroid to centroid of prestressed reinforcement
ε_c	strain in concrete
$\varepsilon_o, \varepsilon'_c$	specified concrete strain in Hognestad's model; 0.00225
ε_{cu}	ultimate concrete strain; 0.003
ε_s	tension reinforcement strain
ε'_s	compression reinforcement strain
E_c	modulus of elasticity of concrete
E_{ci}	modulus of elasticity of concrete at prestress release
f_c, σ_c	Stress in concrete
f'_c	28-day compressive strength of concrete in compression

f'_{ci}	compressive strength of concrete at prestress release
f_{pi}	stress in prestressing strand just prior to release
f_{po}	effective prestress in prestressing strand (after release)
f_{pu}	tensile strength of prestressing steel
f_s	calculated stress in tension reinforcement
f'_s	calculated stress in compression reinforcement
F_i, P_i	initial prestress force just before release
h	overall depth of member
I_G	gross cross-sectional moment of inertia
I_T	transformed cross-sectional moment of inertia
E_{ps}	modulus of elasticity for prestressing strand
E_{ps}	modulus of elasticity for prestressing strand
M_D, M_g	moment due to self weight
M_n	nominal moment strength
n_L	modular ratio (linear analysis)
n_{NL}	modular ratio (nonlinear analysis)
F_o	prestress force immediately after prestress release
P_n	nominal axial load strength
y_{bG}	distance from section centroid to extreme bottom fiber (gross section)
y_{bT}	distance from section centroid to extreme bottom fiber (transformed Section)
y_{tG}	distance from section centroid to extreme top fiber (gross section)
y_{tT}	distance from section centroid to extreme top fiber (transformed Section)
ϕ	strength reduction factor
σ_{top}	stress at top of section
σ_{bot}	stress at bottom of section

Specimen Designation

Shape of Cross-Section
RS – Rectangular Section



RS - 75 S

Tested End
N – North End
S – South End

**Targeted Compression Stress
Level at Release**

75 – $0.75f'_{ci}$

70 – $0.70f'_{ci}$

60 – $0.60f'_{ci}$

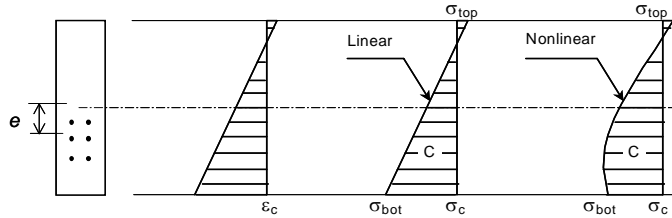
APPENDIX B

Calculated Concrete Stresses in Test Specimens

Concrete Stresses
Specimens: RS-75S, RS-75N

Material Properties				Cross-sectional Properties				Prestress Force Calculation							
Nonlinear		Linear		Gross		Transformed		Strand No.	Microstrain (in/in)				Avg.	f _{ps} (ksi)	F _i (kip)
f' _{ci} (psi)	4225	f' _{ci} (psi)	4225	A _G (in ²)	108	A _T (in ²)	114		Gauge 1	Gauge 2	Gauge 3	Gauge 4			
E _{ci} (ksi)	4225	E _{ci} (ksi)	3705	I _G (in ⁴)	2916	I _T (in ⁴)	2981	1	6292.54	6205.5	6333.16	6309.7	6285	191	173.1
ε' _c (in/in x 10 ³)	2.00			y _{bG} (in)	9	y _{bT} (in)	8.83	2	6235.3	6138.38	6191.24	-	6188	189	
σ _c (psi) = f' _{ci} [2(ε _c /ε' _c) - (ε _c /ε' _c) ²]				y _{iG} (in)	9	y _{iT} (in)	9.17	3	-	6231.7	6202.25	-	6217	189	
f _{ps} (ksi) = (see Calibration curve)				S _{bG} (in ³)	324	S _{bT} (in ³)	338	4	6054.31	6064.16	-	6040.1	6053	185	
				S _{iG} (in ³)	324	S _{iT} (in ³)	325	5	-	-	6113.18	5955.4	6034	185	
								6	6334.2	-	-	6332.3	6333	192	

M_D (kip-in) = 37.969
 F_i (kips) = 173
 e (in) = 3.25
 A_{ps} (in²) = 0.918
 E_{ps} (ksi) = 28500
 n_L = 7.7
 n_{NL} = 6.7



Linear Analysis

Transformed Section Method:

Effective Prestress Force (Elastic Shortening):

$$F_o = [F_i/A_{ps} - (n_L * F_i)/(A_G + (n_L - 1) * A_{ps})] * A_{ps}$$

$$F_o = \mathbf{162.4 \text{ kips}}$$

$$\sigma_{top} = -F_o/A_T + (F_o * e)/S_{iT} - (M_D * y_{iT})/I_T$$

$$\sigma_{top} = \mathbf{23 \text{ psi}}$$

$$\sigma_{bot} = -F_o/A_T - (F_o * e)/S_{bT} - (M_D * y_{bT})/I_T$$

$$\sigma_{bot} = \mathbf{-2872 \text{ psi}}$$

Gross Section Approximate Method:

Effective Prestress Force (Elastic Shortening):

$$F_o = [F_i/A_{ps} - (n_L * F_i)/A_G] * A_{ps}$$

$$F_o = \mathbf{161.8 \text{ kips}}$$

$$\sigma_{top} = -F_o/A_G + (F_o * e)/S_{iG} - (M_D * y_{iG})/I_G$$

$$\sigma_{top} = \mathbf{8 \text{ psi}}$$

$$\sigma_{bot} = -F_o/A_G - (F_o * e)/S_{bG} - (M_D * y_{bG})/I_G$$

$$\sigma_{bot} = \mathbf{-3003 \text{ psi}}$$

Nonlinear Analysis

Nonlinear Analysis Program: Response

(see Appendix)

F_o: Sub. n_{NL} for n_L in trans. section eqn.

$$F_o = \mathbf{163.6 \text{ kips}}$$

$$\varepsilon_{top} (x10^{-3}) = \mathbf{0.053}$$

$$\varepsilon_{bot} (x10^{-3}) = \mathbf{-0.789}$$

$$\sigma_{top} = \varepsilon_{top} * E_{ci}$$

$$\sigma_{top} = \mathbf{224 \text{ psi}}$$

$$\sigma_{bot} = f'_{ci} [2(\varepsilon_{bot}/\varepsilon'_c) - (\varepsilon_{bot}/\varepsilon'_c)^2]$$

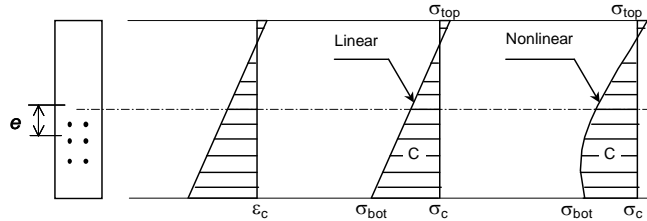
$$\sigma_{bot} = \mathbf{-2676 \text{ psi}}$$

Figure B.1 Calculation of Concrete Stresses for Specimens RS-75S and RS-75N

Concrete Stresses
Specimens: RS-70S, RS-70N

Material Properties				Cross-sectional Properties				Prestress Force Calculation							
Nonlinear		Linear		Gross		Transformed		Strand No.	Microstrain (in/in)				Avg.	f _{ps} (ksi)	F _i (kip)
									Gauge 1	Gauge 2	Gauge 3	Gauge 4			
f' _{ci} (psi)	4550	f' _{ci} (psi)	4550	A _G (in ²)	108	A _T (in ²)	114	7	5847.49	6069.5	6122.24	5843.1	5971	183	171.5
E _{ci} (ksi)	4550	E _{ci} (ksi)	3845	I _G (in ⁴)	2916	I _T (in ⁴)	2981	8	5989.1	5997.87	5995.03	5939.5	5980	183	
ε' _c (in/in x 10 ³)	2.00			y _{bG} (in)	9	y _{bT} (in)	8.83	9	6026.7	6054.87	6006.08	-	6029	184	
σ _c (psi) = f' _{ci} [2(ε _c /ε' _c) - (ε _c /ε' _c) ²]				y _{tG} (in)	9	y _{tT} (in)	9.17	10	6233.46	6164.77	6134.17	6300.3	6208	189	
f _{ps} (ksi) = (see Calibration curve)				S _{bG} (in ³)	324	S _{bT} (in ³)	338	11	6272.76	6213.05	-	-	6243	190	
				S _{tG} (in ³)	324	S _{tT} (in ³)	325	12	6292.24	-	-	-	6292	191	

M_D (kip-in) = 37.969
 F_i (kips) = 171
 e (in) = 3.25
 A_{ps} (in²) = 0.918
 E_{ps} (ksi) = 28500
 n_L = 7.4
 n_{NL} = 6.3



Linear Analysis

Transformed Section Method:

Effective Prestress Force (Elastic Shortening):

$$F_o = [F_i/A_{ps} - (n_L * F_i)/(A_G + (n_L - 1) * A_{ps})] * A_{ps}$$

$$F_o = \mathbf{161.2 \text{ kips}}$$

$$\sigma_{top} = -F_o/A_T + (F_o * e)/S_{iT} - (M_D * y_{iT})/I_T$$

$$\sigma_{top} = \mathbf{22 \text{ psi}}$$

$$\sigma_{bot} = -F_o/A_T - (F_o * e)/S_{bT} - (M_D * y_{bT})/I_T$$

$$\sigma_{bot} = \mathbf{-2852 \text{ psi}}$$

Gross Section Approximate Method:

Effective Prestress Force (Elastic Shortening):

$$F_o = [F_i/A_{ps} - (n_L * F_i)/A_G] * A_{ps}$$

$$F_o = \mathbf{160.7 \text{ kips}}$$

$$\sigma_{top} = -F_o/A_G + (F_o * e)/S_{tG} - (M_D * y_{tG})/I_G$$

$$\sigma_{top} = \mathbf{7 \text{ psi}}$$

$$\sigma_{bot} = -F_o/A_G - (F_o * e)/S_{bG} - (M_D * y_{bG})/I_G$$

$$\sigma_{bot} = \mathbf{-2982 \text{ psi}}$$

Nonlinear Analysis

Nonlinear Analysis Program: Response
(see Appendix)

F_o: Sub. n_{NL} for n_L in trans. section eqn.

$$F_o = \mathbf{162.8 \text{ kips}}$$

$$\epsilon_{top} (x10^{-3}) = \mathbf{0.047}$$

$$\epsilon_{bot} (x10^{-3}) = \mathbf{-0.727}$$

$$\sigma_{top} = \epsilon_{top} * E_{ci}$$

$$\sigma_{top} = \mathbf{214 \text{ psi}}$$

$$\sigma_{bot} = f'_{ci} [2 (\epsilon_{bot} / \epsilon'_c) - (\epsilon_{bot} / \epsilon'_c)^2]$$

$$\sigma_{bot} = \mathbf{-2707 \text{ psi}}$$

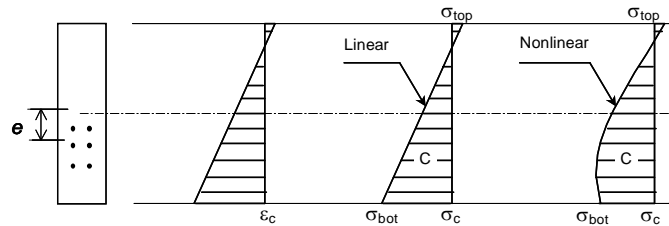
Figure B.2 Calculation of Concrete Stresses for Specimens RS-70S and RS-70N

Concrete Stresses Specimens: RS-60S, RS-60N

Material Properties				Cross-sectional Properties				Prestress Force Calculation							
Nonlinear		Linear		Gross		Transformed		Strand No.	Microstrain (in/in)				Avg.	f_{ps} (ksi)	F_i (kip)
f'_{ci} (psi)	5225	f'_{ci} (psi)	5225	A_G (in ²)	108	A_T (in ²)	114		Gauge 1	Gauge 2	Gauge 3	Gauge 4			
E_{ci} (ksi)	5225	E_{ci} (ksi)	4120	I_G (in ⁴)	2916	I_T (in ⁴)	2981	1	6300.08	-	-	-	6300	192	173.8
ϵ'_c (in/in x 10 ³)	2.00			y_{bG} (in)	9	y_{bT} (in)	8.83	2	6529	6422	6570	5914	6359	193	
σ_c (psi) = $f'_{ci} [2(\epsilon_c/\epsilon'_c) - (\epsilon_c/\epsilon'_c)^2]$				y_{tG} (in)	9	y_{tT} (in)	9.17	3	6068.34	-	6055.55	6023.4	6049	185	
f_{ps} (ksi) = (see Calibration curve)				S_{bG} (in ³)	324	S_{bT} (in ³)	338	4	6082.49	6110.41	-	-	6096	186	
				S_{tG} (in ³)	324	S_{tT} (in ³)	325	5	6234.05	6199.01	6239.28	-	6224	190	
								6	6243.72	6282.13	6298.56	-	6275	191	

M_D (kip-in) = 37.969
 F_i (kips) = 174
 e (in) = 3.25
 A_{ps} (in²) = 0.918
 E_{ps} (ksi) = 28500
 n_L = 6.9
 n_{NL} = 5.5

6



Linear Analysis

Transformed Section Method:

Effective Prestress Force (Elastic Shortening):

$$F_o = [F_i/A_{ps} - (n_L * F_i)/(A_G + (n_L - 1) * A_{ps})] * A_{ps}$$

$$F_o = \mathbf{164.1 \text{ kips}}$$

$$\sigma_{top} = -F_o/A_T + (F_o * e)/S_{tT} - (M_D * y_{tT})/I_T$$

$$\sigma_{top} = \mathbf{24 \text{ psi}}$$

$$\sigma_{bot} = -F_o/A_T - (F_o * e)/S_{bT} - (M_D * y_{bT})/I_T$$

$$\sigma_{bot} = \mathbf{-2904 \text{ psi}}$$

Gross Section Approximate Method:

Effective Prestress Force (Elastic Shortening):

$$F_o = [F_i/A_{ps} - (n_L * F_i)/A_G] * A_{ps}$$

$$F_o = \mathbf{163.6 \text{ kips}}$$

$$\sigma_{top} = -F_o/A_G + (F_o * e)/S_{tG} - (M_D * y_{tG})/I_G$$

$$\sigma_{top} = \mathbf{9 \text{ psi}}$$

$$\sigma_{bot} = -F_o/A_G - (F_o * e)/S_{bG} - (M_D * y_{bG})/I_G$$

$$\sigma_{bot} = \mathbf{-3039 \text{ psi}}$$

Nonlinear Analysis

Nonlinear Analysis Program: Response (see Appendix)

$$F_o: \text{Sub. } n_{NL} \text{ for } n_L \text{ in trans. section eqn.}$$

$$F_o = \mathbf{166.1 \text{ kips}}$$

$$\epsilon_{top} (x10^{-3}) = \mathbf{0.043}$$

$$\epsilon_{bot} (x10^{-3}) = \mathbf{-0.649}$$

$$\sigma_{top} = \epsilon_{top} * E_{ci}$$

$$\sigma_{top} = \mathbf{225 \text{ psi}}$$

$$\sigma_{bot} = f'_{ci} [2(\epsilon_{bot}/\epsilon'_c) - (\epsilon_{bot}/\epsilon'_c)^2]$$

$$\sigma_{bot} = \mathbf{-2841 \text{ psi}}$$

Figure B.3 Calculation of Concrete Stresses for Specimens RS-60S and RS-60N

APPENDIX C

Plots of Prestressing Strand Force History

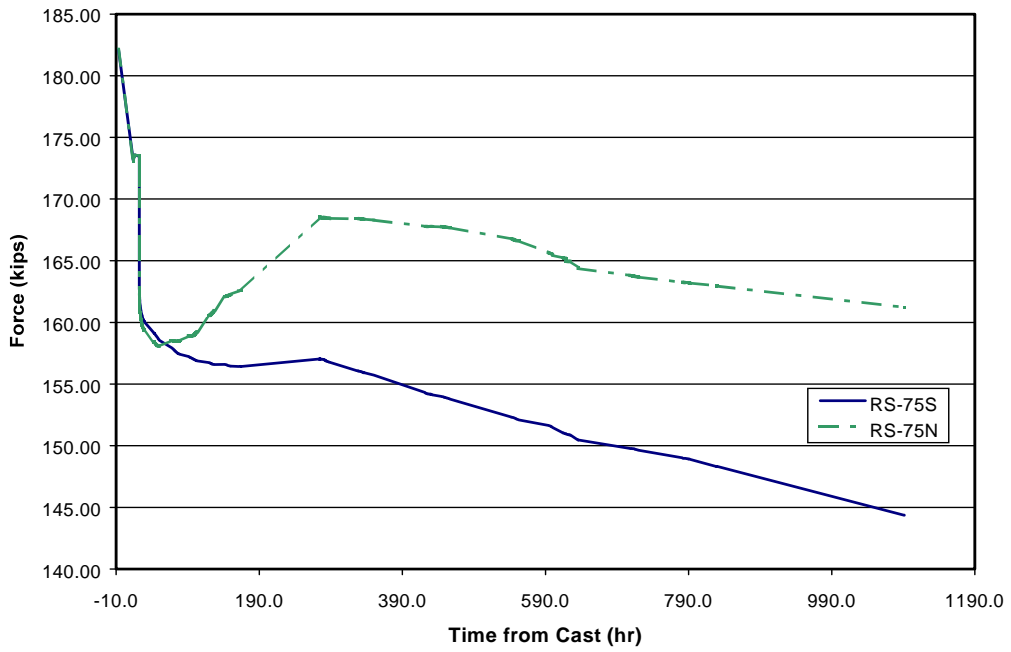


Figure C.1 Prestress Force vs. Time Plot for Specimens RS-75S and RS-75N

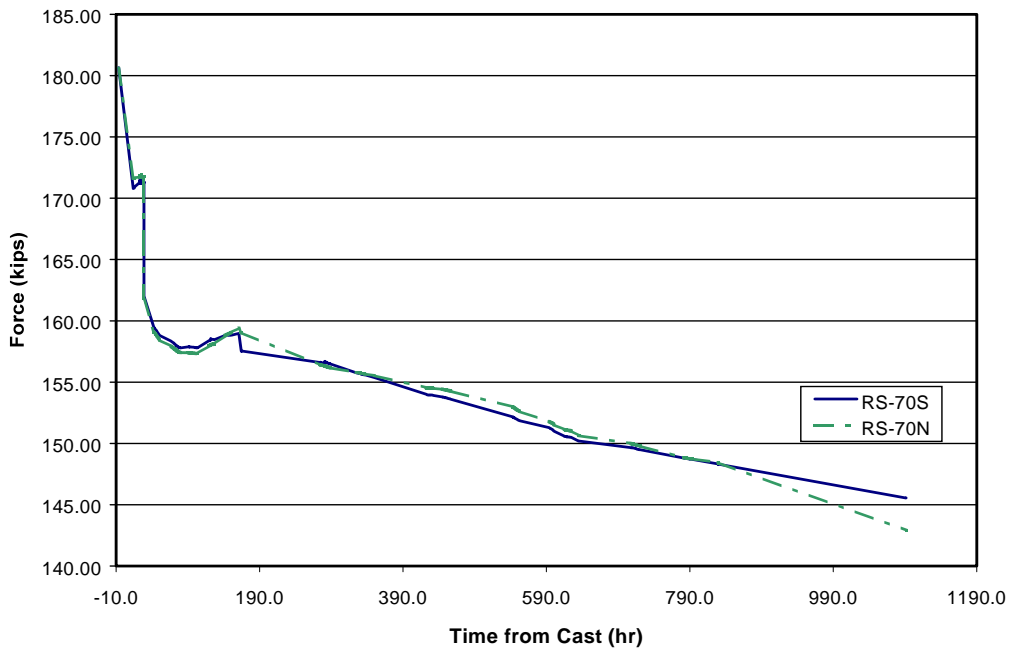


Figure C.2 Prestress Force vs. Time Plot for Specimens RS-70S and RS-70N

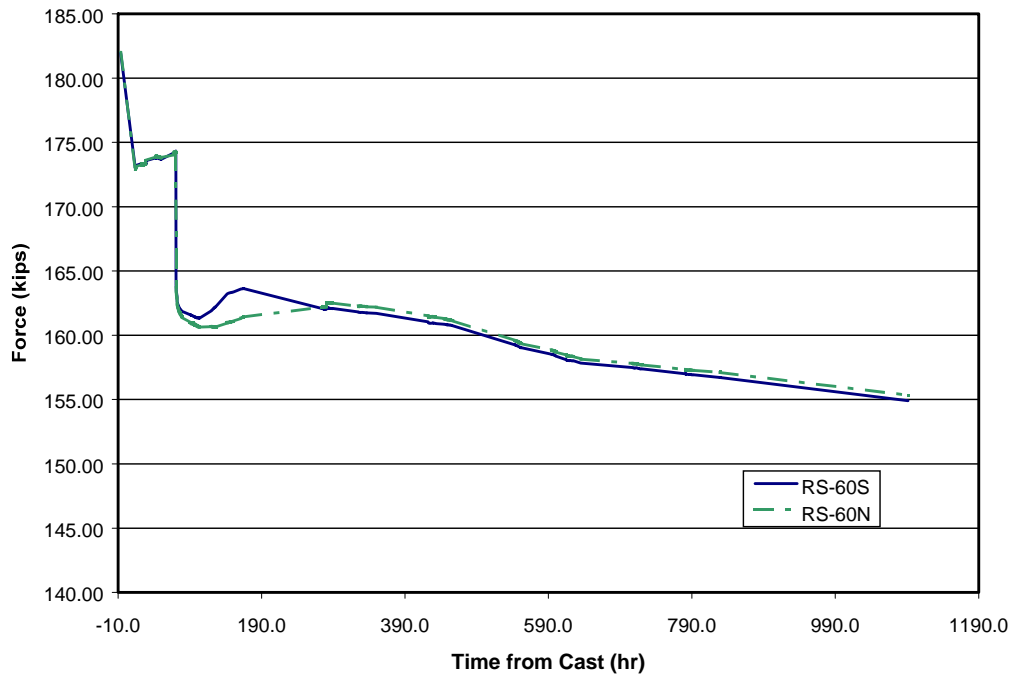


Figure C.3 Prestress Force vs. Time Plot for Specimens RS-60S and RS-60N

APPENDIX D

Measured and Predicted Specimen Camber

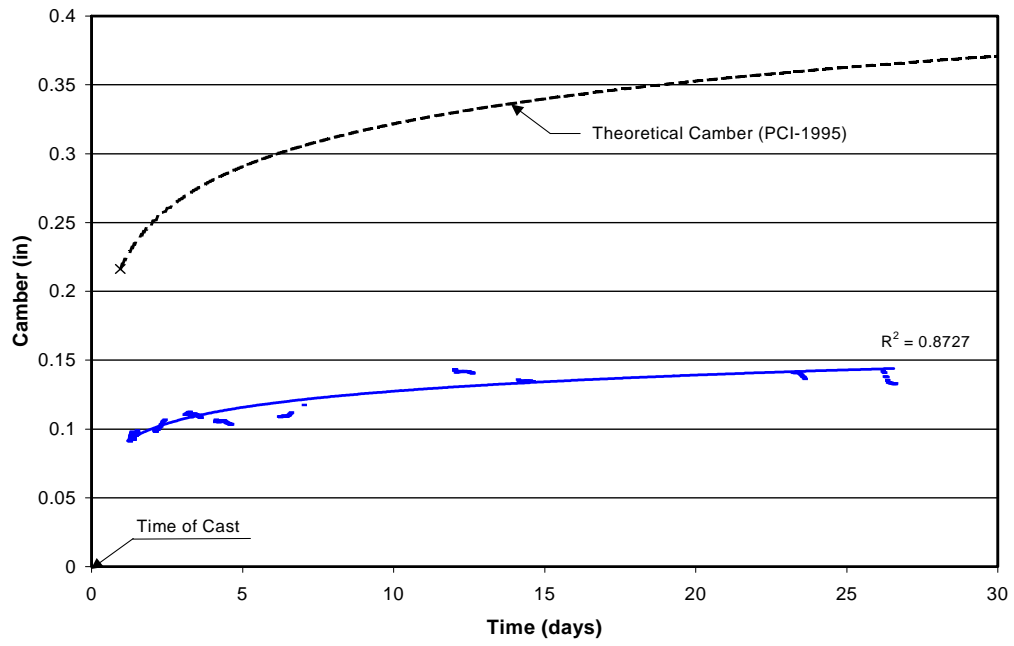


Figure D.1 Camber of Specimen RS-75S

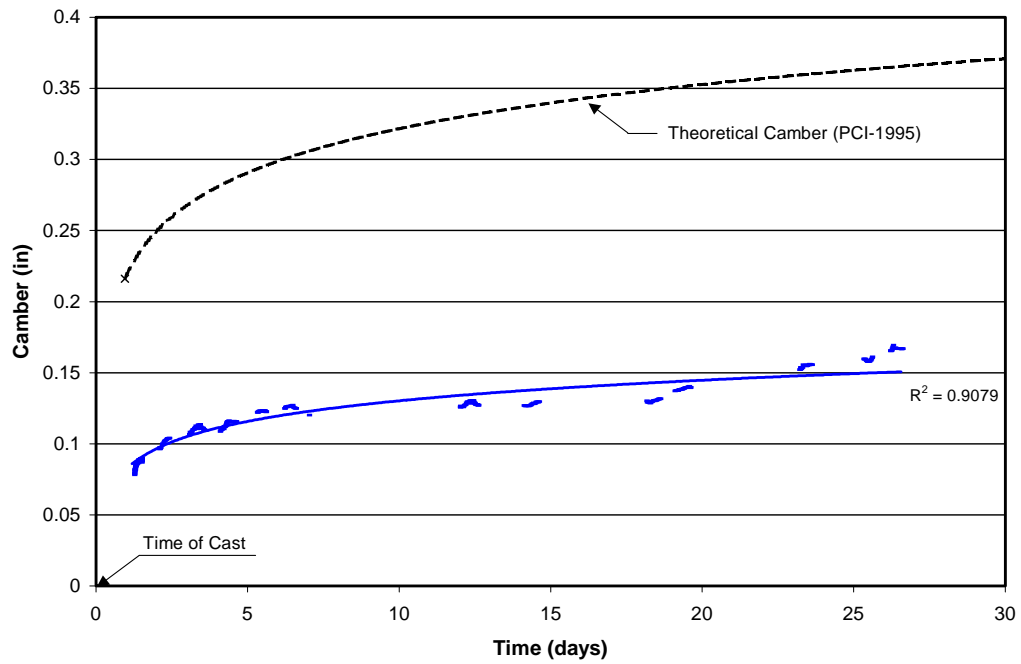


Figure D.2 Camber of Specimen RS-75N

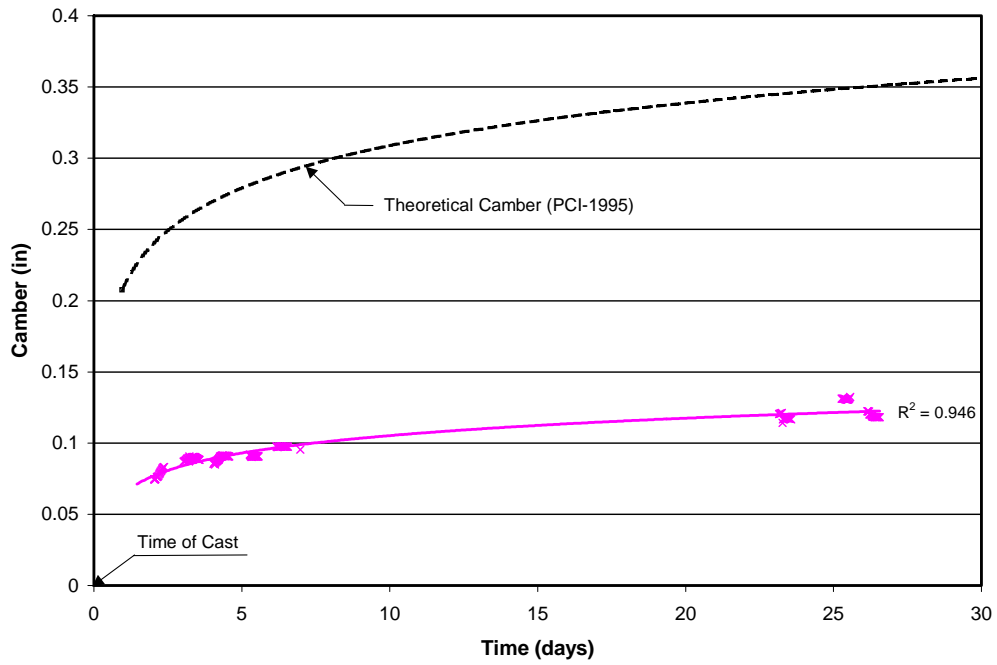


Figure D.3 Camber of Specimen RS-70S

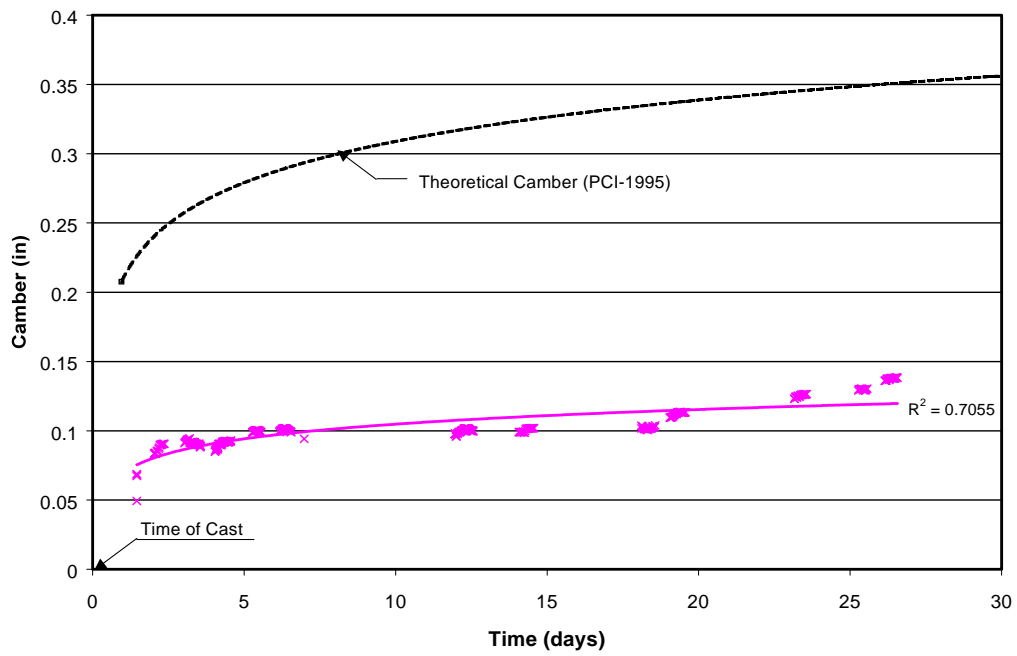


Figure D.4 Camber of Specimen RS-70N

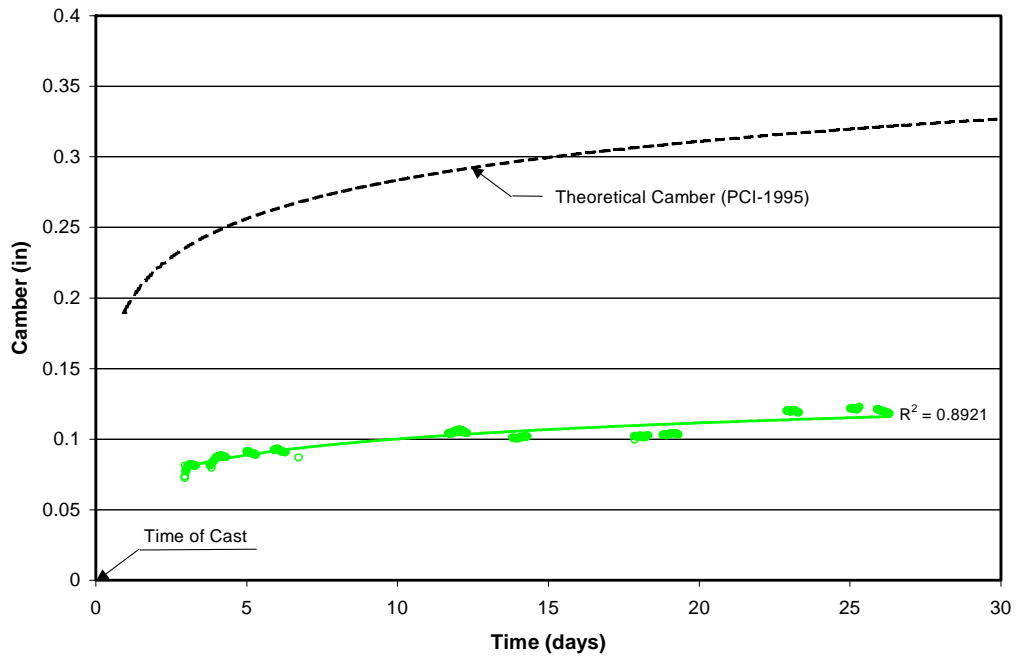


Figure D.5 Camber of Specimen RS-60S

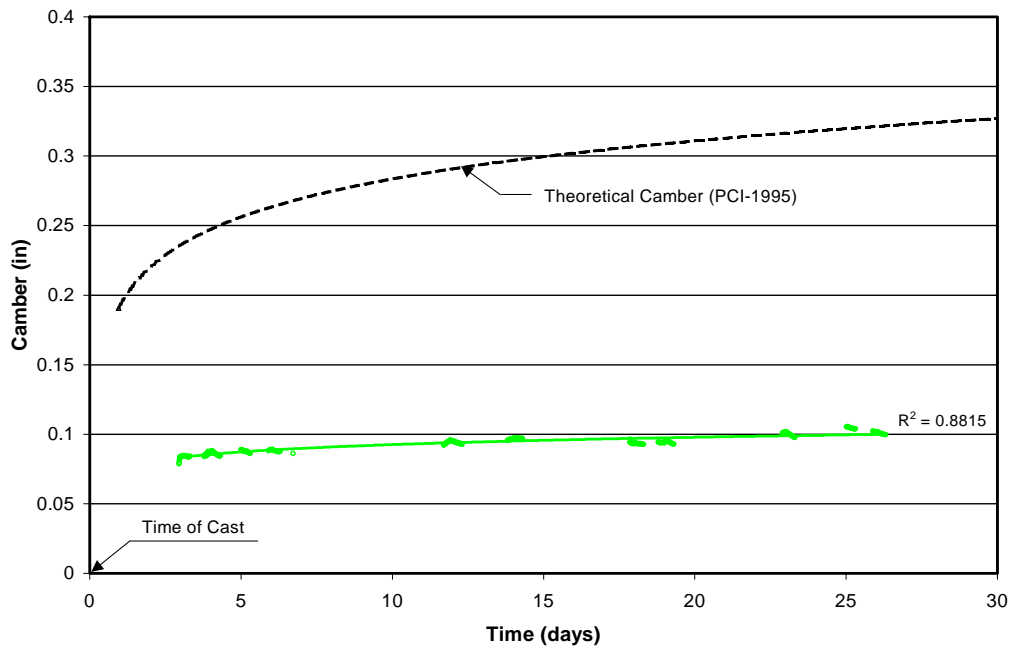


Figure D.6 Camber of Specimen RS-60N

APPENDIX E

DEMEC Strain Profiles

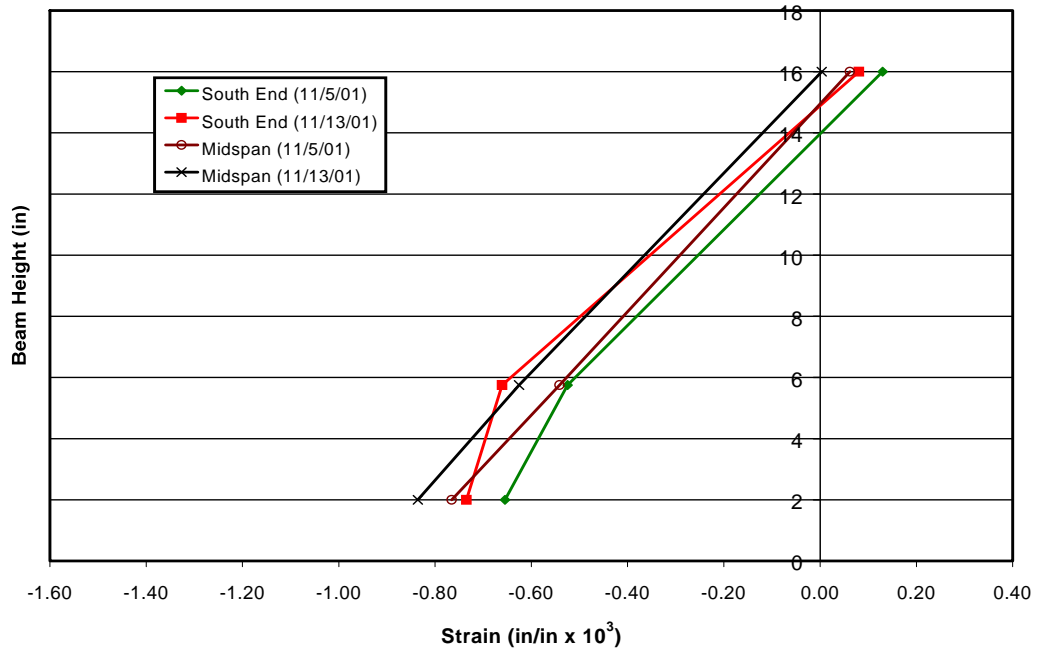


Figure E.1 DEMEC Strain Profile for RS-75S

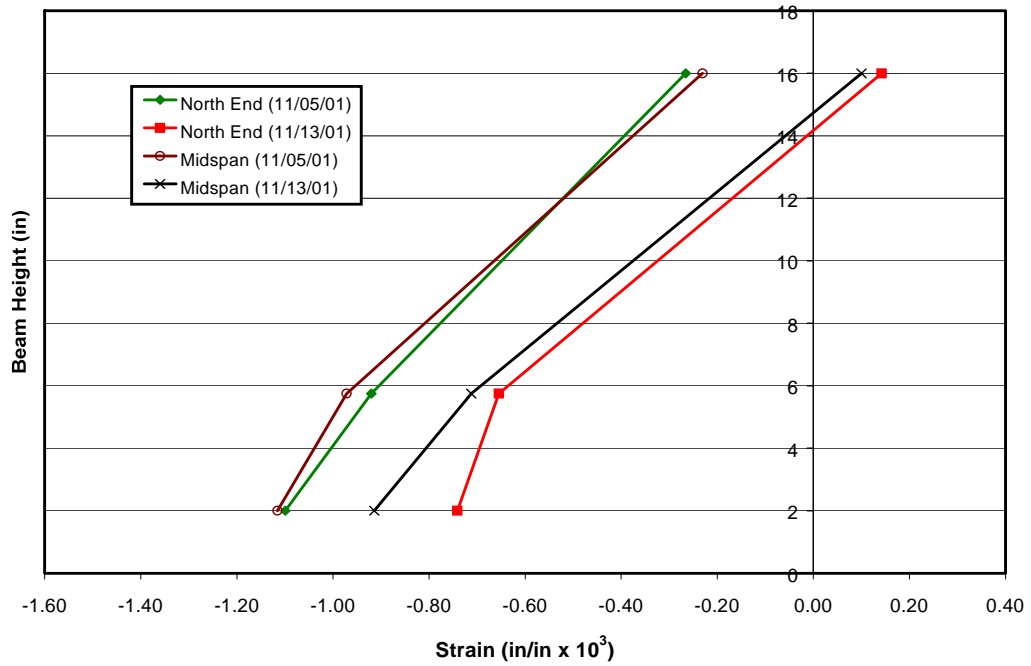


Figure E.2 DEMEC Strain Profile for RS-75N

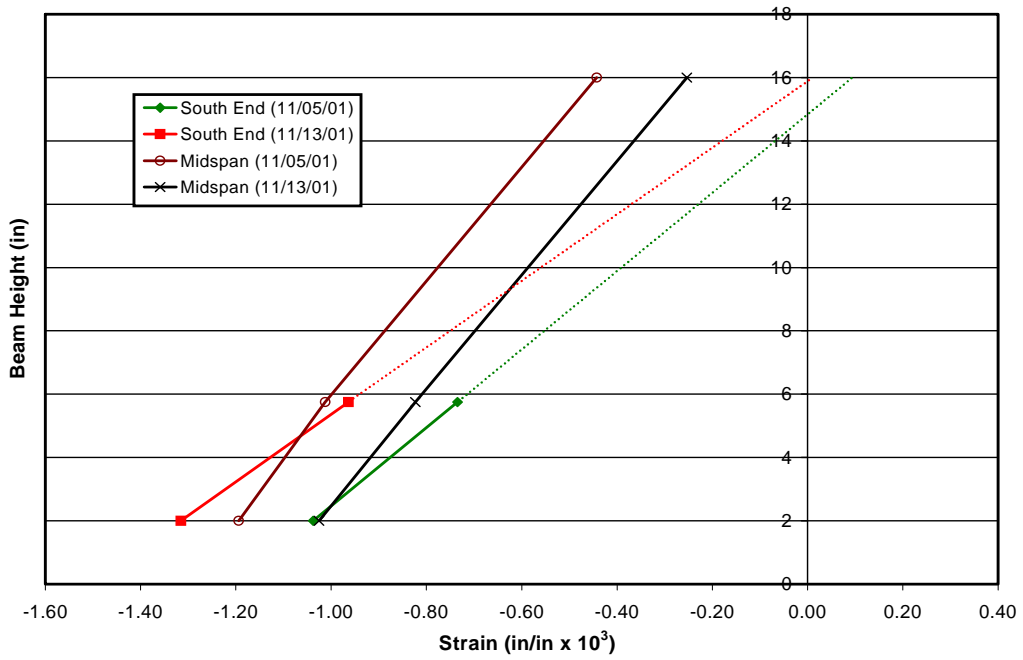


Figure E.3 DEMEC Strain Profile for RS-75S

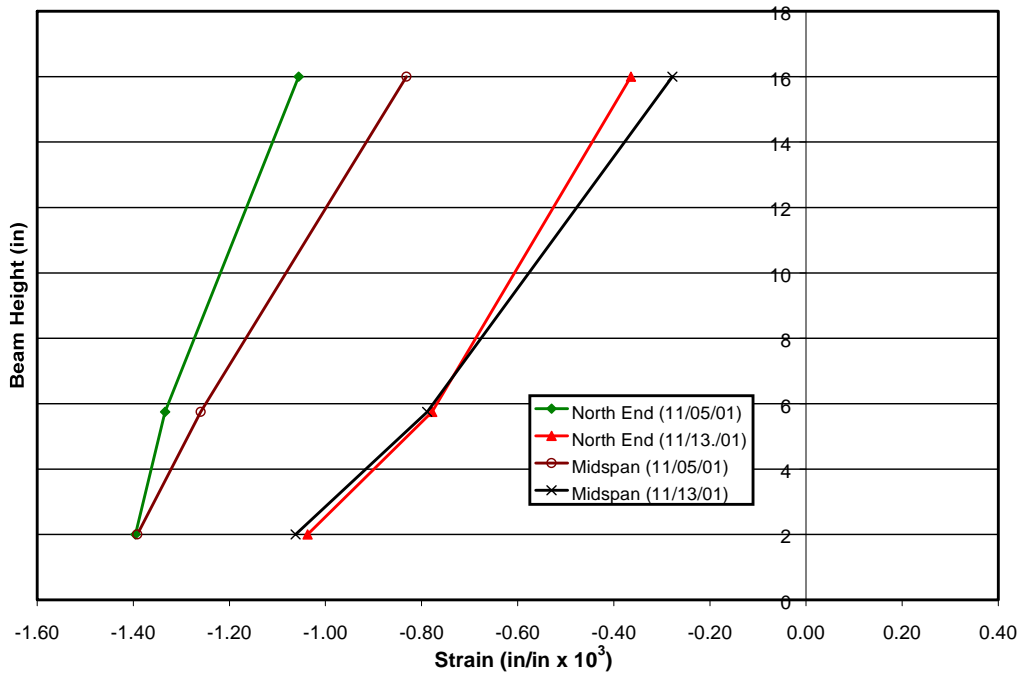


Figure E.4 DEMEC Strain Profile for RS-75S

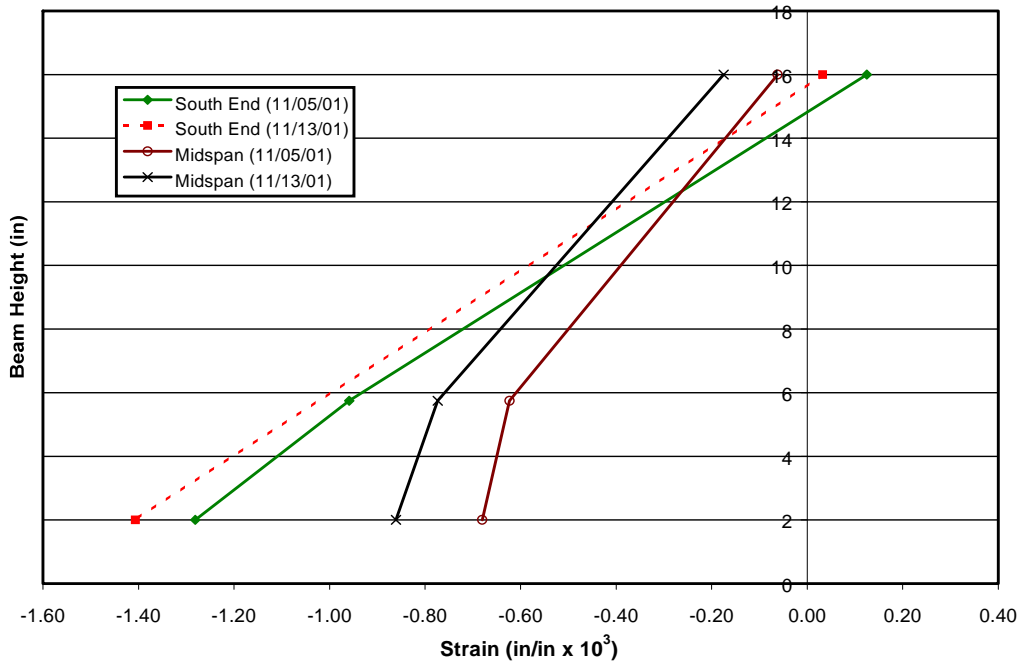


Figure E.5 DEMEC Strain Profile for RS-75S

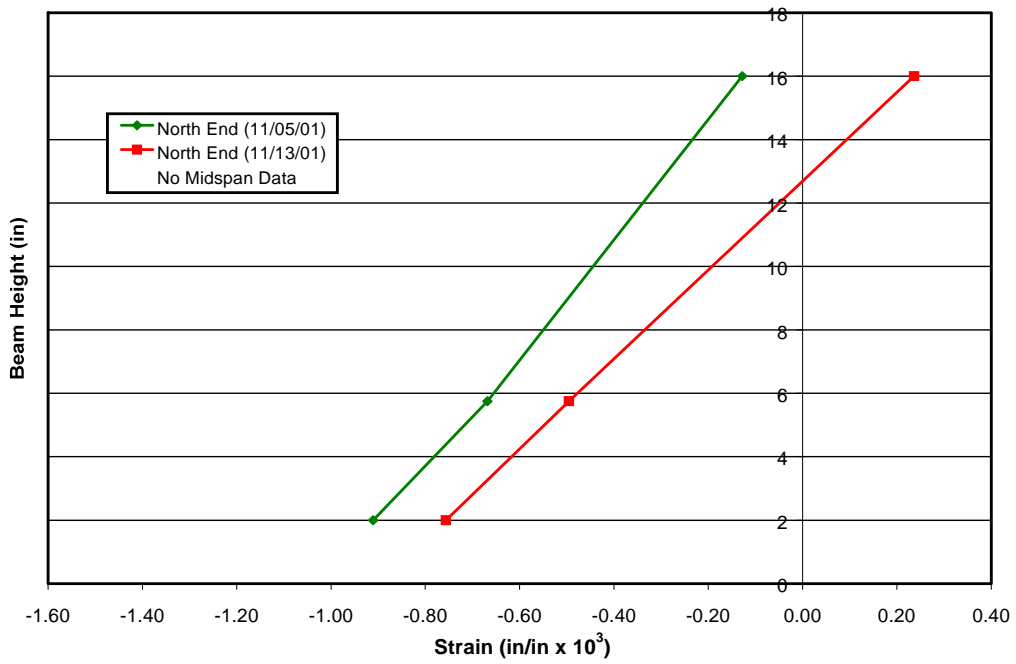


Figure E.6 DEMEC Strain Profile for RS-75S

APPENDIX F

Prestressing Strand Tension Test Results

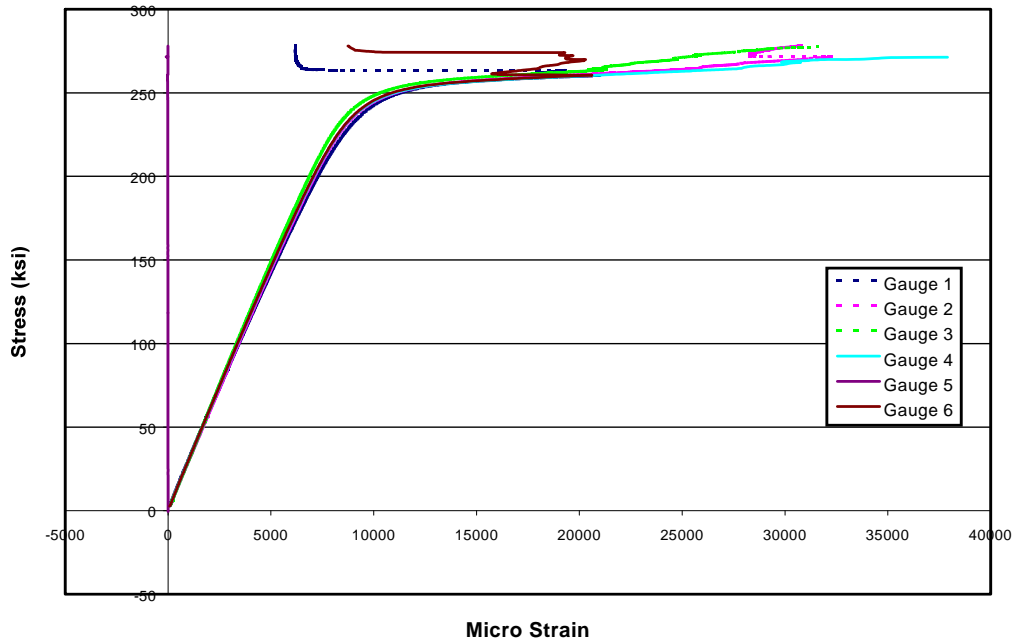


Figure F.1 Stress vs. Strain plot for Strand with Ground Wires (V-Grips)

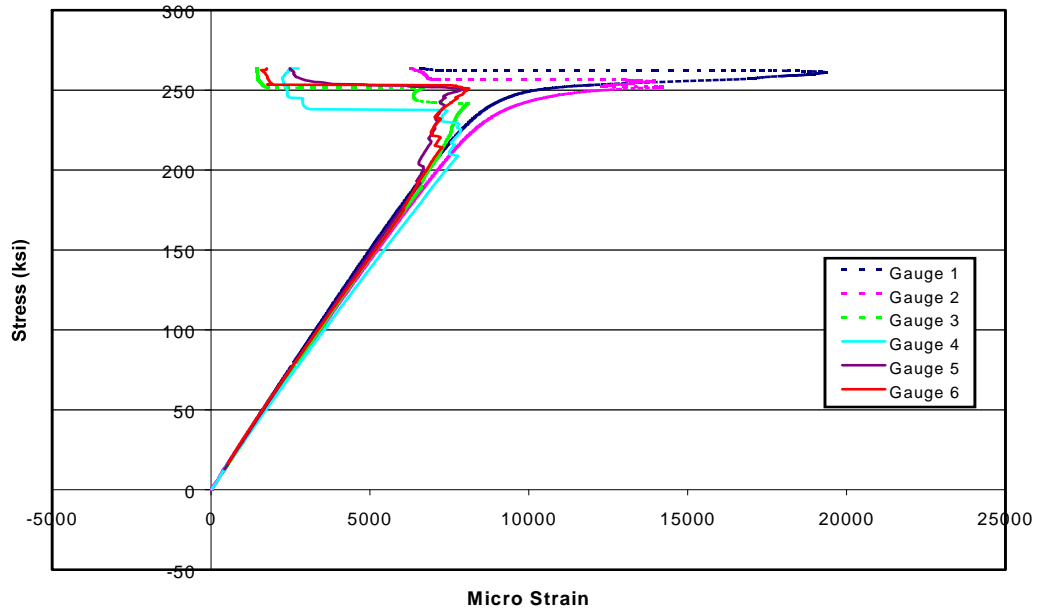


Figure F.2 Stress vs. Strain plot for Strand with Ground Wires (V-Grips)

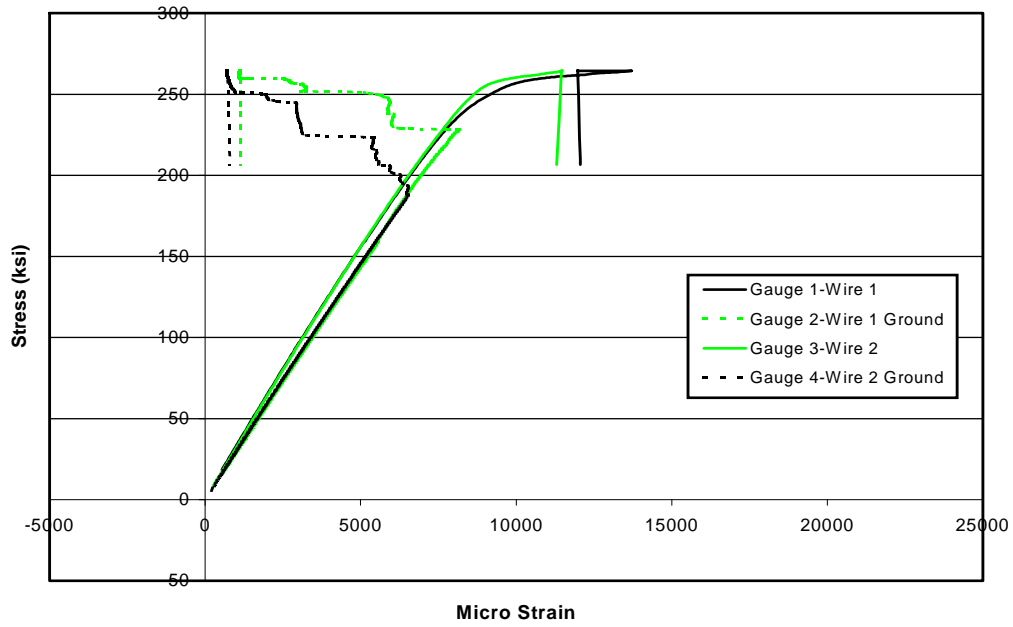


Figure F.3 Stress vs. Strain plot for Strand with Ground and Smooth wires (V-Grips)

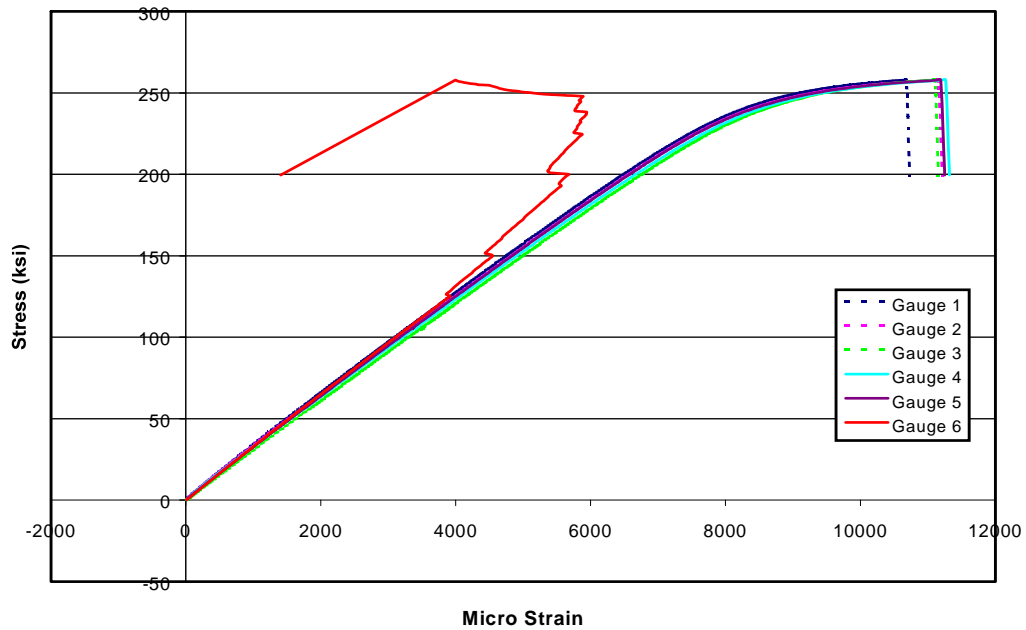


Figure F.4 Stress vs. Strain plot for Strand with no Ground Wires (w/ Chucks)

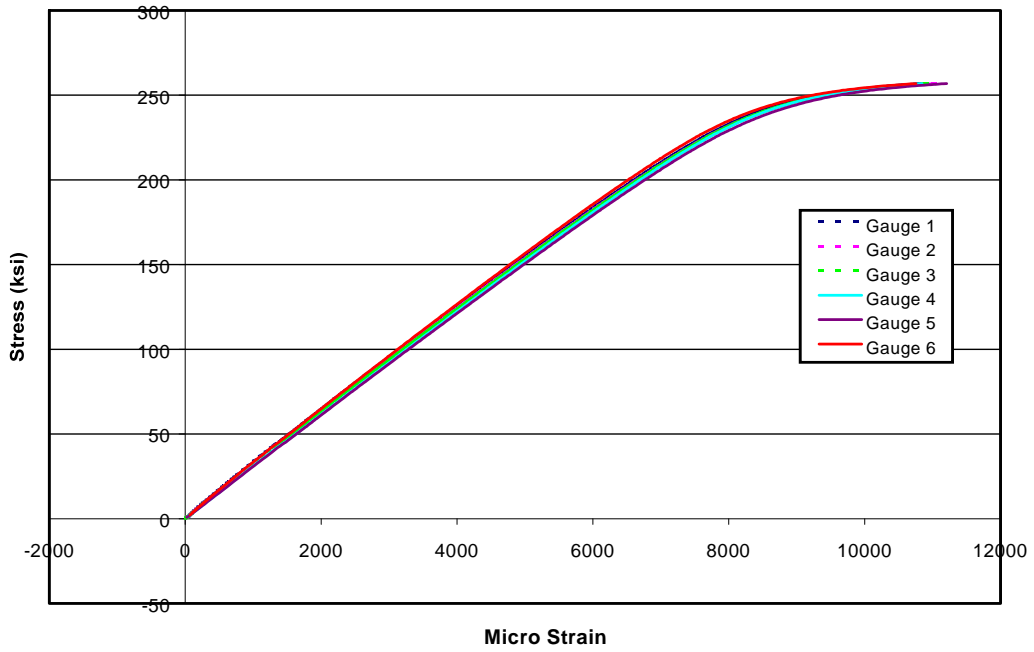


Figure F.5 Stress vs. Strain plot for Strand with no Ground Wires (w/Chucks)

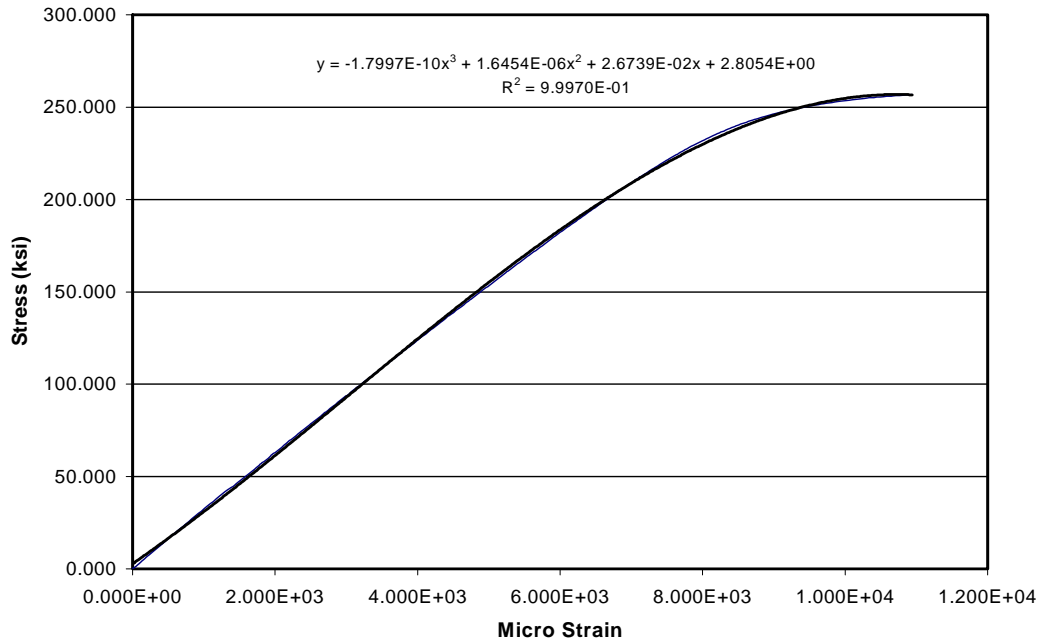


Figure F.6 Calibration Curve for Prestressing Strands

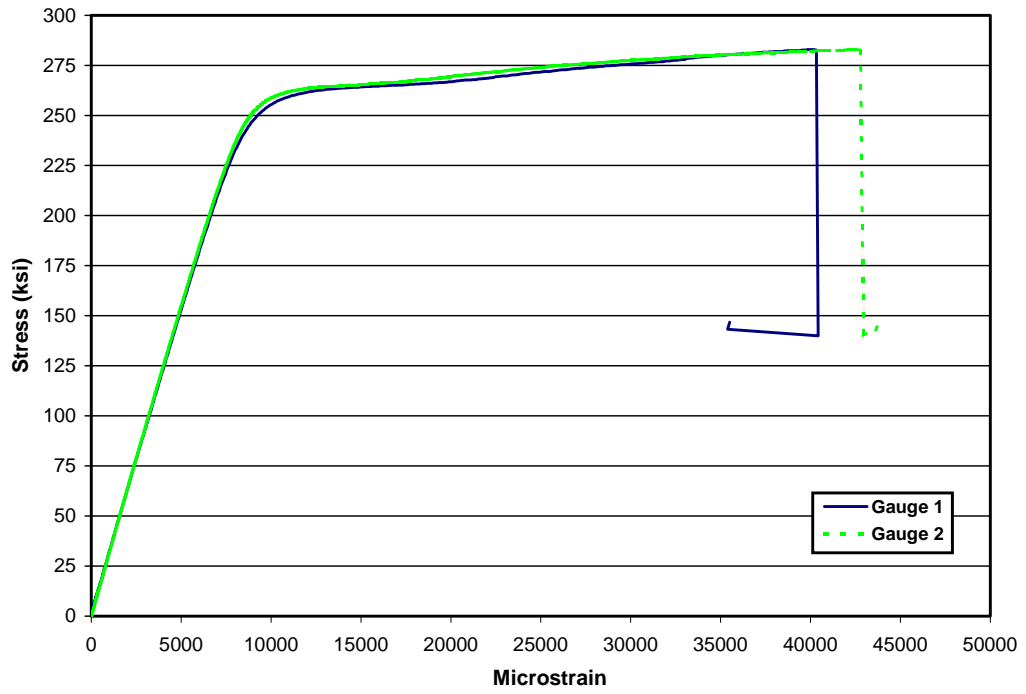


Figure F.7 Stress-Strain Curve for Strand Utilizing CN Adhesive and Polyurethane Coating

REFERENCES

1. Hawkins, N.M., "Impact of Research on Prestressed Concrete Specimens." ACI SP-72, American Concrete Institute, Detroit, 1981. p. 163-176.
2. Kerekes, Frank and Reid, Harold B., *Fifty Years of Development in Building Code Requirements for Reinforced Concrete*, Journal of the American Concrete Institute, Vol. 25, No.6, Detroit, MI, February, 1954. p. 441-470.
3. Henley, H.C. (Chairman), *Report of Committee on Laws and Ordinances*, Proceedings of the National Association of Cement Users, Vol. 3, Washington, D.C., 1907, p. 272-281.
4. Henley, H.C. (Chairman), *Report of Committee on Reinforced Concrete*, Proceedings of the National Association of Cement Users, Vol. 4, Washington, D.C., 1908. p. 233-239.
5. Henley, H.C. (Chairman), *Proposed Standard Building Regulations for the Use of Reinforced Concrete*, Proceedings of the National Association of Cement Users, Vol. 4, Washington, D.C., 1909, p. 438-449.
6. Committee on Building Laws, *Report of Committee on Building Laws*, Proceedings of the National Association of Cement Users, Vol. 6, Washington, D.C., 1910, p. 343-348.
7. Moore, E.J. (Chairman), *Report of the Committee on Reinforced Concrete and Building Laws*, Proceedings of the National Association of Cement Users, Vol. 12, Detroit, MI, 1916, p. 172-180.
8. Committee 501-Standard Building Code, *Proposed Revisions of Building Regulations for Reinforced Concrete*, Journal of the American Concrete Institute, Vol. 36, Detroit, MI, 1940, p. 237-260.

9. Bureau of Public Roads, *Criteria for Prestressed Concrete Bridges*, U.S. Department of Commerce, 1954.
10. ACI-ASCE Joint Committee 323, *Tentative Recommendations for Prestressed Concrete*, Journal of the American Concrete Institute, Detroit, January 1958. Vol. 29, No 7, p. 545-578.
11. American Association of State Highway Officials, *Standard Specifications for Highway Bridges*, Washington D.C., 1961.
12. ACI Committee 318, *Building Code Requirements for Reinforced Concrete*, Detroit, MI, 1963.
13. Siess, C. P., *Research, Building Codes and Engineering Practice*, Journal of the American Concrete Institute, Vol. 56, No. 11, May 1960, p. 1105-1122
14. Private Communication with Prof. Siess, University of Illinois at Urbana-Champaign.
15. Lin, T. Y., *Recommendations for Prestressed Concrete*, Journal of the American Concrete Institute, Detroit, MI, Part 2 September 1958, p.1232-1233.
16. Pang, J. P., *Allowable Compressive Stresses for Prestressed Concrete*. PCI Research Report, 1996.
17. Huo, Xiaoming, and Tadros, Maher, Ph.D., *Allowable Compressive Strength of Concrete at Prestress Release*, PCI Journal, January-February 1997, p. 95-99.
18. Noppakunwijai, Panya and Tadros, Maher, Ph.D., *Strength Design of Pretensioned Flexural Concrete Members at Prestress Release*, PCI Journal, January-February 2001, p. 34-52.

19. Huo, X., Savage, J.M., and Tadros, M. K., *Re-examination of Service Load Limit Compressive Stress in Prestressed Concrete Members*, ACI Structural Journal, V. 92, No.2, March-April 1995, p. 199-210
20. Russell, B., *Design Guidelines for Transfer, Development and Debonding of Large Diameter Seven Wire Strands in Pretensioned Concrete Girders*, Dissertation, The University of Texas at Austin, 1992.
21. PCI Technical Activities Council and PCI Committee on Building Code, *PCI Standard Design Practice*, PCI JOURNAL, V. 41, No. 4, July-August 1996, p. 31-43.
22. Tadros, M.K., Ghali, A., and Meyer, A.W., *Prestress Loss and Deflection of Precast Members*, PCI JOURNAL, V. 38, No. 1, January-February 1985, p. 114-141.
23. Arrellaga, J.A., *Instrumentation Systems for Post-Tensioned Segmental Box Girder Bridges*, Thesis, The University of Texas at Austin, 1991.
24. ACI Committee 318, *Building Code Requirements for Reinforced Concrete (ACI 318-99)*, American Concrete Institute, Detroit, Michigan, 1999.
25. AASHTO, *Standard Specifications for Highway Bridges*, 14th Edition, American Association of State Highway and Transportation Officials, Washington, D.C., 1989.
26. PCI, *PCI Design Handbook*, Fourth Edition, Precast/Prestressed Concrete Institute, Chicago, IL, 1992.
27. Collins, M.P. and Mitchell, D., *Response (Version 1.0) for Prestressed Concrete Structures*, Department of Civil Engineering, University of Toronto, 1990.
28. Integrated Engineering Software, *Visual Analysis*, Bozeman, MT. 1998.